DEVELOPMENT OF PREDICTION MODELS OF HIGH TEMPERATURE CRUMB RUBBER MODIFIED BINDERS

A Dissertation
Presented to
the Graduate School of
Clemson University

In Partial Fulfillment
of the Requirements for the Degree
Doctor of Philosophy
Civil Engineering

---

by
Carl Christian Thodesen
May 2008

Accepted by:
Serji Amirkhanian, Committee Chair
William Bridges
Bradley Putman
Prasad Rangaraju

UMI Number: 3306696

ProQuest Information and Learning Company
300 North Zeeb Road
P.O. Box 1346
Ann Arbor, MI 48106-1346

ABSTRACT

The purpose of this research was to identify and model critical elements of the asphalt rubber matrix contributing to the crumb rubber modified (CRM) binder properties as measured by Superpave testing procedures. Current models are neither applicable (due to new testing procedures) nor practical (due to the difficulty of application or lack of accuracy). Therefore, this research investigated the development of predictive models for estimating binder properties within a specified range of accuracy.

Multiple crumb rubber sources were evaluated in order to gain an understanding of the differences between the various crumb rubbers. This analysis permitted identification of the important parameters, thus allowing for an accurate model to be developed. Analysis of the crumb rubber particles involved the determination of the glass transition temperature, chemical and visual analysis by scanning electron microscope.

Once the critical parameters were established, other test data was obtained from research projects conducted at other labs. This allowed a broader model to be developed, a model which would not be specific to one specific tester and lab facility. Ultimately a total of 17 virgin binder sources from 10 separate regions were evaluated; a further 12 crumb rubber sources were used in conjunction with the various binder sources.

The nonlinear empirical models for estimation of CRM binder properties were developed using the nonlinear least squares method. The accuracy of the various models was evaluated by identifying 95% confidence intervals for the binder property estimation. Validation of the models was performed using a fractional factorial design with

previously untested CRM binders and this step confirmed the accuracy of the various models.

Findings suggest that the effect of the crumb rubber in the binder tends to enhance the effects of the base binder. This indicates that, for CRM binder, the properties of the base binder typically have a greater influence on CRM binder properties than the properties of the crumb rubber used in the matrix. It was possible to develop empirical models depicting the changes in viscosities, G*/sinδ values, and failure temperatures. The Rubber coefficient for viscosity (R_{cv}) and G*/sinδ (R_{cg}) were important parameters when estimating CRM binder properties. These coefficients are representative of the effects of the various crumb rubbers on the binders; generally, it was seen that ambient crumb rubbers had higher R_{cv} and R_{cg} values than cryogenic rubbers.

DEDICATION

I would like to dedicate this work to my family; I know that without their support this would not have been possible.

ACKNOWLEDGMENTS

I would like to acknowledge everyone that has contributed to this dissertation. Specifically, I would like to thank Dr. Serji Amirkhanian for his help and guidance over the years. He allowed me to choose a direction of study and go with it, for better or worse. I am fortunate to have had an advisor such as Serji, and can only hope that one day my children will have a mentor like him.

Special thanks to my other committee members, Dr. Billy Bridges, Dr. Brad Putman, and Dr. Prasad Rangaraju for their countless hours of advising and input into my research. This research would not have been completed in as timely a manner had it not been for their collective efforts.

Thanks to everyone at the Asphalt Rubber Technology Service (ARTS) and the Clemson Civil Engineering Department for making my time here so enjoyable. I would like to thank the Government of Norway and Laanekassen for funding my American adventure. Also, I would like to acknowledge the Istituto Tecnico Guglielmo Marconi in Asmara, Eritrea. This was where my interest in Civil Engineering started all those years ago.

Mom, Dad, and Epi: thanks for always being there and giving me a sense of direction. Finally, my deepest thanks to Bridget who had to deal with me on a daily basis; without a personal cheerleader like you, I don't know how I would have finished.

TABLE OF CONTENTS

Page

Table of Contents (Continued)

Page

Table of Contents (Continued)

Page

Table of Contents (Continued)

Page

LIST OF TABLES

List of Tables (Continued)

Table Page

List of Tables (Continued)

Table Page

List of Tables (Continued)

Table Page

List of Tables (Continued)

Table Page

List of Tables (Continued)

Table Page

List of Tables (Continued)

Table Page

LIST OF FIGURES

List of Figures (Continued)

Figure Page

List of Figures (Continued)

Figure Page

CHAPTER ONE

INTRODUCTION

With the introduction of the Strategic Highway Research Program (SHRP), a number of tests have been adopted in an effort to uniformly evaluate binder properties during all critical stages of its performance life. Such tests allow engineers to perform laboratory evaluations of binders, thus obtaining detailed information specific to the binder resulting in pavement improvements.

Polymer modified binders have been a driving factor behind the adoption of SHRP testing procedures as these binders are typically able to withstand higher performance temperatures without exhibiting the distresses usually associated with elevated temperatures. Of the polymer modified asphalts, Crumb Rubber Modified (CRM) asphalt is widely considered to be the most environmentally friendly. This is largely due to the fact that the modifying agent involved is derived from the shredding of old automobile tires (Yilidirim, 2007). Although the use of natural rubber in asphalt has been around since the 1840s (Heitzman, 1992), the technique of using ground tires in asphalt was first introduced by Charles McDonald in 1963. Initially used as a crack sealant, today his process has been modified and adopted by a number of state agencies for use in highways and other such high volume pavement structures (California Department of Transportation, 2003).

The purpose of this research was the development of empirical relationships to be used in conjunction with some of the SHRP binder properties to determine modified binder properties given only the virgin binder properties. In order to do so, numerous

binder sources need to be studied to provide a statistical platform upon which the empirical relationship could be built. The establishment of such a model would prove beneficial to the industry as well as to the scientific community as it would provide an immediate reference from which binder properties may be estimated given only basic starting parameters, such as base binder viscosity, base binder G*/sinδ, and crumb rubber grinding procedure.

Similarly to other polymer modified asphalts, CRM asphalts tend to cost more than their non modified counterparts. This cost increase is attributed to the addition of the crumb rubber particles; therefore, there is a need to optimize the cost as much as possible. The developed predictive model could be a useful tool to accomplish this. Asphalt behavior is temperature dependent; as such, any subsequent relationship would be required to consider the binder temperature as well as crumb rubber properties.

Preliminary studies indicated that such a relationship is present; findings suggest that a clear relationship between various binder properties and crumb rubber concentration exists. However, the difficulty lies in presenting a universal model that may be used for all binders and crumb rubber types. In particular, this research focused on the prediction of three binder properties: viscosity as determined by rotational viscometer, high failure temperature as determined by dynamic shear rheometer (DSR), and the rutting parameter G*/sinδ as determined by DSR.

Statistical analysis software, SAS, was used to develop the nonlinear relationship present between crumb rubber concentration, temperature, and binder properties. Non linear regressions were utilized in an effort to uniformly describe the behavior of rubber

modified binders at high temperatures. There are currently no predictive models for the determination of properties of binders containing crumb rubber. Past studies have attempted to correlate the viscosity of an asphalt binder with temperature; however, SHRP procedures were not being used at that time (Puzinauskas, 1967).

Significance of Work

It is desirable in the construction business to have well-established relationships for predicting the performance of various materials. Such relationships permit cost estimates to be made well in advance allowing contractors to prepare the most competitive bid while also giving some indication of the engineering properties of the materials.

These relationships can be found in virtually every sub-sector of civil engineering for which empirical equations are available. Such as calculating the compressive and tensile strength of reinforced concrete, estimating the amount of friction head loss in a pipe, predicting hydration products of concrete, and correlating wood grain orientation to compressive and tensile strength of the wood, etc.

Such relationships provide a measure of security to the designer as they indicate that the material is tried and tested, and as such can be, to some extent, trusted. To date, no relationships exist for predicting the high temperature properties of asphalt binders containing crumb rubber. Such relationships would not only provide an invaluable design resource when estimating the amount of crumb required for a certain performance grade,

but they would also indicate that CRM binders are a consistent construction material for which properties can be reliably predicted using well-established testing procedures.

Furthermore, given the temperature dependent viscoelastic nature of asphalt binder, being able to predict the viscosity of an asphalt binder at certain temperatures would also permit more accurate cost estimates of the required fuel costs for reaching the desired pumping temperatures within the asphalt plant.

From an environmental standpoint, it is vital that CRM binders be recognized as a reliable construction material. The EPA reports, "As the environmental impact of buildings becomes more apparent, a new field called green building is gaining momentum. Green or sustainable building is the practice of creating healthier and more resource-efficient models of construction, renovation, operation, maintenance, and demolition" (Environmental Protection Agency, 2007). Specifically the EPA targets six main elements of green building, these include:

- Energy Efficiency and Renewable Energy,
- Water Stewardship,
- Environmentally Preferable Building Materials and Specifications,
- Waste Reduction,
- Toxics,
- Indoor Environment, and
- Smart Growth and Sustainable Development.

The addition of crumb rubber to asphalt binders results in an established environmental building material which promotes sustainable development; additionally,

CRM binder reduces the amount of waste disposed in limited landfill space, as well as eliminating potentially hazardous storage conditions (fire hazards and mosquito breeding). It would appear that CRM binder is the ideal paving material given the aforementioned issues, but to date, pavements incorporating CRM binder are still not the norm in the US or around the world.

The improvements in engineering properties typical of rubberized asphalt pavements are well-documented, however, many of these studies also discuss the inconsistent effects of different crumb rubber types on different binder sources. It is therefore vital that efforts be made to establish the consistency of CRM binder as a construction material.

Objectives

The main objective of this study was the identification, quantification, and subsequent estimation of the effects of crumb rubber in various CRM binders. Specifically, the objectives may be summarized as follows:

1. Conducting an extensive literature review regarding the use, performance, and estimation of SHRP properties of various CRM binders,
2. Evaluating the high temperature binder properties as per SHRP testing procedures (RV and DSR),
3. Conducting statistical analysis of laboratory tested and published data, followed by establishment of nonlinear empirical models for estimation of CRM binder properties,

4. Conducting an error analysis of empirical models, performed by identifying 95% confidence intervals for binder property estimation, and
5. Validating the models by follow up spot checks of binder properties on previously untested binders.

Scope

This study will be concluded following the completion of the steps outlined below:

1. Identification and analysis of previous studies used to evaluate SHRP binder properties. A minimum of 25 unique CRM binders (combinations of at least: five unique virgin binders and five unique crumb rubbers) was deemed the minimum requirement for initial model development.
2. A total of 32 laboratory mixtures were prepared to supplement the literature data for initial model development, specifically CRM binders in the laboratory containing the following materials were prepared:
    a. 5%, 10%, 15%, and 20% crumb rubber content by weight of virgin asphalt binder,
    b. Crumb rubber produced by cryogenic and ambient grinding processing methods,
    c. Crumb rubber derived from various tire sources (e.g., truck tire and passenger car tire), and

d. Asphalt binders from two different sources (Venezuelan and an unidentified blend) meeting PG 64-22 requirement. These binder sources were selected as the Venezuelan source is a commonly used binder throughout the US, while the blended source was used to provide data about the effects of crumb rubber properties on blended virgin binders.

3. Laboratory evaluation of high temperature CRM binder properties as per SHRP testing procedures:
    a. Rotational viscometer (RV) (minimum of three repetitions per sample) and
    b. Dynamic shear rheometer (DSR) (minimum of two repetitions per sample).
4. The SAS program was used to perform statistical analysis of literature and research data:
    a. Identification of appropriate model form,
    b. Perform regression fit of collected data to model, and
    c. Identification of 95 % confidence interval encapsulating predicted values.

Validation testing of model accuracy was accomplished by randomized testing of SHRP binder properties using randomly selected CRM binder compositions of previously untested binder source.

Organization of Dissertation

A literature review of related research is presented in Chapter 2. This review discusses the use of scrap tires in asphalt as wet process CRM binder. SHRP testing procedures are also discussed in detail, specifically the asphalt viscosity and high temperature properties are explained. The literature review also reviews the earlier predictive models used for the determination of binder properties. Chapter 3 includes information regarding the materials and methods used to complete this study. The statistical procedures used for this study are explained in detail in Chapter 4. Model development for the various models is presented in Chapter 5. Experimental results and discussion of the applied models are presented in Chapter 6. This study concludes with Chapter 7, where a summary of the findings is presented along with conclusions and recommendations for future related research.

CHAPTER TWO

LITERATURE REVIEW

To gain an understanding of testing procedures established by SHRP and how they apply to rubberized asphalt, it is first necessary to properly introduce rubberized asphalt and the specific tests developed by SHRP. Therefore, first CRM binder and its components are introduced below, after which the SHRP tests are also presented along with documented cases of such tests being performed in conjunction with CRM binder.

Background

The introduction of CRM binder as an engineering material has occurred due to the occurrence of a number of events. The work done by Charles McDonald on asphalt rubber as a crack sealant in Arizona has proved to be a precursor for the growing environmental sustainability movement. Coupled with dwindling resources, increased environmental problems, and the quest for improved paving materials, CRM binder has emerged as an efficient and "green" alternative to conventional polymer modified binders.

Waste Tire Problem

In 1999, lightning struck a tire dump in Westley, California; the resulting smoke plume impacted nearby farming communities and caused widespread concern of potential health effects from exposure to the smoke emissions (Environmental Protection Agency, 2007). The tire fire produced large quantities of pyrolitic oil which flowed off the slope

and into the drainage of a nearby stream. The pyrolitic oil was also ignited and caused significant smoke emissions on the ground due to the raging oil fire. Local and state agencies were unable to respond to the oil and tire fires, thus requiring the EPA regional coordinator to intervene using the Oil Pollution Act of 1990. In the end, the tire fire lasted for 30 days and the EPA response costs were estimated to be $3.5 million (Environmental Protection Agency, 2007).

While tire fires are infrequent, they cause a serious concern to public safety as well as being expensive to remedy. This danger becomes more apparent as it is estimated that approximately 300 million scrap tires are generated annually (Rubber Manufacturers Association, 2006). This places the generation of scrap tires at approximately one tire per person per year. As seen in Figure 2.1, the number of open landfills in the United States has been in a steady decline, more than 75% of all landfills have been closed within the past 18 years (Environmental Protection Agency, 2006). As such landfilling can no longer be considered a suitable, or sustainable, disposal practice.

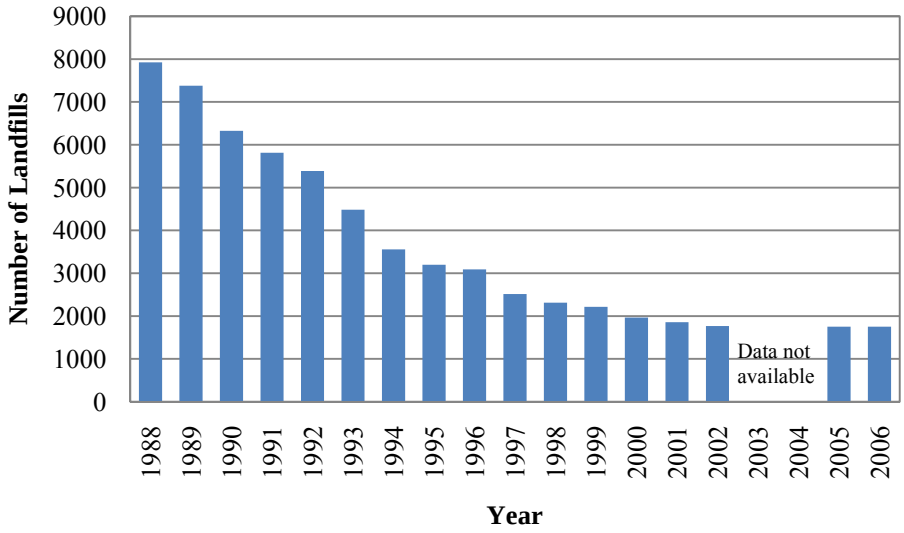

Figure 2.1: Number of Landfills in the United States, 1988-2006 (Environmental Protection Agency, 2006)

Estimates place the number of tires currently in stockpiles and landfills at approximately 188,000,000 (Rubber Manufacturers Association, 2006; Environmental Protection Agency, 2007). The evolution of this problem has prompted the establishment of legislation limiting the disposal options for scrap tires (Rubber Manufacturers Association, 2006). Addition of crumb rubber to binder has been identified as one solution to the scrap tire issue; some studies even suggest that if only 10% of all asphalt pavements laid each year in the U.S. contained 3% rubber by weight of binder, all scrap tires produced for that year would be utilized (Takallou, 1991).

CRM Binder

ASTM D 6114 defines asphalt rubber as "a blend of asphalt cement, reclaimed tire rubber, and certain additives in which the rubber component is at least 15% by weight of the total blend and has reacted in hot asphalt cement sufficiently to cause swelling of

the rubber particles" (American Society of Testing and Materials, 2001). Research has shown that the addition of crumb rubber to virgin asphalt produces binders with improved resistance to rutting , fatigue cracking, and thermal cracking (Dantas Neto et al., 2003; Xiao et al., 2007) as well as reduces the thickness of asphalt overlays and reflective cracking potential (Amirkhanian, 2003).

Research has shown that crumb rubber modification of asphalt binder has many similar effects to polymer modification. The major changes noted by these researchers are seen with the increase in the high temperature stiffness, these are often seen to exceed levels normally achieved by polymer modification. Similarly it has been shown that crumb rubber modifier also results in a reduction of dependency on temperature and loading frequency. However, it has also been suggested that the main function of crumb rubber is that of interactive filler as crumb rubber remains as a particulates even after mixing (Lee & Mahboub, 2006). As the crumb rubber particles do not dissolve in the asphalt, they have been shown to swell in the asphalt resulting in effective volumes that are larger than their initial volume (Bahia & Davis, 1994; Oliver, 1982; Chehoveits et al., 1982).

Tire Composition

Tires are composed of three main components: rubber, steel, and fiber. Rubber contributes the greatest amount of material to the tire, contributing approximately 60% by weight of the tire mass. Typically natural/isoprene rubber is used for both truck and passenger car tires in the tread, sidewall, belt, carcass ply, and inner liner. Differences arise in the amount of styrene butadiene rubber used; truck tires tend to contain higher

amounts of styrene butadiene rubber in the carcass ply and base tread. Higher amounts of butadiene rubber may be found in the base tread of truck tires as well (Toyo Tires, 2001; Ucar et al., 2005).

Crumb Rubber Grinding Procedures

In order for crumb rubber to be added to asphalt it must first be reduced in size; this is generally undertaken by ambient or cryogenic grinding of the scrap tires. The ambient method involves the use of medium to high speed granulators (100-1200 rpm) which utilize a rotor in which fly knives are attached. Prior to being introduced to the fly knives the tires are already ground to approximately 2.5-7.6 cm size. The fly knives move within a close distance of stationary knives which cause a cutting and shearing motion. The size of the ambient ground crumb rubber is controlled by a screen within the machine. Once the material has been processed through primary granulator, it is then passed through a magnetic separation system where a majority of the belt wire steel is removed. The majority of the fiber is removed using an air gravity separation table (Blumenthal, 1994).

The cryogenic process also starts with chunks of tire approximately 2.5-7.6 cm size in size. These chunks are then chilled with liquid nitrogen and ground in a mill, this is followed by the separation of the fiber, metal, and rubber. The ground crumb rubber is then finally sorted according to size; typically 70 to 80% of the crumb rubber is finer than 10 mesh (2 mm) (Blumenthal, 1994).

The principal difference between rubber particles produced using the cryogenic and ambient procedures lies in the shape of the resulting particle. Crumb rubber produced using cryogenic means tends to exhibit a smooth surface, comparable to shattered glass. Ambient grinding tends to yield particles with a rougher surface, thus producing greater surface area than cryogenic particles (Blumenthal, 1994; Putman, 2005).

Mixing Procedure

The incorporation of crumb rubber into the asphalt mixtures is generally performed using the dry process or the wet process. The dry process is characterized by the use of coarse graded rubber as an aggregate with no opportunity for the asphalt and rubber to react before mixing with aggregate. The wet process involves blending the asphalt cement with the crumb rubber prior to the mixing operation. During this process, the rubber reacts with the asphalt binder and changes the binder properties (California Department of Transportation, 2003).

Today, the wet process is the most widely used method of crumb rubber modification, reported advantages of using this procedure include (Amirkhanian, 2003):

- Increased pavement life
- Reduced reflective cracking
- Reduced permanent deformation (rutting)
- Reduced maintenance costs
- Reduced pavement noise generation
- Recycling of waste tires

However, a number of state highway agencies and studies have also suggested that common problems associated with the use of the "wet" process include (Amirkhanian, 2003):

- Higher initial cost: Some highway agencies claim an increase of approximately 25% to over 200% in the cost of the pavement;
- Higher viscosity than conventional asphalt;
- Increased mixing temperature: Asphalt cement and ground tire rubber should be mixed at approximately 204^{o}C to obtain uniform mixture and standard viscosity; and
- There are modifications, in some cases, that may be incurred to the asphalt plant, paving, and compacting equipment.

SHRP Testing

TRB special report 202: *America's Highways: Accelerating the Search for Innovation* first detailed the objectives of the Strategic Highway Research Program. They were identified as follows: "To improve pavement performance through a research program that will provide increased understanding of the chemical and physical properties of asphalt cements and asphalt concretes. The research results would be used to develop specifications and tests needed to achieve and control the pavement performance desired" (Transportation Research Board, 1984).

Emphasis was placed on developing a specification that would be valid for both modified and unmodified asphalt binders. The end product of the binder research

program was called Superpave. The binder specifications were outlined in order to classify binders by performance criteria. Doing so allowed the binder to be evaluated based on performance criteria specific to the application, thus permitting the designer to anticipate the field conditions and ultimately design the pavement accordingly.

Binder Viscosity

AASHTO T 316 is the commonly used SHRP procedure for evaluating asphalt binder viscosity. Achieving asphalt viscosity requirements is of utmost importance for ease of pumping as asphalt is generally stored in asphalt plants at temperatures between 149^{o}C and 177^{o}C depending on the grade or viscosity (US Army Corps of Engineers, 2000). However, fulfilling these requirements becomes more difficult with the increasing viscosity due to modification of the binder by crumb rubber (Stroup-Gardiner et al., 1993) as well as the specifications established by SHRP indicating that asphalt viscosity should not exceed 3.0 Pa-s at 135^{o}C (Asphalt Institute, 2003).

Viscosity at any given temperature and shear rate is essentially the ratio of shear stress to shear strain. At high temperatures such as 135^{o}C, asphalt binders behave as simple Newtonian fluids; that is, the ratio of shear stress to strain is constant. At low temperatures, the ratio of shear stress to shear strain is not a constant, and the asphalt binders behave like non-Newtonian liquids (Roberts et al., 1996).

Research has shown that rubberized asphalt viscosity increases as rubber concentration is increased, regardless of rubber type. Non-Newtonian behavior of the rubber modified binders was also shown to be more pronounced with increasing amounts

of rubber. The same study also concluded that lower viscosity asphalt increases the rate of the modified binder reaction when compared to higher viscosity binders from the same source (Lougheed & Pappagiannakis, 1996).

All combinations of rubber and binder produce a uniquely modified binder, and the resulting viscosity increases occurring with the addition of crumb rubber are due to the amount of aromatic oil absorption and rubber particle swelling. It has been shown that the increase in rubber concentration yielded significant increase in viscosity (Lougheed & Pappagiannakis, 1996). Viscosity of CRM binder is known to be dependent on crumb rubber content (Stroup-Gardiner et al., 1993), particle size and processing method (Putman, 2005), mixing temperature and duration (Abdelrahman M. , 2006), and rubber type (passenger tire or truck tire) (Khalid & Artamendi, 2004).

G*/sinδ and Failure Temperature

Since the implementation of SHRP, the Dynamic Shear Rheometer has been used for the determination of G*/sinδ values as well as the high failure temperature of the binder. Results obtained from the DSR are vital to pavement performance when determining its resistance to rutting (Asphalt Institute, 2003).

The complex shear modulus (G*) and phase angle (δ) are indicators of rutting tendency in the pavement (G*/sinδ) at high temperatures and of fatigue cracking (G*sinδ) at medium range temperatures. AASHTO TP 315 provides specifications and procedures for obtaining experimental values of the complex shear modulus and phase

angle using the DSR (American Association of State Highway and Transportation Officials, 2006).

Loading time and temperature applied on the asphalt binder are the key factors in predicting binder behavior. Information retrieved from the DSR is based on these factors. During the duration of the test, the asphalt binder is sandwiched between two plates, whereby the lower plate is fixed, and the top plate oscillates at a frequency of 10 radians per second.

As specified by previous studies, a gap height of 2 mm was used for testing CRM binder samples, while virgin binders were tested using a 1 mm gap. The differences in gap height were applied to account for the effect of the differing rubber particle sizes present in the CRM binder. Previous studies have shown that if the binders are tested in the linear viscoelastic region, the variation in the gap size will not have a significant impact on the results. Another advantage to using this procedure was the decreased variability noticed when the 2 mm gap data was compared to the 1 mm gap. It has been suggested that the decreased variability of the 2 mm gap data was due to the fact that there was a lower possibility of rubber particles coming in contact with the plates, thus adversely affecting the rheological measurements of the sample (Putman, 2005; Bahia & Davis, 1994; Bahia & Davies, 1996; Tayebali et al., 1990).

The high-temperature portion of the PG grade is determined by measuring the temperature at which the unaged asphalt binder's complex shear modulus divided by the sine of the phase angle ($G^*/\sin\delta$) is at least 1.0 kPa when measured at a frequency of 10

radian per second in accordance with AASHTO M 320 (Asphalt Institute, 2003; Roberts et al., 1996; American Association of State Highway and Transportation Officials, 2005).

Studies have shown that the addition of crumb rubber to asphalt binder tends to increase the G*/sinδ values of the CRM binder. Typically, the addition of crumb rubber to binder is characterized by an increase in G* values and a decrease in phase angle, thus resulting in an overall increased rutting parameter of G*/sinδ (Putman, 2005).

Binder Property Models

Previous studies have shown that viscous flow in any liquid can be regarded as a thermally activated process where molecules must overcome an energy barrier to move to an adjacent vacant site. As temperature goes up, the thermal energy of molecules increases and the vacant site or "holes" in the liquid increases (Salomon & Zhai, 2003). The concept of an activation energy barrier to flow suggests that when a liquid flows, layers of liquid molecules slide over each other and intermolecular forces cause resistance to flow (Eyring, 1936). The viscosity and temperature relationship can be modeled using the Arrhenius equation shown in Equation (2.1) (Ward & Hadley, 1993; Painter & Coleman, 1997).

$$\eta = Ae^{\frac{E_f}{RT}} \qquad \text{Eq.(2.1)}$$

Where,

η: Viscosity of the asphalt binder

T: Temperature (degrees Kelvin)

A: Constant

E_f: Activation energy for flow

R: Universal gas constant (8.314 J.mol^{-1}.K^{-1})

It is more useful to write the Arrhenius equation as shown in Equation (2.2), such an equation produces a linear plot of $\ln\eta$ versus $1/T$ with a slope of E_f/R. Activation has been used in binders to rank their temperature susceptibility. Typically the activation energy is given as the energy in kilojoules needed for one mole of reactants to react. The typical activation energy for an ethylene vinyl acetate (EVA) modified binder was approximately 67kJ/mol (Maze, 1996). An independent study found the average activation energy for unmodified binder to be 205 kJ/mol (Pellinen et al., 2002).

$$ln\eta = \frac{E_f}{RT} + lnA \qquad \text{Eq.(2.2)}$$

Another technique for predicting the temperature susceptibility of asphalt was the binder temperature susceptibility classification (Griffith & Puzinauskas, 1963; Puzinauskas, 1967; Roberts et al., 1996). This index is relatively simple and is given by Equation (2.3):

$$VTS = \frac{log[log(\eta_{T_2})] - log[log(\eta_{T_1})]}{log(T_2) - log(T_1)} \qquad \text{Eq.(2.3)}$$

Where,

T_1 and T_2: Asphalt temperatures at two known points (degrees Rankine)

η_{T1} and η_{T2} : Asphalt viscosities at T_1 and T_2 (Centipoise)

The binder was found to be more temperature susceptible as the VTS value increased. Testing on more than 50 commonly used US binders showed that VTS values tended to range from -3.36 to -3.98 (Puzinauskas, 1967).

A later model proposed by Rasmussen was derived from the definition of Newtonian viscosity and related to penetration (Rasmussen et al., 2002). This equation is based on information produced by the ASTM D5 penetration test for asphalt binders and is given by Equation (2.4):

$$\eta = \frac{\lambda 2 m_n g t_f}{\delta \pi x_f^2} \qquad \text{Eq.(2.4)}$$

Where,

η: Viscosity (Pa-s)

λ: Shear zone thickness (m)

m_n: Mass of the needle assembly (kg, typically 0.10 kg)

g: Acceleration of gravity (at sea level) =9.81 (m/s^2)

δ: Diameter of needle (m)

t_f: Final test time (s) typically 5 s for testing at 25^{o}C

x_f: Final penetration (m)

One model which showed a great deal of promise was developed by Specht et. al., this research focused on modeling the rotational viscosity of asphalt-rubber by statistical analysis and neural networks (Specht et al., 2007). As seen in Equations (2.5) through (2.8) the model was not consistent as the temperature varied from 135 to 195^{o}C.

$$\eta@135 = 0.72 + 1.80(RC) + 1.07(RC)(RC) + 0.83(RC)(TP) + 0.72(RC)(MP) + 0.58(MD) - 0.57(SS) \quad \text{Eq.(2.5)}$$

$$\eta@155 = 0.15 + 0.96(RC) + 0.57(RC)(RC) + 0.42(RC)(MD) + 0.36(RC)(MP) + 0.28(MD) + 0.38(MP)(MT) \quad \text{Eq.(2.6)}$$

$$\eta@175 = -0.0014 + 0.74(RC) + 0.42(RC)(RC) + 0.27(MP)(MD) \quad \text{Eq.(2.7)}$$

$$\eta@195 = -0.40 + 0.80(RC) + 0.40(RC)(RC) + 0.30(MP)(MD) \quad \text{Eq.(2.8)}$$

Where,

η:	Rotational *V*iscosity (Pa-s)
RT:	Read Temperature (^{o}C)
RC:	Rubber Content (% rubber in relation to total mass)
MD:	Mixing Duration (minutes)
MP:	Mixing Temperature (^{o}C)
SS:	Rubber Specific Surface (m^2/kN)

Another issue with this relationship is that it is not applicable for a number of scenarios; this is because at these specified values the model produces negative values. It is not physically possible to exhibit a negative viscosity, therefore additional research is required to be undertaken in order to produce more realistic models.

While some merit has been found in a number of these relationships; they are not representative of the current testing procedures outlined by SHRP, or only functional to a certain degree. Furthermore, none of these methods takes into consideration the addition of crumb rubber to the binder for predicting the G*/sinδ values of the CRM binder.

CHAPTER THREE

MATERIALS AND EXPERIMENTAL PROCEDURES

In this chapter the materials, experimental plan, and experimental methods used to accomplish the research goals are discussed. The materials used in this study are listed as well as any data relevant to the origin of the materials and their engineering properties. The experimental plan is explained in detail, specifically, the goal of each section is discussed as well as its relevance to the overall objectives of the study. Experimental methods are provided and, when relevant, the standard procedure is identified.

Materials

Asphalt Binders

During the model development stage a total of twelve base asphalt binders were evaluated. In addition, during verification five other asphalt binders were evaluated. The binders were selected from many sources to determine the effects of geographic locations of the binders. On some occasions, the same binder source was evaluated over several months to determine if the binder properties were maintained over time. Table 3.1 provides a description of the binders used in this study. The test dates and test locations are also given in order to provide a description of the various dates and locations the binders were evaluated.

As shown in Table 3.1, binders from four different continents were tested; furthermore, the information is a compilation of studies from three independent lab

facilities which studied the binder properties over an eight year span. Three polymer modified asphalt (PMA) binders were also evaluated to provide some information regarding the feasibility of using the developed models in this research work on PMAs as well.

Table 3.1: Description of binder used in this research study

Binder Code	Source	Description	Superpave PG	Test Date	Test Location
A	Venezuela	-	PG 70-22	2006-7	ARTS Lab, Clemson, SC
B	South Carolina	Blend	PG 64-22	2006-7	ARTS Lab, Clemson, SC
C	Russia	-	PG 64-22	2005	Pannonia Lab, Veszprem, Hungary
D	Venezuela	-	PG 70-22	2004-5	ARTS Lab, Clemson, SC
E	Middle East	-	PG 64-22	2004-5	ARTS Lab, Clemson, SC
F	South Carolina	Blend	PG 64-22	2004-5	ARTS Lab, Clemson, SC
G	South Carolina	Blend	PG 64-22	2005	ARTS Lab, Clemson, SC
H	South Carolina	SBS	PG 76-22	2005	ARTS Lab, Clemson, SC
I	Unknown	-	PG 58-28	1999	FHWA Lab, McLean, VA
J	Unknown	-	PG 64-22	1999	FHWA Lab, McLean, VA
K	Unknown	NOVOPHALT	PG 76-22	1999	FHWA Lab, McLean, VA
L	Unknown	STYRELF	PG 82-22	1999	FHWA Lab, McLean, VA
M	Middle East	-	PG 64-22	2007	ARTS Lab, Clemson, SC
N	Texas	-	PG 70-22	2007	ARTS Lab, Clemson, SC
O	Canada 2	-	PG 64-22	2007	ARTS Lab, Clemson, SC
P	West Texas	-	PG 64-22	2007	ARTS Lab, Clemson, SC
Q	Canada 1	-	PG 64-22	2007	ARTS Lab, Clemson, SC

Crumb Rubber

The gradation of the crumb rubber sources was highly varied and therefore, five different gradations were evaluated. The gradations were: Arizona Department of Transportation (ADOT) and South Carolina Department of Transportation's (SCDOT) specifications, 0.850 mm, 0.425 mm, and 0.180 mm. This range of gradations provides both coarse and fine gradations, as well as individual coarse and fine crumb rubber particles. The SCDOT and ADOT gradations are given in Table 3.2.

Crumb rubber data was available for twelve different types of crumb rubber (Table 3.3). The variables that were varied for the crumb rubbers included: production location, grinding procedure, gradation, and tire type. As described in later chapters, many of the crumb rubber sources were added to various asphalt binders at concentrations ranging between 5 and 20% by weight of binder.

Table 3.2: (a) ADOT and (b)SCDOT gradations

(a)

Sieve Number	**No. 10**	**No. 16**	**No. 30**	**No. 50**	**No. 200**
Opening size (mm)	**2.000**	**1.190**	**0.600**	**0.300**	**0.075**
Upper Specification (% passing)	100	100	100	45	5
Lower Specification (% passing)	100	65	20	0	0

(b)

Sieve Number	**No. 20**	**No. 40**	**No. 80**	**No. 100**
Opening size (mm)	**0.850**	**0.425**	**0.180**	**0.150**
Upper Specification (% passing)	100	100	50	30
Lower Specification (% passing)	100	85	10	5

Table 3.3: Description of crumb rubber used in this research study

CRM Designation	Production Location	Grinding	Gradation	Tire Type	Test Date	Test Location
Source 1	South Carolina	Cryogenic	ADOT	Passenger	2006-7	ARTS Lab, Clemson, SC
Source 2	Arizona	Cryogenic	ADOT	Passenger	2006-7	ARTS Lab, Clemson, SC
Source 3	California	Ambient	ADOT	Unknown	2006-7	ARTS Lab, Clemson, SC
Source 4	Florida	Ambient	ADOT	Truck	2006-7	ARTS Lab, Clemson, SC
Source 5	Hungary	Ambient	ADOT	Unknown	2005	Pannonia Lab, Veszprem, Hungary
Source 6	South Carolina	Ambient	SCDOT	Passenger	2005	ARTS Lab, Clemson, SC
Source 7	South Carolina	Cryogenic	0.850 mm	Passenger	2004-5	ARTS Lab, Clemson, SC
Source 8	South Carolina	Cryogenic	0.425 mm	Passenger	2004-5	ARTS Lab, Clemson, SC
Source 9	South Carolina	Cryogenic	0.180 mm	Passenger	2004-5	ARTS Lab, Clemson, SC
Source 10	South Carolina	Ambient	0.850 mm	Passenger	2004-5	ARTS Lab, Clemson, SC
Source 11	South Carolina	Ambient	0.425 mm	Passenger	2004-5	ARTS Lab, Clemson, SC
Source 12	South Carolina	Ambient	0.180 mm	Passenger	2004-5	ARTS Lab, Clemson, SC
Source 13	South Carolina	Cryogenic	SCDOT	Passenger	2007	ARTS Lab, Clemson, SC
Source 14	South Carolina	Ambient	SCDOT	Passenger	2007	ARTS Lab, Clemson, SC
Source 15	South Carolina	Cryogenic	0.850 mm	Passenger	2007	ARTS Lab, Clemson, SC
Source 16	South Carolina	Cryogenic	0.425 mm	Passenger	2007	ARTS Lab, Clemson, SC
Source 17	South Carolina	Cryogenic	0.180 mm	Passenger	2007	ARTS Lab, Clemson, SC
Source 18	South Carolina	Ambient	0.850 mm	Passenger	2007	ARTS Lab, Clemson, SC
Source 19	South Carolina	Ambient	0.425 mm	Passenger	2007	ARTS Lab, Clemson, SC
Source 20	South Carolina	Ambient	0.180 mm	Passenger	2007	ARTS Lab, Clemson, SC

Experimental Plan

The research was completed by carrying out six distinct objectives and resulted in the establishment of equations relating high temperature properties of CRM binders with crumb rubber content and temperature. The experimental plan for this research study is shown in Figure 3.1.

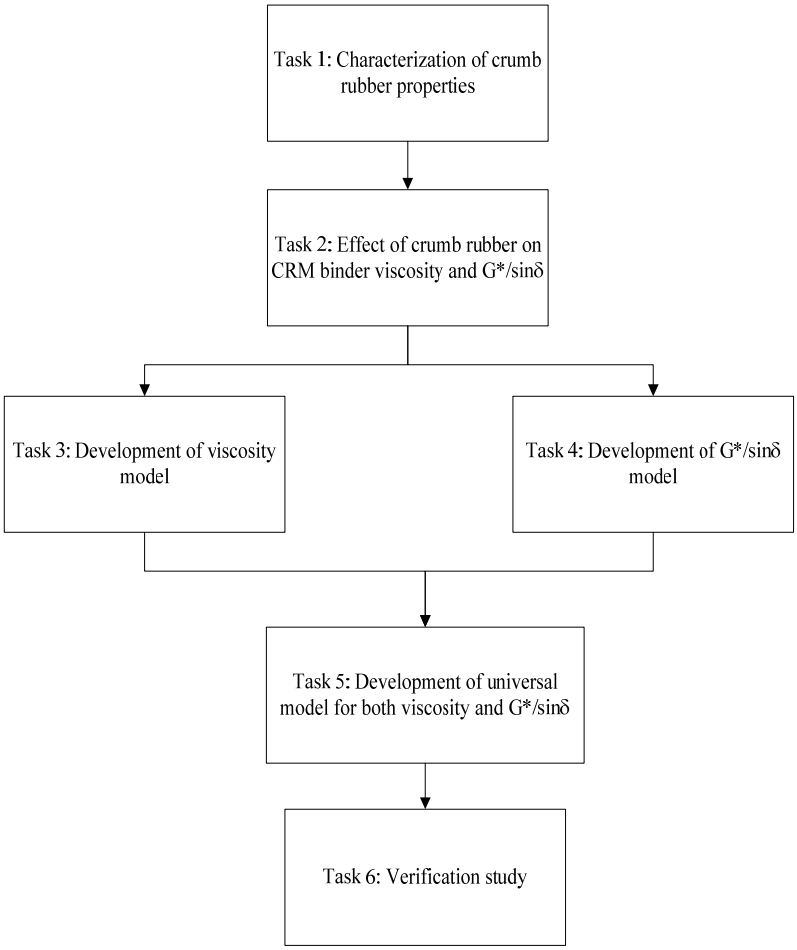

Figure 3.1: Step by step task list

Task 1: Characterization of crumb rubber properties

The first task involved identifying the differences present between crumb rubber materials derived from different manufacturers. This gave an indication of the variability present in the various crumb rubber sources (Figure 3.2). Such an evaluation was necessary because it was important to determine the extent of the differences present from crumb rubber source to source.

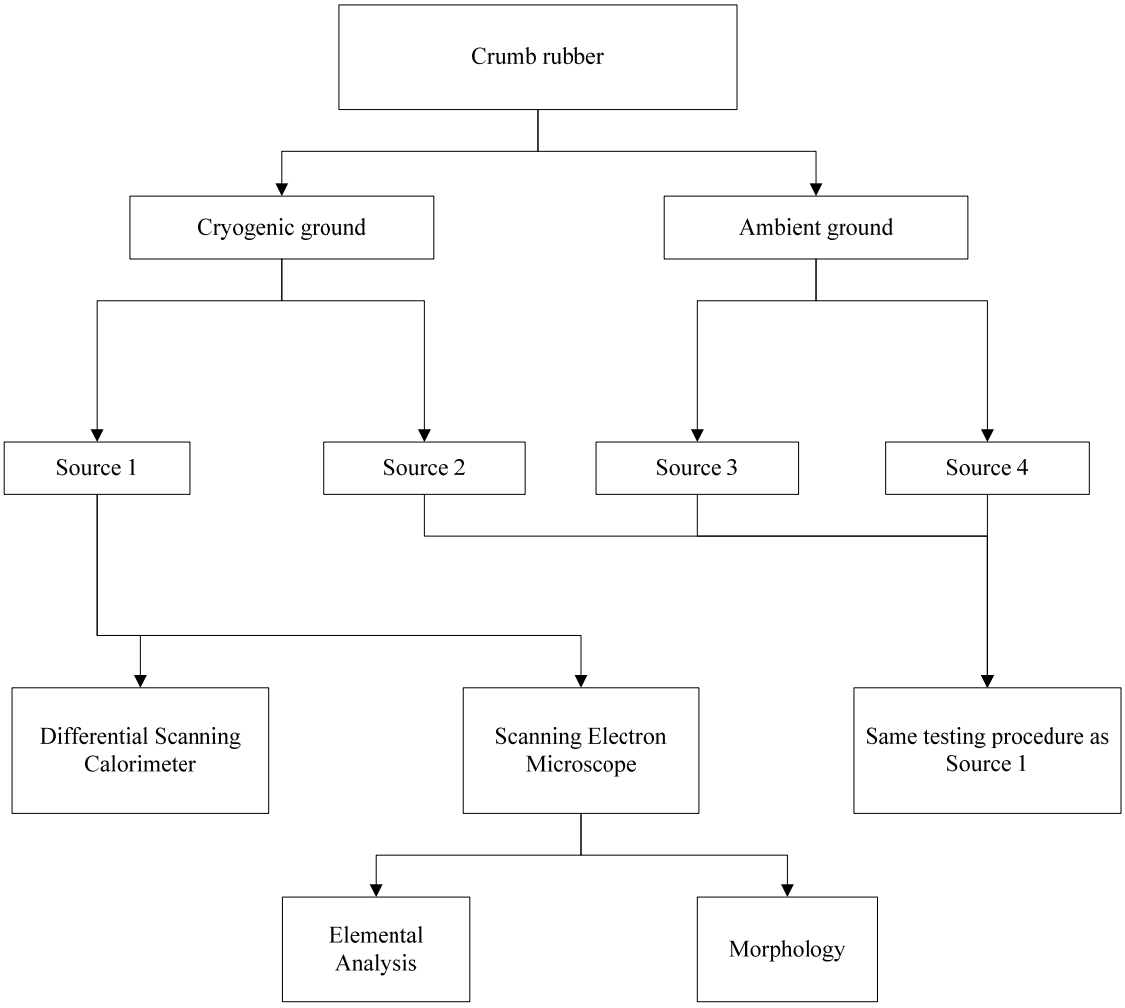

Figure 3.2: Task 1 - Characterization of crumb rubber particles

Task 2: Effect of Crumb Rubber on CRM binder viscosity and G*/sinδ

The second task was reacting the four crumb rubber sources with two binder sources (A and B) and evaluating the viscosity and failure temperature of the various binder-crumb rubber combinations. This evaluation provided data regarding the effect of the different crumb rubber sources on asphalt binder properties. Also, an evaluation of the different effects (particle and interaction) of the crumb rubber on the binder was conducted. In doing so, it was possible to determine whether the effects of the crumb rubber on the asphalt were physical or due to interactions between the crumb rubber and binder.

This evaluation was conducted by determining the effects on binder performance due to particle morphology as opposed to interactions between the particle and binder. Figure 3.3 gives an illustration of the experimental plan pursued during Task 2. In this phase of the research the viscosity and G*/sinδ data were obtained at crumb rubber concentrations between 0 and 20% crumb rubber by weight of binder.

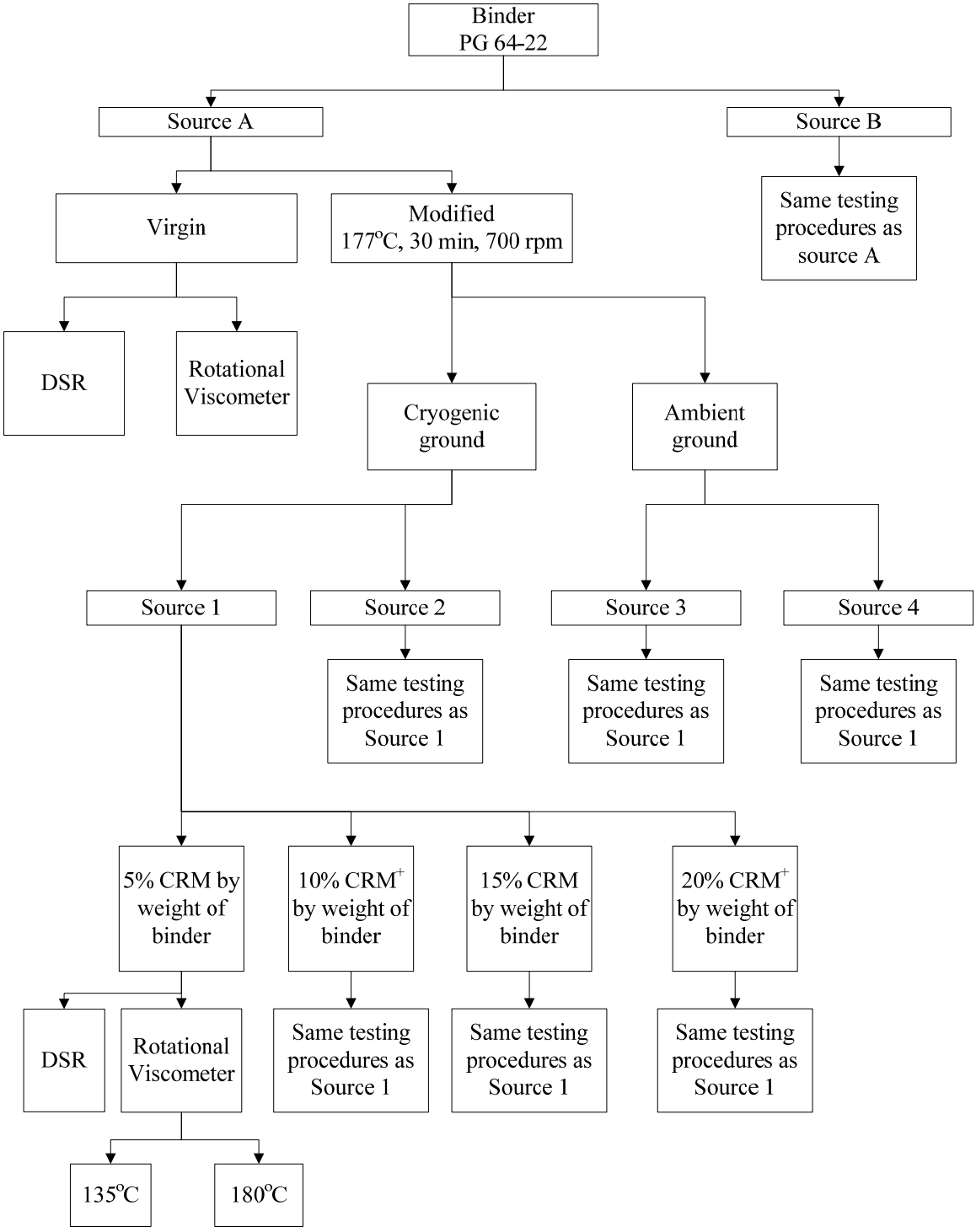

+Drained samples were prepared and tested for DSR and Rotational Viscometer

Figure 3.3: Task 2 - Effect of crumb rubber on CRM binder viscosity and G*/sinδ values

Tasks 3 and 4: Development of G*/sinδ and viscosity model

The third and fourth tasks were completed by supplementing the data from the second task with additional test data obtained from the literature. Then the statistical regression analysis was employed to identify specific relationships for determining failure temperature and viscosity using only the base binder and relevant crumb rubber properties as input parameters.

The various testing variables that were considered during model preparation are shown in Figures 3.4 and 3.5. These figures show the various asphalt binder and crumb rubber sources utilized to develop the models.

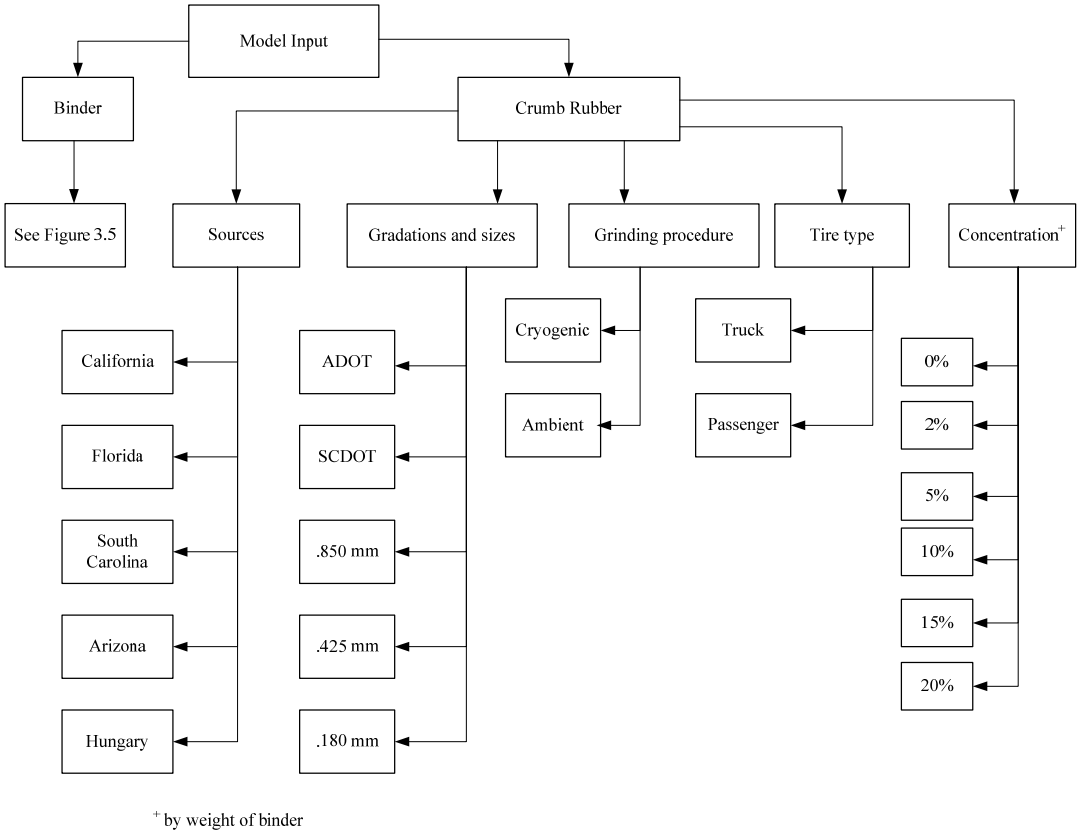

Figure 3.4: Task 3&4 - Various crumb rubber variables considered for model input

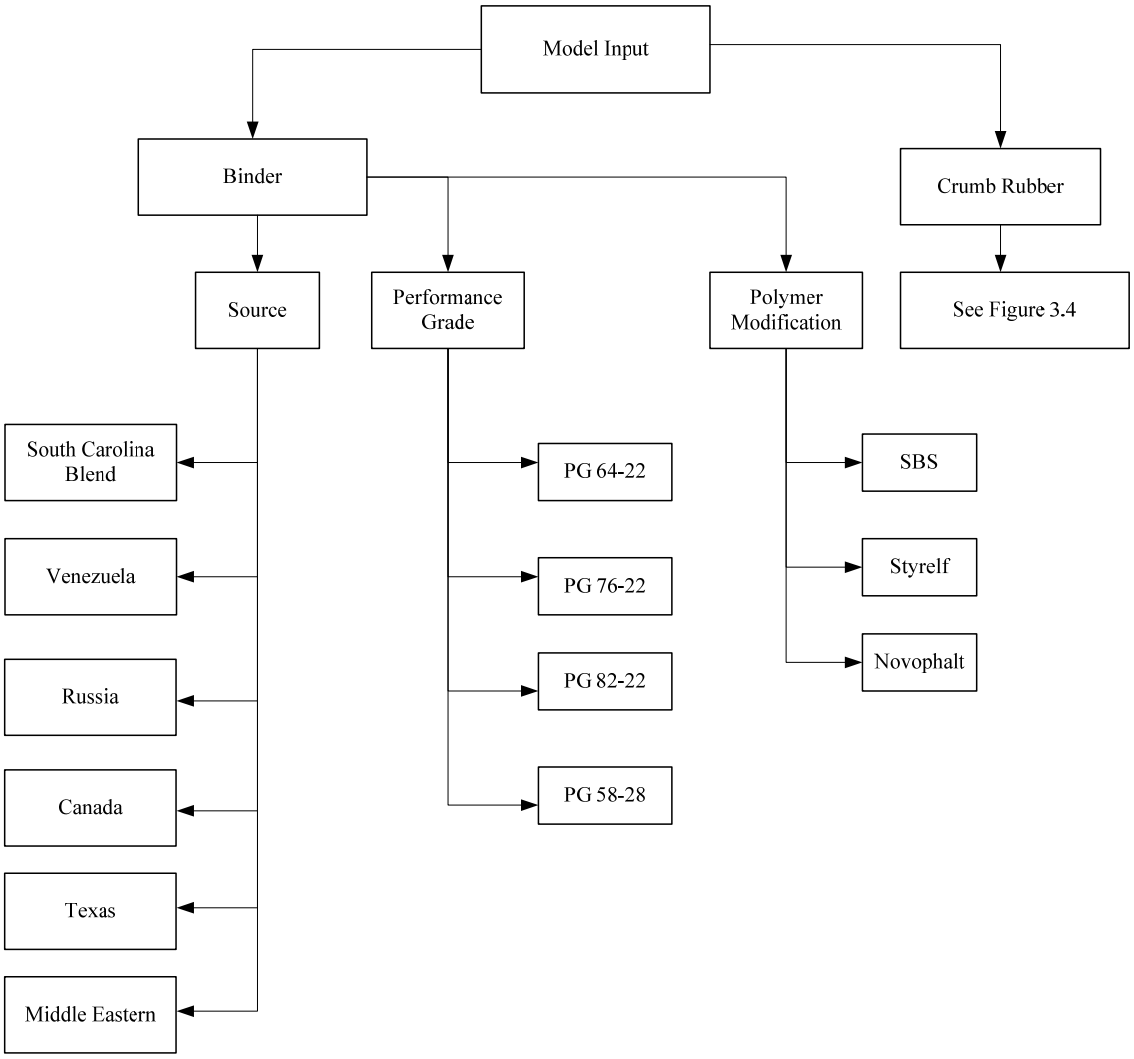

Figure 3.5: Task 3&4 - Various binder variables considered for model input

Task 5: Development of the universal model for both viscosity and G*/sinδ

Upon completion of the fifth task, a universal model relating the high temperature performance grade of the CRM binder to the asphalt viscosity was developed. This relationship permitted data regarding both the viscosity and the high temperature performance grade of the binder to be obtained using a single equation.

Task 6: Verification Study

Finally, the sixth task involved a follow-up study using previously untested materials. This provided an evaluation of the various equations which were developed over the course of the first five tasks. Specifically, the data from this task provided validation of the models for a number of previously untested binders.

The untested materials consisted of many combinations of binder sources, crumb rubber variables, crumb rubber concentrations, and temperatures. Obviously, it was not possible to test all of the combinations of these factors. Instead of trying to test all the possible combinations, a certain subset of the combinations was determined (called a fractional factorial) that allowed a generalization of the results as if all the combinations had been simulated. This generalized testing scheme is shown in Figure 3.6.

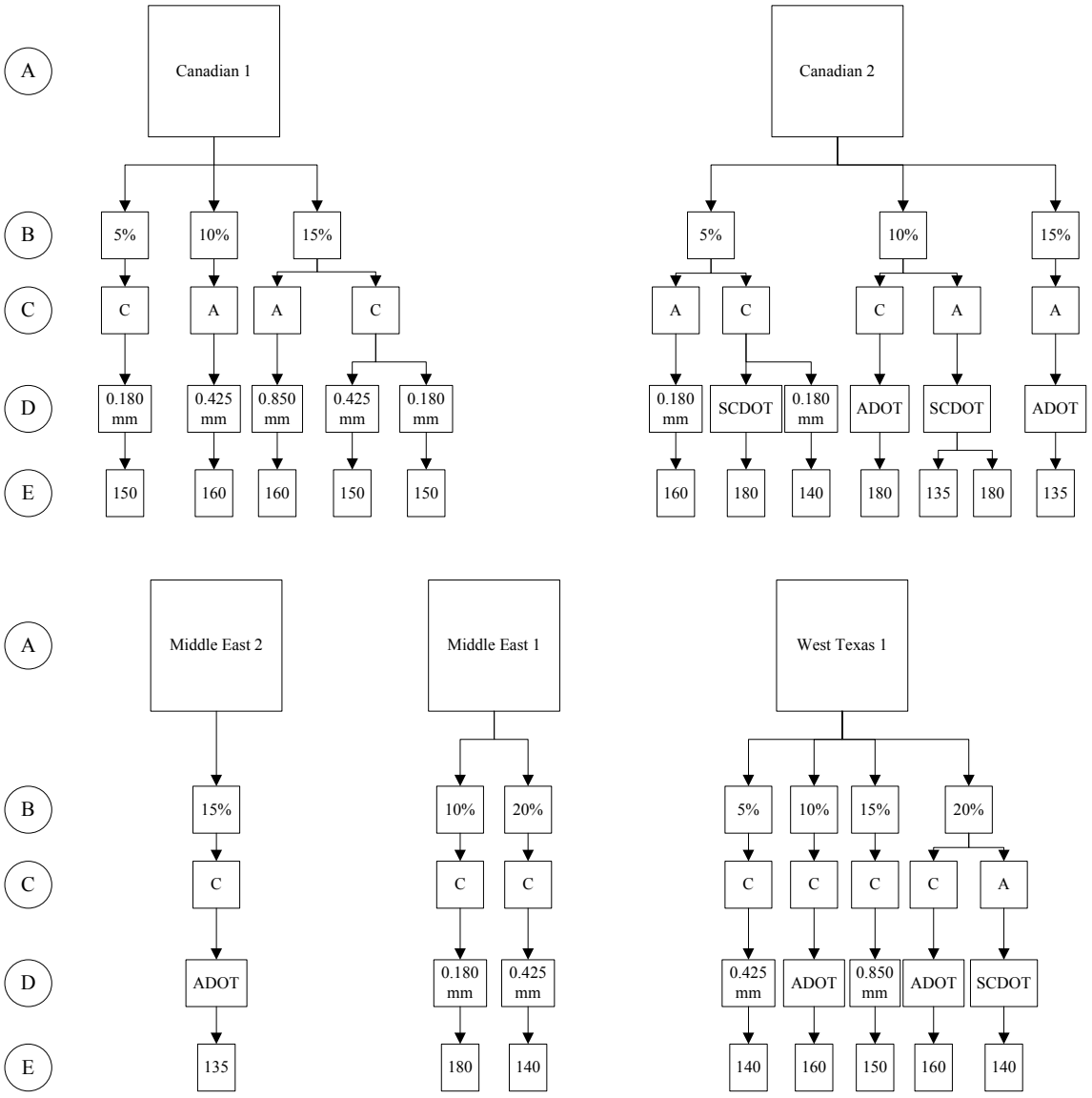

Legend

A Binder Source

B %CRM (by weight of binder)

C Grinding method (Cryogenic or Ambient)

D Gradation

E Viscosity Testing Temperature (^{o}C)

Figure 3.6: Task 6 - Verification study

An important step in the model validation was to check that the sample size of the presented data was large enough to ensure that the models were accurately estimated. The measure that was used for accuracy was the width of the interval estimated around the models and the size of the standard errors of the estimated model coefficients. The widths and sizes were based on three factors: 1) the amount of variation within the data, 2) the confidence levels of the intervals, and 3) the magnitude of the coefficients. Statistical formulas are available that relate the sample size to these three factors. These three factors were determined for this research and the formulas were used to estimate the needed sample size. Further statistical tests are also available to confirm the validity of the sample size selected.

Methods

Sample Preparation

The base binders prepared in the laboratory in this research were generally delivered to the laboratory in 5 gallon buckets from the source. The samples were then reduced to 600 g samples by heating the 5 gallon buckets of binder until the binder flowed easily. The 600 g samples were stored in sealed individual quart cans at room temperature until they were blended with the crumb rubber.

Prior to blending, the specified binder cans were placed in a 163^{o}C oven for approximately 75 minutes. The wet process was used when reacting the crumb rubber with the binders. During blending the individual can of binder was placed on top of a hot plate (maintained at approximately between 400-425^{o}C) with a sand bath. The

mechanical mixer used was a high shear 50.8 mm diameter radial flow impellor; crumb rubber concentrations of 5, 10, 15, and 20% by weight of binder were used to react the materials using a reaction time of 30 minutes while maintaining a constant binder temperature of 177°C and speed of 700 rpm. This temperature was selected as it is a common temperature used to produce CRM binders in the field in South Carolina. Upon completion of blending the crumb rubber with the binder, the can of CRM binder was sealed and allowed to cool for 24 hours at room temperature prior to testing.

Drained binders were also prepared in order to study particle and interaction effects of the crumb rubber on the binder. Separation of the binder from the crumb rubber was done by heating the CRM binder to a temperature of 163°C in an oven, the binder was then mixed thoroughly to ensure uniformity and 100 g of each binder was poured into a 76.2 mm diameter 80 mesh (0.18 mm) sieve and allowed to drain for 30 minutes in an oven maintained at 149°C. Binder recovered from this process was then subjected to the same tests as the CRM binder.

Characterization of Crumb Rubber

Cryogenic processed particles are known to exhibit a crystalline shape as a result of the fracturing occurring following the cryogenic freezing process, whereas ambient ground crumb rubber display rougher edges as a result of the tearing action typical of the ambient grinding procedure. Crumb rubber particles resulting from the two production processes can be identified by magnified imagery. Additionally SEM was utilized to

conduct the elemental analysis of the crumb rubber particles to establish the elemental compositions of the various crumb rubber sources studied.

The SEM analysis was done using a Hitachi S3500N SEM; 30x magnification was selected, as this level of magnification permitted clear identification of the grinding mechanism (ambient/cryogenic) used to reduce the scrap tire into crumb rubber. The sample was prepared by attaching some crumb rubber particles to an aluminum specimen tab with double sided carbon tape. Care was taken to ensure all the crumb rubber particles were firmly attached to the tab; the SEM was calibrated using a copper sample.

In general, truck tires exhibit a higher concentration of natural rubber than passenger car tires; however, the exact amounts of each component are proprietary as well as possibly being varied from time to time or from manufacturer to manufacturer. During the crumb rubber production process, in many cases, tires from numerous sources are collected, shredded, and distributed without particular attention being paid to the nature of each tire type. One of the points of interest for this research study was to determine the effect of these elemental and physical inequalities on the CRM binder properties.

A differential scanning calorimeter (DSC) was used to determine the presence of various rubber compounds in the crumb rubber, by determining the number of glass transition temperatures present. These corresponding temperatures were then used to verify the presence of natural and synthetic rubber. The glass transition temperature of natural rubber (NR) is approximately -70^{o}C whereas the glass transition temperature of synthetic rubber is approximately -108^{o}C. Therefore, confirming the presence of such

glass transition temperatures would permit identification of various rubber types present in the crumb rubber.

Samples were analyzed using a TA instruments Q1000 DSC, where a 7.5 mg sample was enclosed in standard aluminum DSC sample pan and entered into the DSC. The temperature was then varied from -150^{o}C to 100^{o}C at a rate of 20^{o}C/minute, using a N_2 flow rate of 50cm^3/min. The data was analyzed using Universal Analysis Software, glass transition temperatures were obtained from the inflection point of the step function.

Viscosity Testing

AASHTO T316 was used when determining the viscosity at 135^{o}C. During this procedure 8.5 grams of asphalt binder is poured into a standard Brookfield Viscometer test tube, the test tube and asphalt were then placed in temperature control device and the desired temperature selected. The appropriate spindle was selected (#21 for virgin binder), attached to the viscometer, and then submerged in the test tube to the specified depth. The sample was then allowed to heat up for 20 minutes, followed by 10 minutes of the spindle rotating at 20 RPM. Finally, three viscosity measurements are recorded at one minute intervals (American Association of State Highway Officials, 2006).

It should be noted that when CRM binder samples were used 10.5 gram samples were used instead of 8.5 grams samples, subsequently a smaller spindle size (#27) was also selected. Careful attention was placed on ensuring that the CRM binder samples were well mixed prior to pouring into the test tube.

G*/sinδ Testing

AASHTO T315 was used for the DSR testing (American Association of State Highway and Transportation Officials, 2006). The complex shear modulus and phase angle were measured using a Bohlin DSR. Following previous research, a 2 mm gap was used for testing CRM binder samples in the DSR, while a 1 mm gap was used for the virgin binder. Variations in gap were incorporated to take into account the effect of the rubber particle size present in the CRM binder. Previous research suggests that the variation in the gap size does not affect the comparison of results between the CRM binder and the unmodified binder when binders are tested in the linear viscoelastic region. It has been noticed that the 2 mm gap resulted in less variability of data when compared to the 1 mm gap for CRM binders. This lower variability was attributed to the fact that when the 2 mm gap was used there was less possibility of rubber particles coming in contact with the plates, thus adversely affecting the rheological measurements of the sample (Tayebali et al., 1990; Bahia & Davies, 1996; Bahia & Davis, 1994).

CHAPTER FOUR

STATISTICAL ANALYSIS PROCEDURES

This research project required the use of numerous statistical analysis procedures. During Tasks 1 and 2 the ANOVA and LSD procedures were used to determine the significant differences between the binder and crumb rubber property means among the various sources. Tasks 3-5 dealt with the development of nonlinear regression models for the proposed relationships between G*/sinδ, failure temperature, and viscosity, and 95% confidence intervals were used to evaluate the precision of the various models. Finally, the verification testing in Task 6 was performed by using a small subset of the many factor combinations (i.e. a fractional factorial design). Each of these procedures is introduced and expanded upon in this chapter; all relevant equations and notation are included in the discussion.

Analysis of Variance (ANOVA)

The Analysis of Variance (ANOVA) is a method for comparing the means of several populations, this method is an alternative to performing multiple *t* tests to test this hypothesis (Fisher, 1949). This method permits the hypothesis of "multiple means being equal" to be analyzed at a specified probability of Type I error (0.05 for example). The ANOVA procedure is based on the following assumptions:

1. Independence of cases: Independent random samples from their respective populations.
2. Normality: The distributions in each of the groups are normal.

3. Homogeneity of variances: $\sigma_1^2 = \sigma_2^2 = \sigma_3^2 = \sigma_4^2 = \sigma_5^2 = \sigma^2$.

The ANOVA table format is shown in Table 4.1; in this table the second column provides information regarding sums of squares associated with each source of variability. The third column provides the degrees of freedom associated with the sources of variability. In the last column the means squares are calculated and the *F* test for the equality of the *t* population means presented.

Table 4.1: Example of an ANOVA table for a completely randomized design

Source	Sum of Squares	Degrees of Freedom	Mean Square	*F* Test
Between Samples	SSB	t - 1	s^2_B = SSB/(t - 1)	s^2_B/s^2_W
Within Samples	SSW	n_T - t	s^2_W = SSB/(n_T - t)	
Totals	TSS	n_T - 1		

In an ANOVA for *t* populations, the null and alternative hypotheses have the following specific form:

H_0: $\mu_1 = \mu_2 = \mu_3 = \cdots = \mu_t$ (i.e., the *t* population means are equal)

H_a: At least one of the *t* population means differs from the rest.

The ANOVA procedure produces a tests statistic called *F* that is the ratio of the variation among the population to the variation within the population (Equation (4.1)).; if Equation 4.1 exceeds the tabulated value of *F* for $a=\alpha$, $df_1=t-1$, and $df_2=n_T-t$, then the null hypothesis is rejected.

$$F = \frac{S_b^2}{S_w^2} \qquad \text{Eq.(4.1)}$$

Fisher's Least Significant Difference (LSD)

In this research the LSD procedure was used to make specific comparisons between pairs of various CRM binder and crumb rubber properties. This procedure was also developed by R.A Fisher in 1949, and is commonly used for making pairwise comparisons among a set of *t* population means (Fisher, 1949). The Fisher LSD uses the observed difference between two sample means as a test statistic for testing the null and alternative hypothesis.

H_0: $\mu_i = \mu_j$

H_a: $\mu_i \neq \mu_j$

Research has shown that the error rate for the LSD test is controlled on an experimentwise basis at a level approximately equal to the α-level for the *F* test (Cramer & Swanson, 1973).

During this study the MEANS LSD command in the SAS program was used to perform the various LSD tests; however, Ott and Longnecker provide the following step by step procedure for performing Fisher's LSD test (Ott & Longnecker, 2001):

1. Perform an ANOVA test to test H_0: $\mu_1 = \mu_2 = \mu_3 = \cdots = \mu_t$ against the alternative hypothesis that at least on of the means differs from the rest.
2. If there is insufficient evidence to reject H_0 using F = MSB/MSW, proceed no further.
3. If H_0 is rejected, define the LSD to be the observed difference between the two sample means necessary to declare the corresponding population means different.

4. The least significant difference for comparing μ_i to μ_j (at a specified value of α), is computed using Equation (4.2):

$$LSD_{ij} = t_{\propto/2}\sqrt{s_w^2\left(\frac{1}{n_i}+\frac{1}{n_j}\right)} \qquad \text{Eq.(4.2)}$$

Where,

n_i and n_j: Sample size for population i and j, respectively

t: Critical t value for $a=\alpha/2$

s_w^2: Mean square within samples

5. Next, all pairs of sample means are compared. If $\left|\bar{y}_{i.} - \bar{y}_{j.}\right| \geq LSD_{i,j}$, it is possible to identity the corresponding population means μ_i and μ_j different.
6. It is necessary to note that the probability of a Type I error for each pairwise comparison of population means is fixed at a specified value of α.

Regression Analysis

The method of nonlinear least squares was used to estimate the parameters in the various CRM binder property equations, this is because they were nonlinear functions of the parameters. The reason for using a nonlinear model is that often when attempting to model real world phenomena, simple linear models are not accurate enough. According to Jennrich, a nonlinear model is by definition a nonlinear family of functions. The functions themselves may be linear or nonlinear; in simpler terms a nonlinear model is one that is nonlinear in its parameters (Jennrich, 1995)

Jennrich maintains that the world is full of nonlinear models; this is because almost all mathematical models in science are defined by differential equations, and differential equations almost inevitably give rise to nonlinear models. Therefore, the basic task in nonlinear regression involves fitting nonlinear models to data (Jennrich, 1995).

Generally, the nonlinear regression model may be written in the form given in Equation (4.3).

$$y = f(x, \theta) + e \qquad \text{Eq.(4.3)}$$

If we allow $(x_1,y_1),\ldots(x_n,y_n)$ to be a set of n observations of the dependent variable y and the vector independent variables x in the nonlinear regression model (Equation (4.4)). This leads to the data model:

$$y_i = f(x_i, \theta) + e_i \quad i = 1, \ldots, n \qquad \text{Eq.(4.4)}$$

A parameter vector $\hat{\theta}$ in Θ is called a least squares estimate of θ if $\theta = \hat{\theta}$ minimizes the least squares criterion (Equation (4.5)).

$$Q(\theta) = \sum_{i=1}^{n} \big(y_i - f(x_i, \theta)\big)^2 \qquad \text{Eq.(4.5)}$$

over all θ in Θ. A least squares estimate $\hat{\theta}$ need not exist and if it does, one seldom has simple conditions for uniqueness like those in linear regression (Jennrich, 1995).

The observation space representation for the issue of minimizing Equation (4.5) is given in Figure 4.1. In this case the objective is to select $\hat{\theta}$ which minimizes the sum of

squares of the vertical deviations from the fitted curve (or surface) to the observed data points (x_i, y_i).

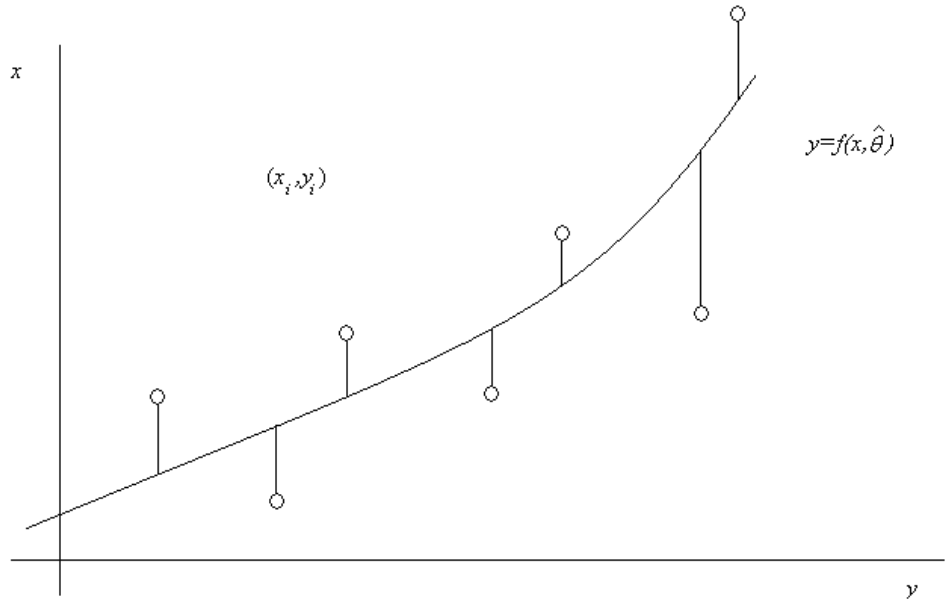

Figure 4.1: Observation space picture of nonlinear least squares fitting (Jennrich, 1995)

By writing the data model Equation (4.5) in vector form, it is also possible to develop the vector space representation (Equation (4.6)).

$$\mathbf{y} = \mathbf{f}(\boldsymbol{\theta}) + \mathbf{e} \qquad \text{Eq.(4.6)}$$

Where **y,f(θ)**, and **e** are vectors in $\Re^n$ (Euclidean *n*-space of column vectors) whose i-th components are y_i, $f_i(\boldsymbol{\theta})=f(\mathbf{x}_i,\boldsymbol{\theta})$and e_i respectively. Using this notation the least squares criterion is given by Equation (4.7).

$$Q(\boldsymbol{\theta}) = \|\mathbf{y} - \mathbf{f}(\boldsymbol{\theta})\|^2, \qquad \boldsymbol{\theta} \in \Theta \qquad \text{Eq.(4.7)}$$

The issue becomes determining a in Θ which allows the vector f($\hat{\theta}$)to be as close as possible to the vector y of observed responses. Shown in Figure 4.2 is a graphical representation of the variable space representation of the least squares fitting problem. The least squares fit is the point on the surface which is as close as possible to *y*.

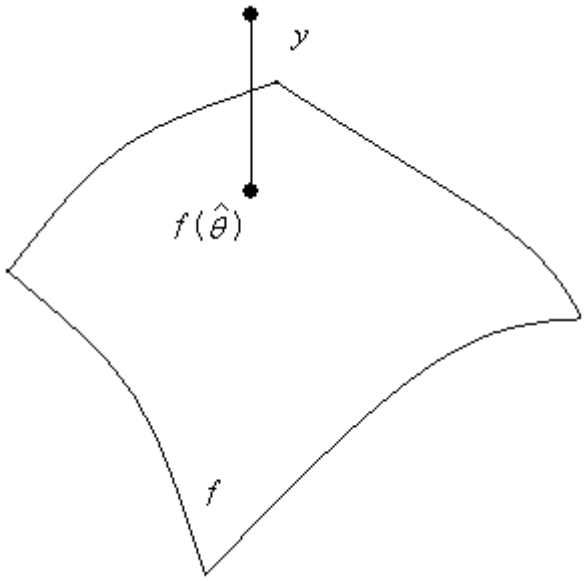

Figure 4.2: Variable space picture of the nonlinear least squares fitting problem (Jennrich, 1995)

Using the nonlinear least squares concept, the regression was determined using the program PROC NLIN in the SAS system. Appropriate starting parameters were selected for the model being proposed, and the method of nonlinear least square was used to estimate of the model parameters.

The parameter estimates are the converged values of the parameters form the iteration procedure. The standard error estimates and approximate 95% confidence intervals are based on asymptotic arguments. The standard errors are computed by

applying formulas from linear regression to a linearized form of the nonlinear model (Jennrich, 1995).

This procedure culminates upon receiving the "convergence criteria met" statement. This indicates that the parameters have been adequately estimated. Typically, the estimation of parameters is specific to each CRM binder property model; where, the parameters are specific to a given set of criteria (e.g. grinding procedure).

95% Confidence Interval

The confidence interval is an interval estimate of a model parameter of interest. Confidence intervals provide two numbers (the lower confidence limit (LCL) and the larger the upper confidence limit (UCL)) that are likely to contain the true parameter value. The 95% refers to the confidence coefficient, this is indicative of the probability that the interval will actually capture the parameter being estimated (Rieck, 2005).

An example of confidence interval for a population mean is as follows. Assuming the standard deviation is known and the sample is obtained from a normal distribution, then Equation (4.8) may be used to determine the 95% confidence interval.

$$\left(\bar{Y} - 1.96\frac{\sigma}{\sqrt{n}}, \bar{Y} + 1.96\frac{\sigma}{\sqrt{n}}\right) \qquad \text{Eq.(4.8)}$$

Where,

$\bar{Y}$: Sample mean

σ: Standard deviation

n: Sample size

Factors affecting the confidence interval include the value of the standard deviation, the value of the confidence coefficient, and the value of the sample size. As seen in Equation (4.8), the confidence interval shrinks as the sample size increases and the standard deviation decreases. The confidence coefficient is also important as it determines the value of the constant in Equation (4.8). This value will tend to increase as the confidence coefficient decreases, however, this results in a larger and therefore less precise confidence interval (Figure 4.3).

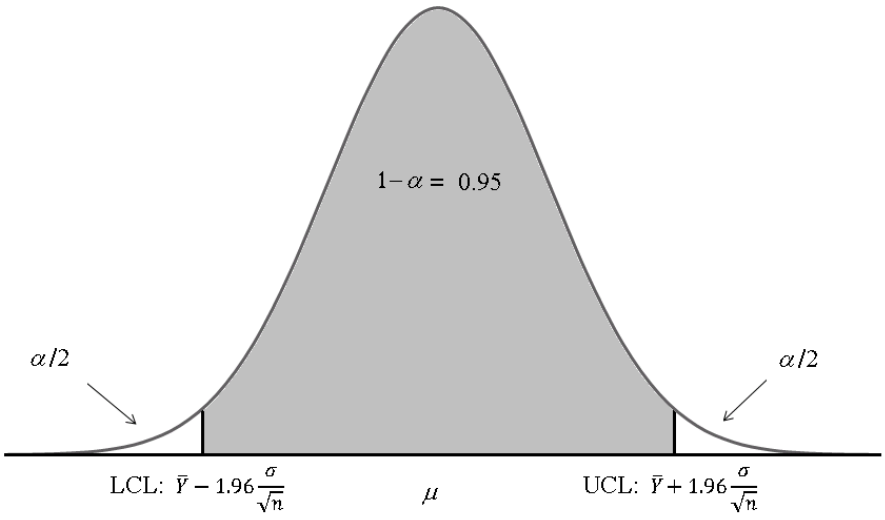

Figure 4.3: LCL and UCL for 95% Confidence Interval

Fractional Factorial Design

The fractional factorial design method was employed in conducting the verification study. This method permits the testing of a certain subset of CRM binder combinations to evaluate the factors, rather than trying to test all the possible combinations. It allows a generalization of the results as if all the combinations had been

simulated. Equation (4.9) provides the notation usually used for expressing a fractional factorial designs:

$$I^{n-p} \qquad \text{Eq.(4.9)}$$

Where,

I: number of levels of each factor investigated

n: number of factors

p: number of design generators

The fraction of the full factorial design is given by $1/(I^{p})$, and the number of aliases by is given by $(I^{p}-1)$. The number of aliases refers to the number of effects which are confounded with each other (Toler, 2006).

Usually in fractional factorial designs there are two levels of each factor investigated, a "high" value and a "low" value. Therefore for a half a replicate (1/2) one design generator is necessary, and the number of aliases for each effect is $(2^{1}-1) = 1$.

The standard order approach is used to determine treatment combinations to be used in the experiment. If a study using three factors A,B, and C is considered, then the coefficients for factor A are determined by alternating – and + signs. The coefficients of factor B are determined by alternating pairs of – and + signs. The coefficients of factor C are determined by alternating four – and four + signs. The coefficients of the remaining factors are determined using an alias or with either one of the design generators. The + and – coefficients for all *n* factors must be determined in order to decide which treatment combinations should be included in the experiment (Table 4.2) (Toler, 2006).

Table 4.2: Standard order approach for fractional factorial design

A	B	C	D=ABC	Treatment Combination
-	-	-	-	(1)
+	-	-	+	ad
-	+	-	+	bd
+	+	-	-	ab
-	-	+	+	cd
+	-	+	-	ac
-	+	+	-	bc
+	+	+	+	abcd

CHAPTER FIVE

MODEL DEVELOPMENT

Models were developed for determining SHRP test properties of various CRM binders. Emphasis was placed on the determination of CRM binder properties given only the virgin binder properties obtained using standard SHRP binder tests and crumb rubber content and type. This chapter describes the development of models for determining:

- CRM binder viscosity using virgin binder viscosity data;
- CRM binder's G*/sinδ and failure temperature data using virgin binder's G*/sinδ data; and
- CRM binder's G*/sinδ and failure temperature data using virgin binder's viscosity data.

Viscosity Model

The model was developed in two parts; first, the effects of the addition of crumb rubber to the virgin binders were studied. Once a working model was developed for the addition of the crumb rubber to the virgin binders, the model for temperature variation was developed. Such a division assumes that once the binder viscosity is set at 135^{o}C, binder viscosities will vary with temperatures greater than 135^{o}C in the same fashion. Therefore, the starting point for the model is described by Equation (5.1), given by:

$$\eta_{x,t} = \eta_{0,135}(Rubber\ Factor)(Temperature\ Factor) \qquad \text{Eq.(5.1)}$$

Where $\eta_{x,t}$ is the viscosity with rubber content x at temperature t, and $\eta_{0,135}$ is the neat binder viscosity at 135°C. The Rubber Factor and Temperature Factor components of the model are discussed in the following sections.

Rubber Factor

The rubber factor was considered first because preliminary experimental results indicated that when crumb rubber was added to the binder, the asphalt viscosity consistently increased. However, it was also seen that this increase was dependent on the virgin binder viscosity; therefore, it was necessary to normalize the data in order to analyze the extent of the viscosity increase. When analyzing viscosity changes due to the addition of crumb rubber, the virgin binder was held as the reference point, all subsequent CRM binder viscosities were then divided by the virgin viscosity. Ultimately, a unitless ratio of crumb rubber concentration to virgin binder viscosity relationship was found.

When these ratios were plotted against their corresponding crumb rubber percentages, it became clear that the nature of the viscosity increase was consistent for all CRM modified binders. It was seen that viscosity ratio change with respect to crumb rubber percent followed an exponential trend. As all the viscosity ratios started at 0% crumb rubber the starting point was always 1; therefore, the nature of the change could be quantified by a single entity. This factor was referred to as the rubber coefficient for viscosity (R_{cv}). Figure 5.1 provides a visual reference for identifying the rubber coefficient for viscosity; the R_{cv} was identified as a suitable parameter for describing the

rubberized asphalt interaction as it provides a numerical value relating the viscosity increase in the CRM binder to the specific crumb rubber source.

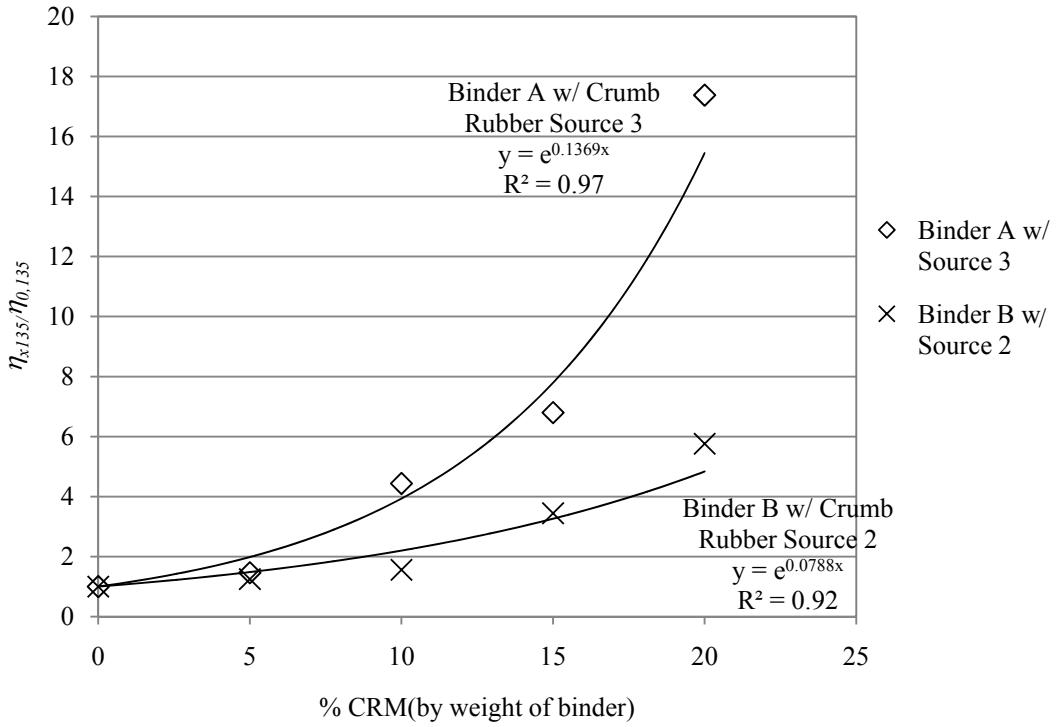

Figure 5.1: Method of R_{cv} determination

Therefore, the Rubber Factor in the model has the form given in Equation (5.2):

$$\eta_x = e^{R_{cv}x} \qquad \text{Eq.(5.2)}$$

Where, R_{cv} is the rubber coefficient for viscosity and x is the rubber content.

Temperature Factor

The effect of temperature on binders was also studied; here too the asphalt binder viscosity was normalized. However, in this case the viscosity at 135°C was used as the

reference. A temperature of 135°C is commonly used by many testing agencies as the reference for Brookfield viscometer viscosity measurements.

The Arrhenius equation was used as the starting point of establishing the temperature factor component of the model. The Arrhenius equation is used for modeling viscous behavior of thermo-rheologically simple materials; thermo-rheologically simple materials are those materials whose chemical structure is stable at the testing temperatures (135-210°C). The form of the Arrhenius equation is given in Equation (5.3):

$$\eta_t = Ae^{\frac{E_a}{Rt}} \quad \text{Eq.(5.3)}$$

Where,

η_t: Viscosity of the asphalt binder at temperature t

A: Constant

E_a: Activation energy

R: Universal gas constant (8.314 J.mol^{-1}.K^{-1}).

The model was normalized by allowing the viscosity to be predicted at a desired temperature (Equation (5.4)):

$$\eta_t = Ae^{\beta t} \quad \text{Eq.(5.4)}$$

Where,

A and β: Constants

t: Temperature in degrees Celsius

The Combined Model

The rubber and temperature factors were combined to produce Equation (5.5):

$$\eta_{x,t} = \eta_{0,135}(e^{R_{cv}x})(Ae^{\beta t}) \quad \text{Eq.(5.5)}$$

Since the values for $\eta_{0,135}$ and R_{cv} are known constants which have been previously derived, only the values for parameters A and β need to be estimated. The method of nonlinear least squares was used to estimate the parameters A and β. All calculations were performed using the Statistical Analysis System (SAS) procedure, whereby a nonlinear regression model was fitted to the data.

Failure Temperature Model

The model was developed in two parts; first, the effects of the addition of crumb rubber to the virgin binder were studied. Once a working model was developed for the addition of the crumb rubber to the virgin binder, the model for temperature variation was developed. Equation (5.6) illustrates the starting point for the model:

$$\left(\frac{G*}{sin\delta}\right)_{x,t} = \left(\frac{G*}{sin\delta}\right)_{0,64} (Rubber\ Factor)(Temperature\ Factor) \quad \text{Eq.(5.6)}$$

Where,

$G^*/\sin\delta_{x,t}$: Complex shear modulus divided by the sine of the phase angle with rubber content x at temperature t

$G^*/\sin\delta_{0,64}$: Virgin binder $G^*/\sin\delta$ value at 64°C

The Rubber Factor and Temperature Factor components of the model are discussed next.

Rubber Factor

The rubber coefficient for G*/sinδ (R_{cg}) was introduced as a means of quantifying the unique effects of crumb rubber on the specific binder; it is defined as the exponential coefficient by which the crumb rubber concentration is multiplied when values of CRM binder are normalized with the neat binder of the same source. It can be seen in Figure 5.2 that the normalized values follow an exponential trend with increasing crumb rubber concentrations.

This procedure yielded high R squared values when used to describe the change in behavior of the binder with respect to crumb rubber concentration. The R_{cg} values were calculated for all CRM-Binder combinations, consistent with Figure 5.2, the relationship between crumb rubber concentration and G*/sinδ was seen to be adequately presented by Equation (5.7).

$$\frac{\left(\frac{G*}{sin\delta}\right)_{x,64}}{\left(\frac{G*}{sin\delta}\right)_{0,64}} = e^{R_{cg}x} \qquad \text{Eq.(5.7)}$$

Where $(G^*/sin\delta)_{x,64}/(G^*/sin\delta)_{0,64}$ is the ratio of G*/sinδ values at 64°C, between 0 and x% crumb rubber by weight of binder, R_{cg} is the rubber coefficient for G*/sinδ and x is the crumb rubber concentration by weight of binder. Equation (5.7) illustrates the exponential growth witnessed by CRM binders with regards to G*/sinδ values. Therefore, at a temperature of 64°C the rutting susceptibility of a binder with varying crumb rubber concentrations may be predicted using Equation (5.7).

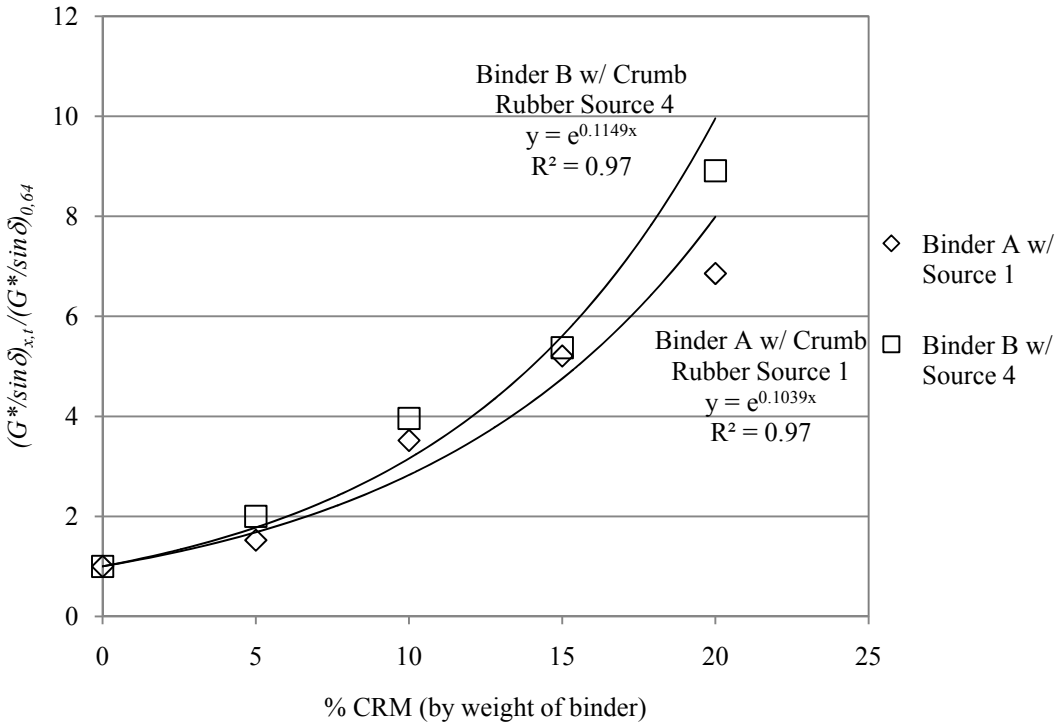

Figure 5.2: Method of R_{cg} determination

Temperature Factor

In order to vary the G*/sinδ behavior with respect to temperature, an inverse log relationship was seen to have the best correlation when the data was analyzed with the Statistical Analysis System (SAS). In this case, the binder G*/sinδ value was normalized (i.e., the G*/sinδ value at 64°C was used as the reference). The Arrhenius equation, shown below in Equation 5.8, was used as the starting point of the temperature factor component of the model.

$$\left(\frac{G*}{sin\delta}\right)_t = Ae^{\frac{E_a}{Rt}} \qquad \text{Eq.(5.8)}$$

Where,

$(G^*/\sin\delta)_t$: complex shear modulus divided by sine of phase angle given at the desired temperature *t* (> 64°C)

t: Temperature in degrees K

A: Constant, E_a is the activation energy

R: Universal gas constant (8.314 J.mol-1.K-1).

As shown in Equation (5.9), the model was normalized by allowing the G*/sinδ value to be predicted at a desired temperature. The resulting equation is:

$$\left(\frac{G*}{sin\delta}\right)_t = Ke^{\phi t} \qquad \text{Eq.(5.9)}$$

Where,

K and ϕ: Constants

t: Temperature in degrees Celsius

The Combined Model

The rubber and temperature components were combined to produce Equation (5.10):

$$\left(\frac{G*}{sin\delta}\right)_{x,t} = \left(\frac{G*}{sin\delta}\right)_{0,64} (e^{R_{cg}x})(Ke^{\phi t}) \qquad \text{Eq.(5.10)}$$

Where,

$G^*/\sin\delta_{x,t}$: Complex shear modulus divided by the phase angle at the desired crumb rubber concentration and temperature

$G^*/\sin\delta_{0,64}$: Complex shear modulus divided by the phase angle at a crumb rubber concentration of zero at 64°C

R_{cg}: Rubber coefficient for G*/sinδ

x: Concentration of crumb rubber by weight of binder

K and ϕ: Constants

t: Temperature in ^{o}C.

The method of nonlinear least squares was used to estimate the parameters K and ϕ. All calculations were performed using the nonlinear modeling procedure in SAS.

High End Failure Temperature Model

Failure temperature of a binder is defined as the temperature at which the G*/sinδ value of the unaged binder falls below 1000 Pa (Asphalt Institute, 2003). Therefore, by rearranging the preceding relationship and solving for temperature when the G*/sinδ is set to 1000 it is possible to predict the high temperature failure temperature of the binder, doing so yields Equation (5.11):

$$\frac{\left(\frac{G*}{sin\delta}\right)_{x,t}}{\left(\frac{G*}{sin\delta}\right)_{0,64}\left(e^{R_{cg}x}\right)} = Ke^{\phi t} \qquad \text{Eq.(5.11)}$$

Equation (5.12) is produced by taking the natural logarithm of both sides,

$$ln\left[\frac{\left(\frac{G*}{sin\delta}\right)_{x,t}}{\left(\frac{G*}{sin\delta}\right)_{0,64}\left(e^{R_{cg}x}\right)}\right] = ln(K) + ln\left(e^{\phi t}\right) \qquad \text{Eq.(5.12)}$$

solving for T yields Equation (5.13),

$$\frac{ln\left[\frac{\left(\frac{G*}{sin\delta}\right)_{x,t}}{\left(\frac{G*}{sin\delta}\right)_{0,64}(e^{R_{cg}x})}\right] - ln(K)}{\phi} = t \qquad \text{Eq.(5.13)}$$

Therefore, as shown in Equation (5.14), the failure temperature may be determined by substituting in $(G^*/\sin\delta)_{x,t}$ = 1000 Pa.

$$ft = \frac{ln\left[\frac{1000}{\left(\frac{G*}{sin\delta}\right)_{0,64}(e^{R_{cg}x})}\right] - ln(K)}{\phi} \qquad \text{Eq.(5.14)}$$

Where,

ft: Failure temperature (high end)

$G^*/\sin\delta_{0,64}$: Complex shear modulus divided by the phase angle at a crumb rubber concentration of zero at 64°C

R_{cg}: Rubber coefficient for $G^*/\sin\delta$

x: Concentration of crumb rubber by weight of binder

Universal model

The experimental data was processed using the Statistical Analysis System, specifically the nonlinear regression function was used in this software package to find the optimum empirical relationship between $G^*/\sin\delta$ and the unmodified viscosity while varying temperature and crumb rubber concentration. This procedure resulted in the exponential described by Equation (5.15):

$$\frac{G*}{sin\delta} = \eta_{135,0} a e^{(bx+c(t))} \quad \text{Eq.(5.15)}$$

Where,

$G^*/sin\delta$:	Complex shear modulus divided by sine of phase angle (kPa)
$\eta_{135,0}$:	Unmodified binder viscosity at 135°C determined by Brookfield viscometer (Pa-s)
x:	Percent crumb rubber added by weight of binder (% crumb rubber)
t:	User defined temperature (64 – 88 °C)
a, b, and c:	Coefficients

The differences in CRM binder of differing origin (ambient versus cryogenic) is well established (Stroup-Gardiner et al., 1993), similarly the differences in rutting susceptibility between CRM binder and unmodified binder are also known (Xiao et al., 2007). Therefore, to produce the most accurate results, the binders were classified by modification procedure (virgin, ambient crumb rubber, or cryogenic crumb rubber) and coefficients calculated accordingly.

Failure Temperature Model

To solve for failure temperature, it was necessary to rearrange Equation (5.13), solving for t using a G*/sinδ value of 1 kPa would provide the necessary input to solve for failure temperature. Therefore, taking Equation (5.15) and dividing by ($\eta_{135,0}$ a) yields Equation (5.16),

$$\frac{\frac{G*}{sin\delta}}{(\eta_{135,0}a)} = e^{(bx+c(t))} \quad \text{Eq.(5.16)}$$

Taking the natural logarithm of both sides produced Equation (5.17),

$$ln\left[\frac{\frac{G*}{sin\delta}}{(\eta_{135,0}a)}\right] = bx + c(t) \quad \text{Eq.(5.17)}$$

If Equation (5.17) is then solved as a function of *t*, Equation (5.18) is produced,

$$t = \frac{1}{c}\left\{ln\left[\frac{\frac{G*}{sin\delta}}{(\eta_{135,0}a)}\right] - bx\right\} \quad \text{Eq.(5.18)}$$

Finally, *t* is defined as the failure temperature (*ft*) when G*/sinδ is less than 1 kPa, thus producing Equation (5.19),

$$ft = \frac{1}{c}\left\{ln\left[\frac{1}{(\eta_{135,0}a)}\right] - bx\right\} \quad \text{Eq.(5.19)}$$

Crumb Rubber Concentration Model

Rearranging Equation (5.13) for crumb rubber concentration (*x*), yields Equation (5.20)

$$x = \frac{1}{b}\left\{ln\left[\left(\frac{G*}{sin\delta}\right)\frac{1}{(\eta_{135,0}a)}\right] - ct\right\} \quad \text{Eq.(5.20)}$$

Similarly, the required amount of crumb rubber for a desired failure temperature may be obtained by setting the G*/sinδ value to 1 kPa as shown in Equation (5.21),

$$x = \frac{1}{b}\left\{ln\left[\frac{1}{(\eta_{135,0}a)}\right] - c(ft)\right\} \quad \text{Eq.(5.21)}$$

CHAPTER SIX

EXPERIMENTAL RESULTS AND DISCUSSION

In this chapter the results of the tests performed in Tasks 1-6 are presented and discussed. The first section of the chapter deals specifically with the crumb rubber testing outlined in Task 1. The next section presents the experimental data obtained from the binder testing of the various CRM binders outlined Task 2. The remainder of the chapter is dedicated to the presenting and discussing the various model results and verification outlined in Tasks 3-6.

Task 1: Characterization of Crumb Rubber Properties

SEM Characterization of Crumb Rubber

As seen in the SEM images given in Figure 6.1, the effects of processing procedure on crumb rubber surface characteristics were confirmed, two of the crumb rubber sources (Sources 1 and 2) exhibited smooth fractured edges consistent with cryogenic grinding. The remaining samples (Sources 3 and 4) exhibited a rougher morphology typical of ambient ground crumb rubber. The SEM was also utilized to determine the elemental composition of the crumb rubber particles (Figure 6.2).

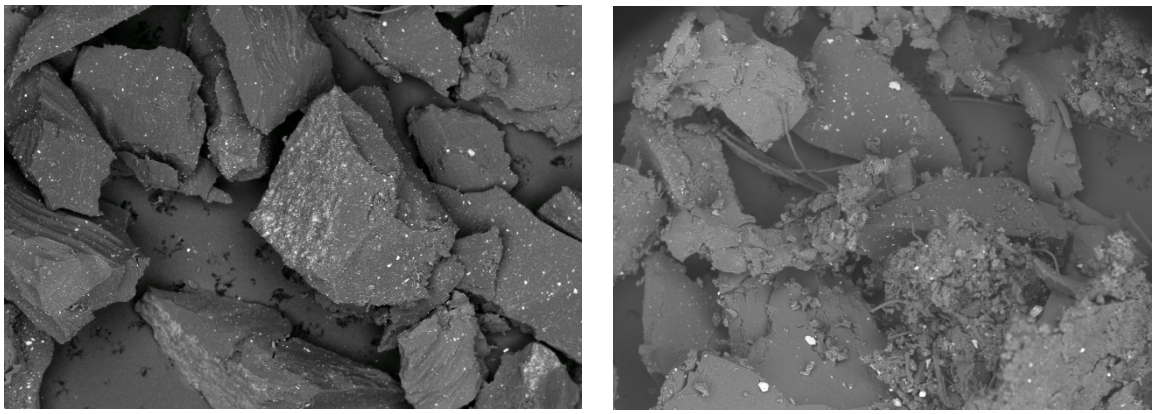

(a) **(b)**

Figure 6.1: SEM micrographs of (a) cryogenically and (b) ambient Ground crumb rubber at 30x magnification

Elemental composition was seen to vary slightly from source to source, however of the major constituents of the crumb rubber, the only element to vary significantly was the oxygen in Source 4 crumb rubber. This lower oxygen content may be indicative of a significant presence of truck tire in this source of crumb rubber (Ucar et al., 2005). Results indicate that the amounts of carbon were similar regardless of the grinding procedure; however, oxygen levels in the cryogenically ground particles were found to be statistically greater than those in the ambient ground particles (Figure 6.2).

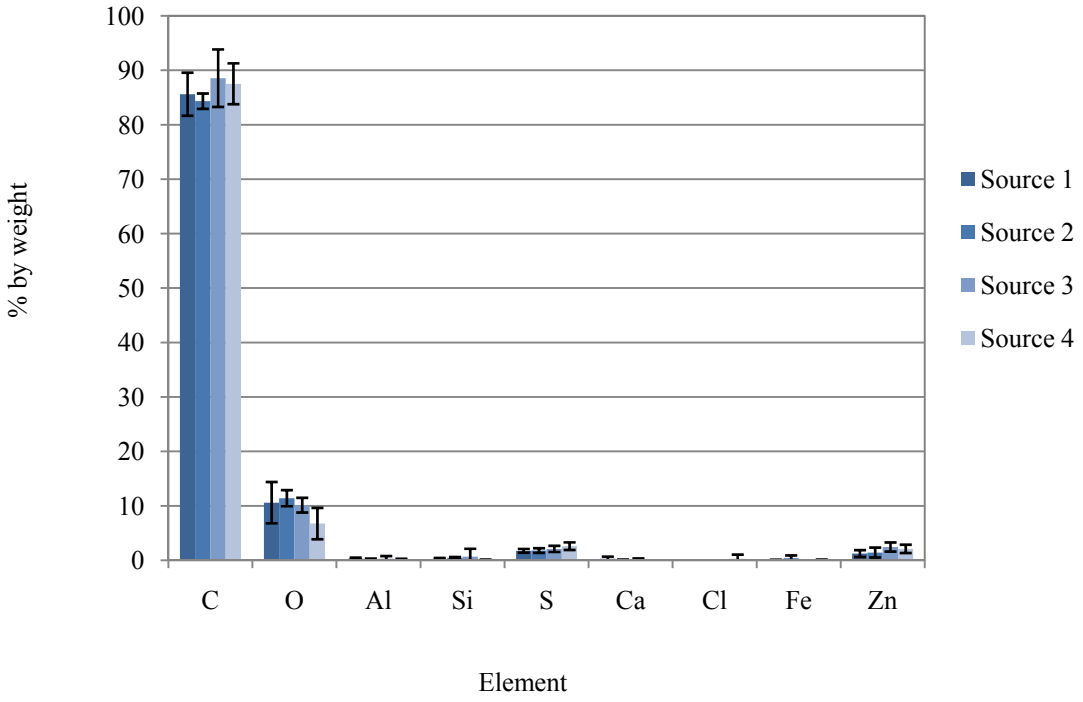

Figure 6.2: Elemental composition by weight

Glass Transition Temperature (T_g)

Analysis of the glass transition temperatures was conducted. Generally, crumb rubber glass transition temperatures were found to be quite similar with the exception of Source 4. Major differences found in the DSC profiles of the various crumb rubber types involved the presence of more than one glass transition temperature for some crumb rubber types. Multiple glass transition temperatures are indicative of the presence of more rubber types within the crumb rubber. The glass transition temperatures for natural rubber (NR) were generally lower for cryogenic rubbers than for ambient ground rubber sources.

Findings from the DSC tests were consistent with the SEM tests, crumb rubber Sources 3 and 4 exhibited no visible T_g in the Synthetic Rubber (SR) range thus indicating the presence of a significant concentration of truck tire rubber. As shown in Figure 6.3, crumb rubber Sources 1 and 2 exhibited T_gs at both the natural rubber (NR) and the synthetic rubber (SR) ranges thus illustrating significant presence of both types of rubber. Source 3 crumb rubber was seen to exhibit some characteristics of truck and passenger tire rubbers.

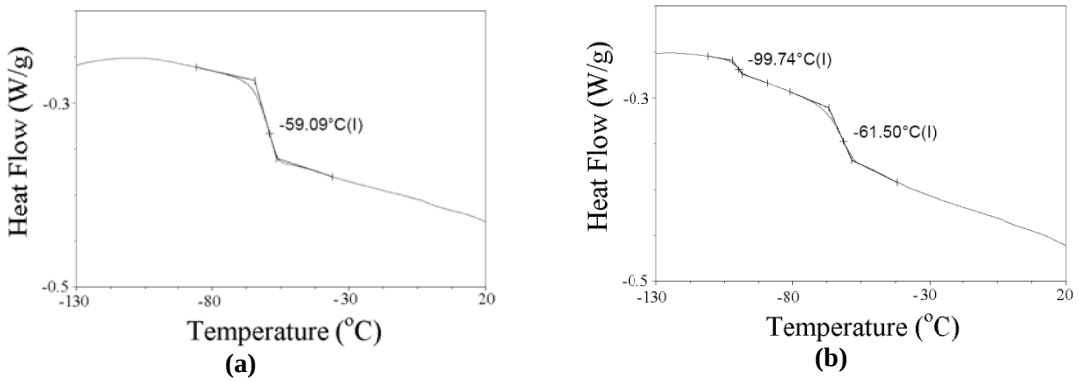

Figure 6.3: DSC Profiles of a) Source 4 crumb rubber and b) Source 1 crumb rubber

Figure 6.3 clearly demonstrates the differences in the steps present in the DSC profiles for the different crumb rubber sources. For example, this figure shows that Source 1 exhibited two clear steps in the profile consistent with the glass transition temperatures of natural and synthetic rubber. However, only one step was apparent in the DSC profile of Source 4 crumb rubber, this indicates a lack of material present at the SR glass transition zone. Source 2 crumb rubber illustrated a step similar to the one shown for Source 1, while Source 3 demonstrated two steps similar to the ones present in Source 4.

Task 2: Effect of crumb rubber on binder properties

Viscosity

Previous research results have indicated that binder modified by ambient ground crumb rubber will exhibit greater viscosities than binder modified by cryogenically ground crumb rubber (Stroup-Gardiner et al., 1993). In addition, literature also states that greater quantities of natural rubber will also increase the viscosity; therefore, it might be assumed that Source 4 crumb rubber would exhibit the greatest viscosities as crumb rubber tests indicated a substantial presence of natural rubber within Source 4. This was generally the case as binder modified with Source 4 crumb rubber yielded the highest viscosities for three of the four concentrations studied. Similarly the ambient ground crumb rubber was seen to consistently provide the higher CRM binder viscosities.

Figure 6.4 shows the experimental values of the viscosities determined by Brookfield viscometer at 135^{o}C. Both binders clearly exhibit a viscosity increase with increasing crumb rubber concentrations; however the extent to which these are quantified depends on the binder being modified and the properties of the crumb rubber used to make modifications.

At a concentration of 5% crumb rubber by weight of binder, the results were generally quite similar. However, as the crumb rubber increased, the differences in the crumb rubber started to manifest themselves. The CRM binders at 20% provided the greatest contrasts between the binders; however, even then the results were not consistent with Source 3 exhibiting the highest viscosity for Binder B while Source 4 had the highest viscosity for Binder A.

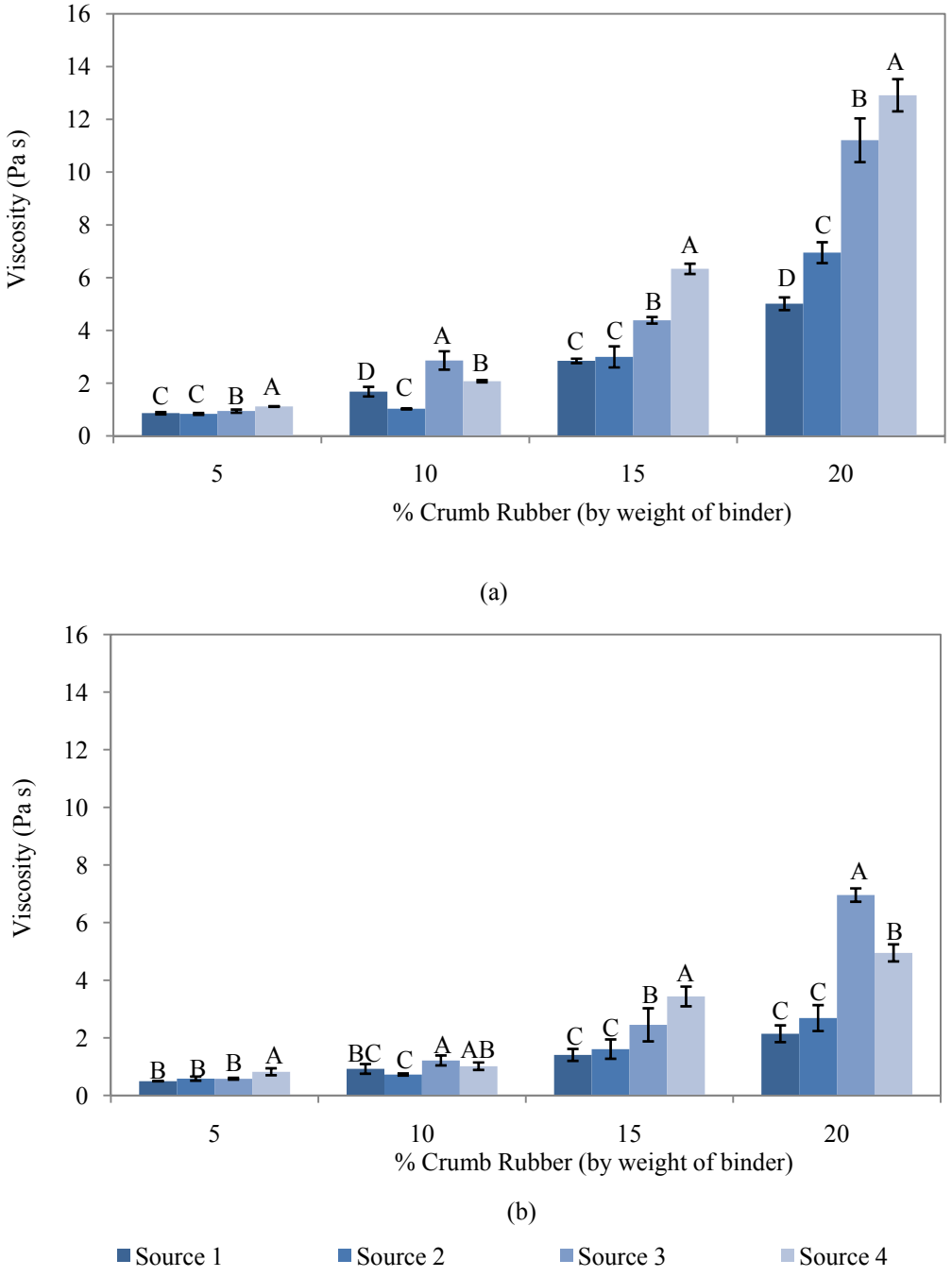

Figure 6.4: Viscosity data for (a) Binder A and (b) Binder B with crumb rubber sources 1-4(Treatments containing at least one common letter within a single CRM size produced statistically similar responses)

When examining the binder viscosities using grinding procedure as a blocking factor, the importance of grinding procedure was confirmed for determination of viscous properties of the CRM binder. Binder source, in this limited study, played a key role in dictating the viscous properties of the CRM binder; when binder source was used as a blocking factor, statistical differences were noted for every crumb rubber concentration.

When the crumb rubber concentration was used as a blocking factor, the relative effects of the various crumb rubber sources could be analyzed. From Figure 6.4, it can be seen that Source 4 crumb rubber consistently exhibited higher viscosities regardless of the binder source. When the grinding procedures were compared, the ambient ground crumb rubber samples yielded statistically significant higher viscosities regardless of the crumb rubber concentration. This suggests that the morphology of the crumb rubber plays an important role in the viscous performance of the binder, as the smooth crystalline particles generated by the cryogenic procedure yielded less viscous binder than their rougher ambient counterpart. It was concluded that the base binder plays an influential role in determining the viscosity of the CRM binder, when the binder source was used as a blocking factor, Binder A consistently had a statistically higher viscosity than Binder B.

Particle and Interaction Effects on Viscosity (PEV & IEV)

Particle Effect and Interaction Effect were determined for viscosity. Doing so permitted the analysis of interaction and particle effects on binder properties. PEV and IEV identified as the contribution to the binder viscosity due to the interaction between crumb rubber and the binder (IEV) and as the effect of the crumb rubber particles as inert

filler in the binder (PEV). Precise identification of the contribution of each was necessary to determine the cause of the change in properties of the CRM binder (Equations (6.1) and (6.2)).

$$IE = \frac{Drained - Base}{Base} \quad \text{Eq. (6.1)}$$

$$PE = \frac{CRM - Drained}{Base} \quad \text{Eq. (6.2)}$$

Where,

IE: Interaction effect

PE: Particle effect

Drained: Drained binder property

Base: Virgin binder property

CRM: CRM binder property

Results indicated that at a crumb rubber concentration of 10%, the interaction effect for viscosity was statistically consistent regardless of crumb rubber source; this indicates that at the 10% level the CRM binder effects due to interaction between particle and binder were independent of the source. Results also indicated that at the 10% level very small interactions occur regardless of crumb rubber, binder source, or grinding procedure when viscosity results are considered.

Figure 6.5 illustrates the differences in IE and PE for the two binder Sources (A and B) when modified with crumb rubbers from four different sources. Clearly, the IE

increases significantly as the amount of crumb rubber is increased, thereby suggesting that any reactions occurring between the crumb rubber and binder are dependent on the amount of crumb rubber used. The base binder used also appears to play a major role on the development of the IE as the interactions were noted to be consistently higher for Binder A than Binder B.

As shown in Figure 6.5, the PE clearly increases as the crumb rubber concentration increases, thus suggesting that the effect of the particle in the binder matrix is magnified as the number of particles increases. At 10% crumb rubber, there appears to be some variation between binder and crumb rubber sources. However, these differences are more apparent when the 20% crumb rubber concentration is studied. At 20% rate, the ambient ground crumb rubber sources yielded the highest PEs, furthermore the base Binder A also tended to exhibit higher PEs than Binder B. These findings suggest that the ability of the particle as an inert filler in the binder matrix to modify the asphalt properties is highly dependent on the base binder viscosity as well as the morphological properties of the crumb rubber.

Emphasis must be placed on the fact that PE was generally 12 times greater than the IE, thereby suggesting that the bulk of the viscous effects due to the presence of crumb rubber in the binders were attributed to the effects of the crumb rubber as inert filler. The grinding procedure was seen to consistently affect the properties of the binders where the ambient ground binders were generally seen to demonstrate the highest viscosity.

Source 4 crumb rubber consistently produced the most viscous binder; crumb rubber testing also indicated that this rubber source contained a significant portion of truck tire crumb rubber. Therefore, it appears that the source of tire used as a modifier plays some role in the viscosity of the modified binder. It is unclear whether this is due to chemical differences in tire source, and thus interaction between tire and binder. Tire composition and properties depend on tire grade, age, and manufacturer (Kyari et al., 2005), differences in natural and synthetic rubber content in tire sources may contribute to different particle morphology, such as surface area of the particles. Tire compounds exhibit differing properties with respect to aging (oil resistance, sunlight aging, and oxidation) and physical distresses (abrasion resistance, tear resistance, and maximum tensile strength); therefore, variability in these may contribute to varied particle morphologies thus resulting in varied CRM binder properties.

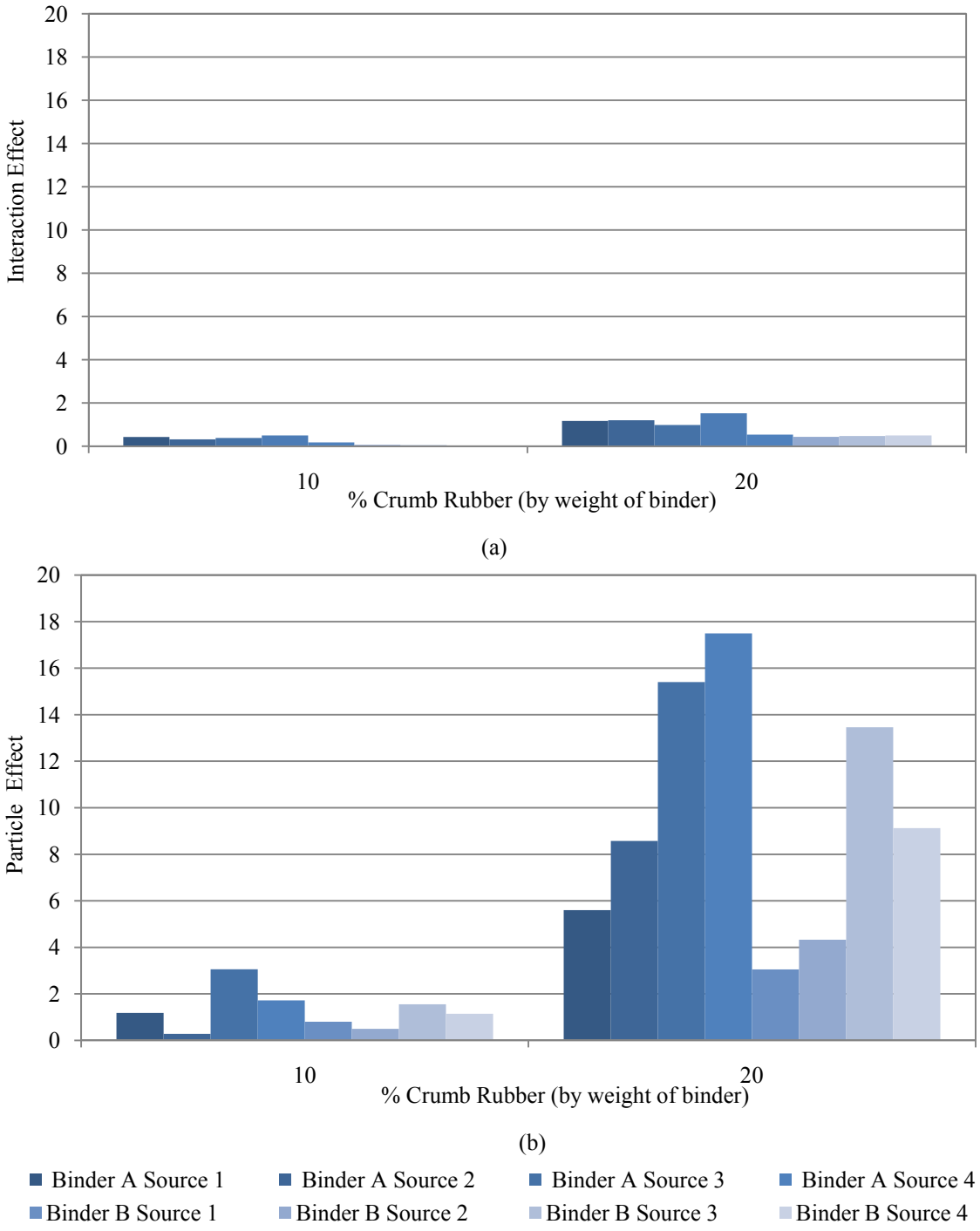

Figure 6.5: Viscosity (a) Interaction Effect and (b) Particle Effect

G*/sinδ and FT testing

Statistically, no significant difference was found when failure temperatures and G*/sinδ of ambient and cryogenic crumb rubbers were compared at 5% crumb rubber concentration. When comparing the failure temperature and the G*/sinδ by grouping the grinding procedures, the ambient ground CRM binders consistently produced higher values. These findings suggest that the extent of failure temperature and G*/sinδ modification is dependent on the grinding process used to render the tire, with ambient ground tires consistently producing higher failure temperatures and G*/sinδ.

When the effect of binder type was examined, Binder A produced significantly higher failure temperatures regardless of crumb rubber source used. These findings suggest differences in crumb rubber source, used in this research project, appear to be less influential than the base binder properties.

Figures 6.6 and 6.7 illustrate the general trend exhibited with the addition of crumb rubber to the asphalt binder. The findings were consistent with the literature as the addition of crumb rubber tended to increase both the high end failure temperature and the G*/sinδ values.

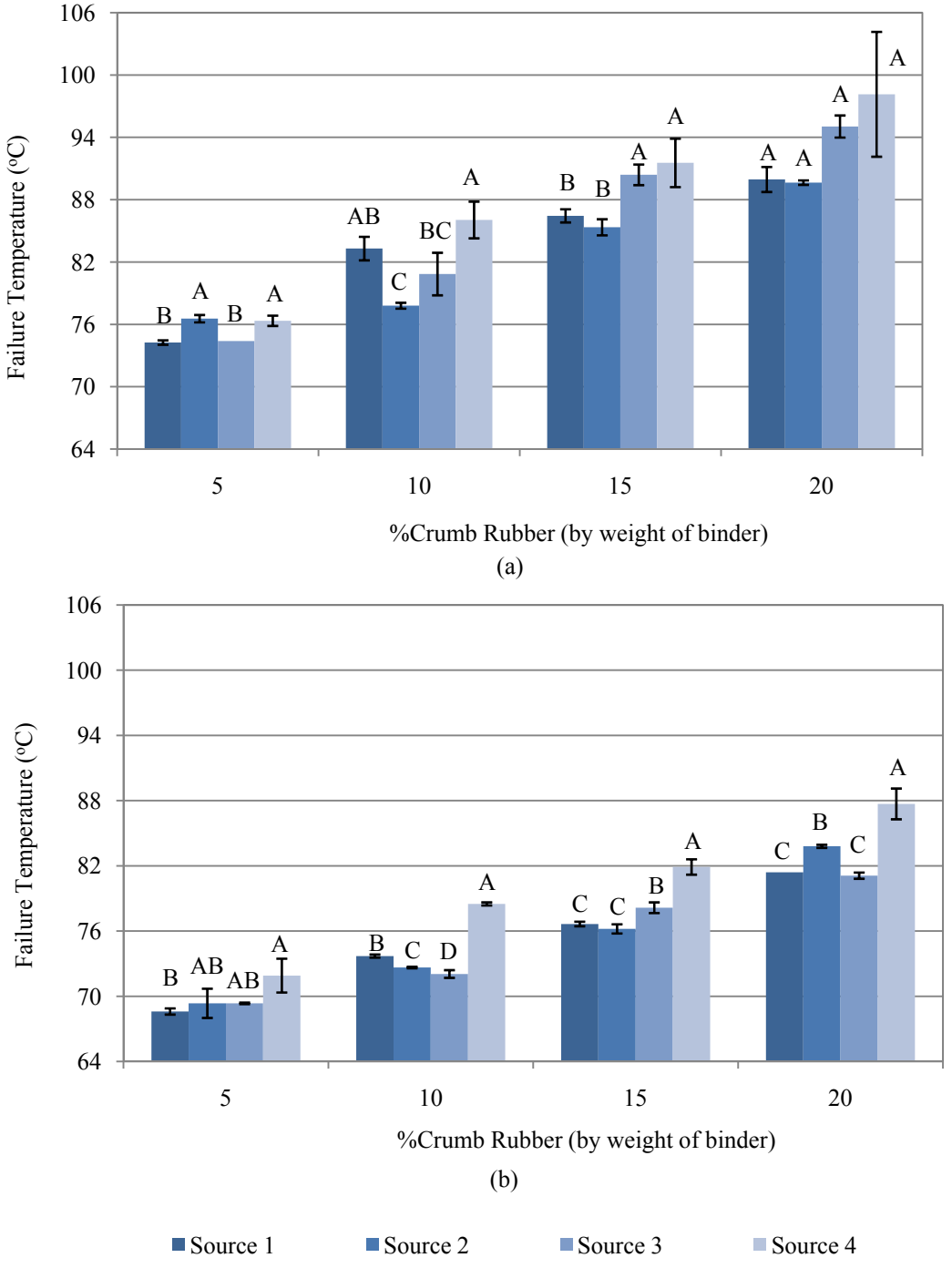

Figure 6.6: Failure temperature of (a) Binder A and (b) Binder B (Treatments containing at least one common letter within a single CRM concentration produced statistically similar responses)

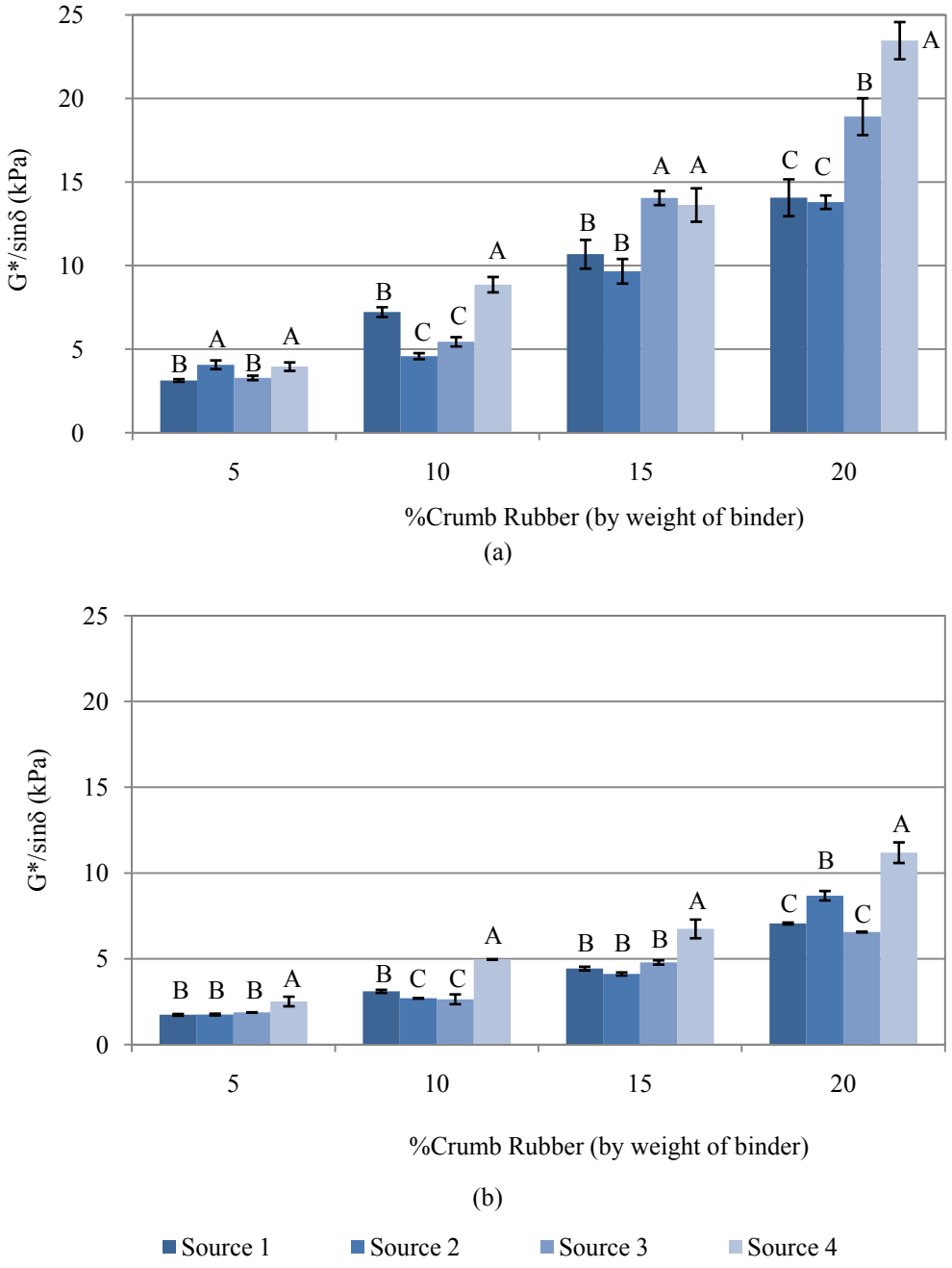

Figure 6.7: G*/sinδ of (a) Binder A and (b) Binder B (Treatments containing at least one common letter within a single CRM concentration produced statistically similar responses)

As shown in Figures 6.6 and 6.7, modified binders made with Source 4 crumb rubber yielded the highest failure temperatures and G*/sinδ regardless of concentration, such findings suggest that ambient ground truck tire rubber yielded the highest failure temperatures and G*/sinδ. The results of modified binders made with Source 3 crumb rubber (ambient) were insufficient to conclude that this crumb rubber source produced results which are significantly different from the two cryogenic crumb rubbers studied.

Particle Effect (PE) and Interaction Effect (IE) on G*/sinδ and Failure Temperature

The PE and IE on failure temperature and G*/sinδ values were calculated. Precise identification of the contribution of each was necessary to determine the cause of the change in properties of the CRM binder. Figures 6.8 and 6.9 illustrate the differences in IE for the two binder types (A and B) when modified with crumb rubbers from 4 different sources. The IE and PE increase significantly as the amount of crumb rubber is increased, thereby suggesting that any reactions occurring between the crumb rubber and the binders are dependent on the amount of crumb rubber used.

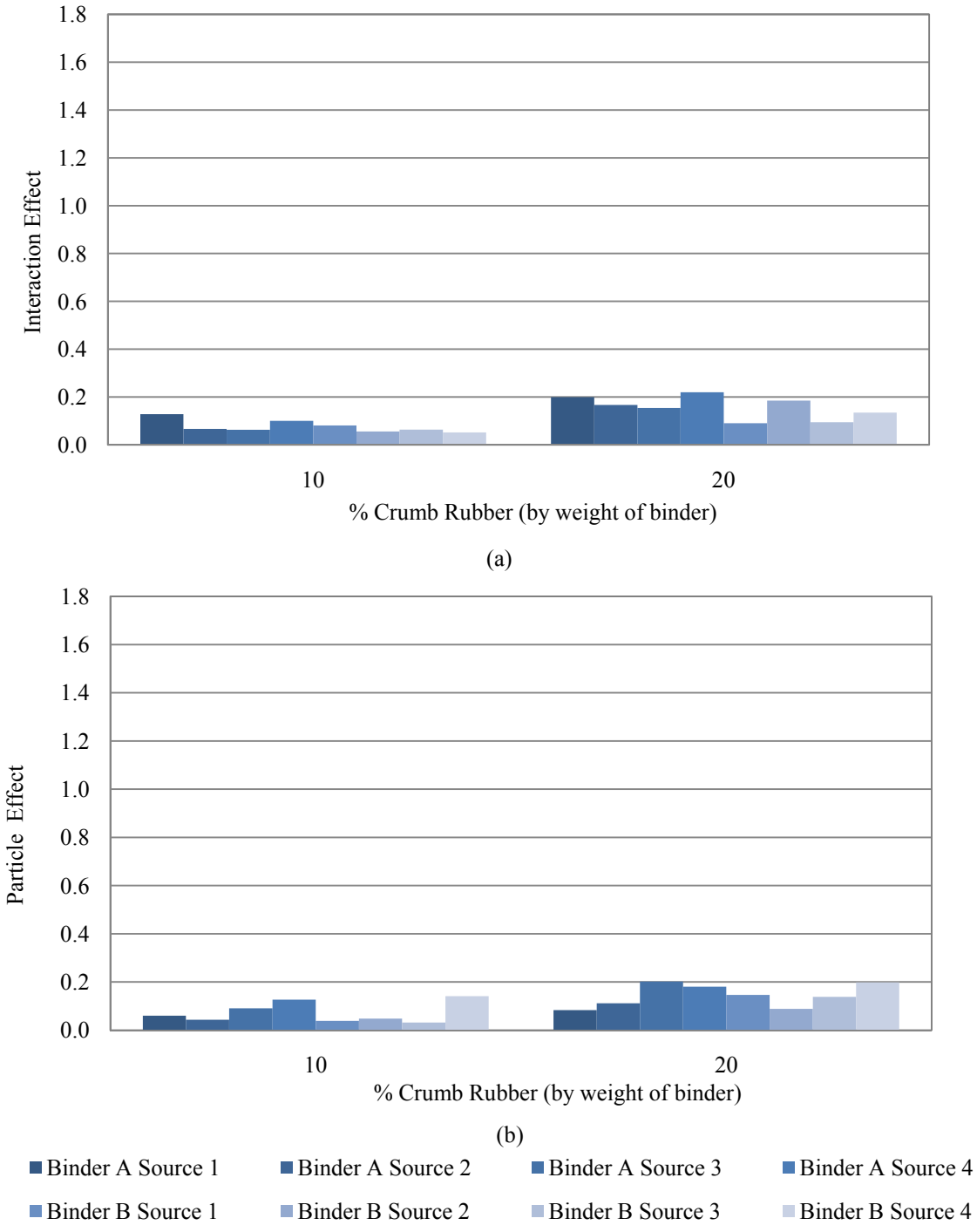

Figure 6.8: Failure temperature (a) Interaction Effect and (b) Particle Effect

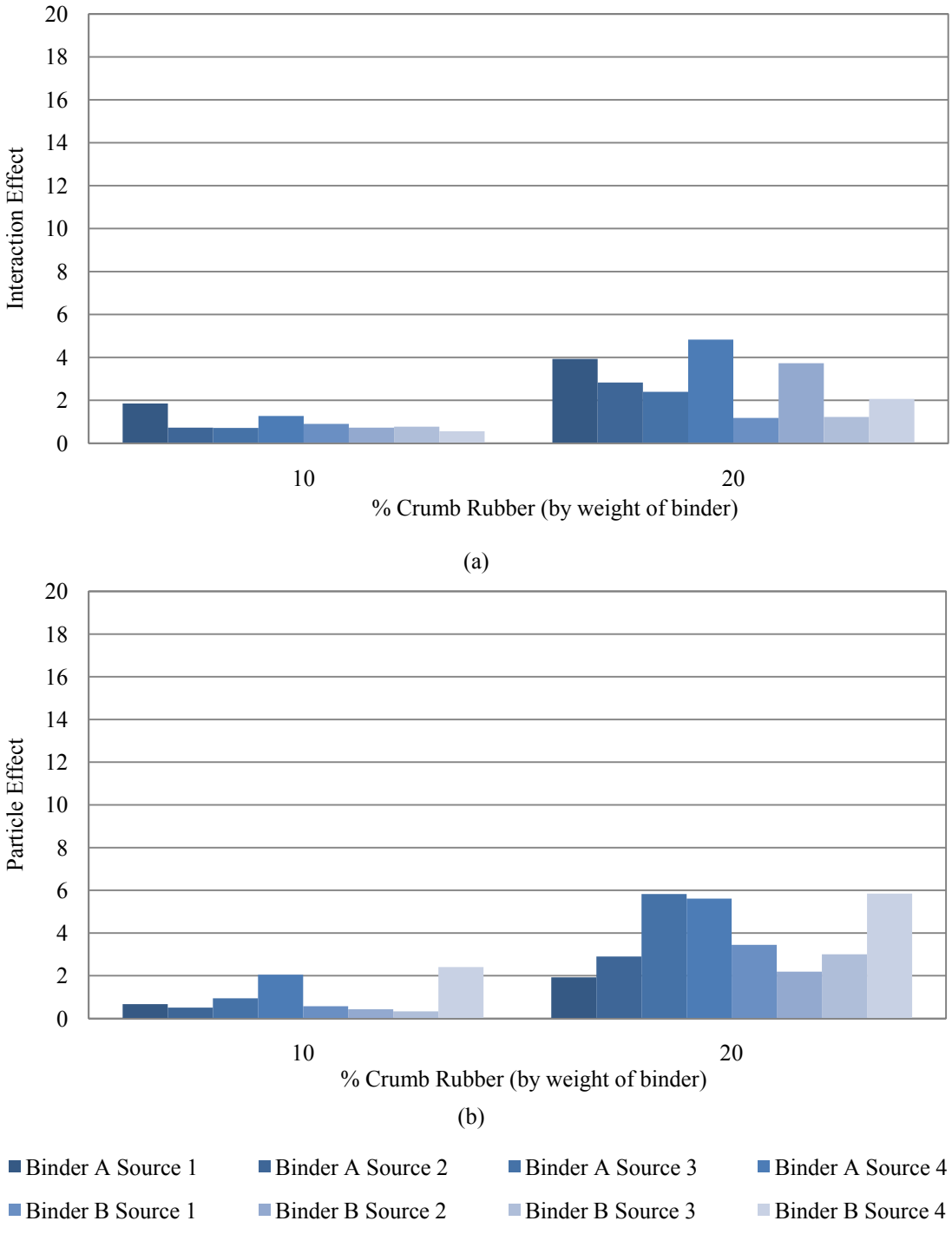

Figure 6.9: G*/sinδ (a) Interaction Effect and (b) Particle Effect

When the results were analyzed by grinding procedures, the IEs were generally quite consistent for both ambient and cryogenic crumb rubbers (at similar crumb rubber concentrations). This behavior was unexpected as the literature suggests that crumb rubber produced by the ambient procedure produces crumb rubber with larger surface areas than those produced cryogenically. Finer crumb rubbers, in general, provide a larger surface area for chemical interactions to occur, therefore, it was expected that as surface area increased, the interaction effect would follow suit. This suggests that the interaction effect between crumb rubber particles and binder is independent of the surface morphology.

When the PEs were compared by the grinding procedure, the crumb rubbers produced using the ambient procedure resulted in higher values than the one produced cryogenically. As expected such results suggest that the PE is influenced by the particle morphology. Such findings indicate that emphasis should be placed on the grinding procedure rather than the tire composition. Tire composition does appear to play a role in the development of $G^*/\sin\delta$ and failure temperature values, however this role appears to be within the context of the particle effect.

The analysis of the interaction and particle effects produced some unexpected results. Of particular note were the inconsistencies in the PE and IE for CRM binder modified with Source 1 crumb rubber. Figures 6.8 and 6.9 show that at 20% crumb rubber by weight of binder Source 1 crumb rubber produced a high IE and a low PE when reacted with Binder A. However, when Binder B was reacted with the same crumb rubber source, it produced a low IE and a high PE. This suggests that the effect of crumb

rubber is dependent on the base binder properties, by examining the IE and PE it is evident that the same crumb rubber source might have different effect on different binder types exhibiting the same performance grade and similar base viscosities.

These findings reinforce the conclusion that little interaction effects are taking place, as reported by others (Putman, 2005). In the event of interactions between binder and crumb rubber, it would be natural to assume that ambient crumb rubber would produce greater interaction effects as ambient particles provide a greater surface area. It was also seen that as the crumb rubber concentration increased, the differences between the various CRM binders became more pronounced, this reinforces the conclusion that binder modification is dependent on the crumb rubber concentration.

Task 3: Viscosity model results

Equation (6.3) describes the resulting estimated equation using SAS:

$$\eta_{x,t} = \eta_{0,135}(e^{R_{cv}x})(211.8e^{-0.040t}) \quad \text{Eq. (6.3)}$$

With the standard error of A and β found to be 28.4084 and 0.00096. Equation (6.3) was used to predict values of viscosity for an array of binder and temperature combinations. Upper and lower prediction intervals, were also estimated from Equation (6.3). The predicted values and the prediction intervals were plotted along with the actual values. Whenever the actual values fell within the prediction intervals, the predictions based on the model were considered to be accurate. Analysis of the model showed that 94% of the time the actual values fell within the prediction intervals.

While R^2 is a popular method of determining the goodness of fit of a model, it does not provide an indication of the range of accuracy of the model. Therefore, 95% confidence intervals were used as a method of determining the accuracy of the model, as well as to provide the user an indication of the accuracy of the model. An additional benefit of using the 95% confidence interval is that if used properly the confidence interval allows the user to incorporate a factor of safety into the predicted value. For viscosity values it is conservative to use the upper 95% confidence interval value when making predictions, doing this provides a value that is slightly higher than the actual value. However, it is sufficiently accurate to provide an indication of the viscosity, while also reducing the risk of exceeding the upper confidence interval to 2.5%.

Values for the R_{cv} were calculated and are summarized in Tables 6.1 and 6.2. As seen in these tables, statistically significant differences are present depending on the binder source and grinding procedure. The highest R_{cv} was exhibited by the Russian binder source; it is thought that this elevated R_{cv} is due to the high shear mixing procedure and higher temperature used during reaction, rather than unique crumb rubber and binder properties. This is likely the case as the Russian binder, whose viscosity was similar to the other binders tested, was modified with ambient crumb rubber. For the remaining binders, the R_{cv} values tended to decrease with decreasing virgin viscosity, thus suggesting that as the virgin binder viscosity decreases so too does the corresponding CRM binder viscosity.

Table 6.1: Mean R_{cv} by Binder Source

Source	Binder	Mean R_{cv}	Observations	LSD
Russia	C	0.187	1	a
Blend	B	0.120	6	b
Venezuela	A,D	0.120	17	b
Middle Eastern	E	0.110	6	b c
Blend	F	0.094	4	c

Table 6.2: R_{cv} by Grinding Procedure

Grinding	Mean R_{cv}	Observations	LSD
Ambient	0.133	17	a
Cryogenic	0.100	17	b

Tables 6.1 and 6.2 use the Fisher LSD procedure to distinguish statistically significant differences present among the R_{cv} values. This procedure is a commonly used statistical analysis method to determine the difference between two sample estimates necessary to declare the corresponding differences between population means. R_{cv} values having at least one LSD letter in common produced statistically similar values.

The influence of the R_{cv} on CRM binder viscosity is quite profound, for example if a binder of 0.5 Pa-s was reacted with a crumb rubber yielding an R_{cv} of 0.1 and another of 0.12 the two binder viscosities produced would be of approximately 3.7 and 5.5 Poise, respectively. This difference in predicted viscosity is dependent on the R_{cv}, as seen in Table 6.2 ambient ground particles typically tend to produce higher R_{cv} values than cryogenically ground particles. The difference in grinding procedures was seen to produce statistically different R_{cv} values, by definition the R_{cv} of a binder containing no crumb rubber is zero. Preliminary results also indicate that the R_{cv} tends to increase for ambient ground particles with increasing fineness, no such increase was found for cryogenic particles of differing fineness.

The experimental results are plotted along side with the predicted values and the corresponding 95% confidence interval in Figure 6.10. The confidence intervals which went below zero Pa-s were omitted as they do not present realistic values.

Figure 6.10 provides a graphical representation of the average values of the data points at various temperatures; it is evident from these charts that the nonlinear model used for predicting CRM binder was accurate. As with any empirical model, it is difficult to make exact predictions; therefore, the 95% confidence interval was also included thus providing an indication of the reliability of the model. For all temperatures, the 95 % confidence interval was encapsulated by +/- 0.8 Pa-s of the predicted value. This is indicative of a model that has a 95% chance of encapsulating the true value within +/- 0.8 Pa-s. Therefore, depending on the application in question, the upper or lower limit would provide a conservative estimate of the parameter of interest.

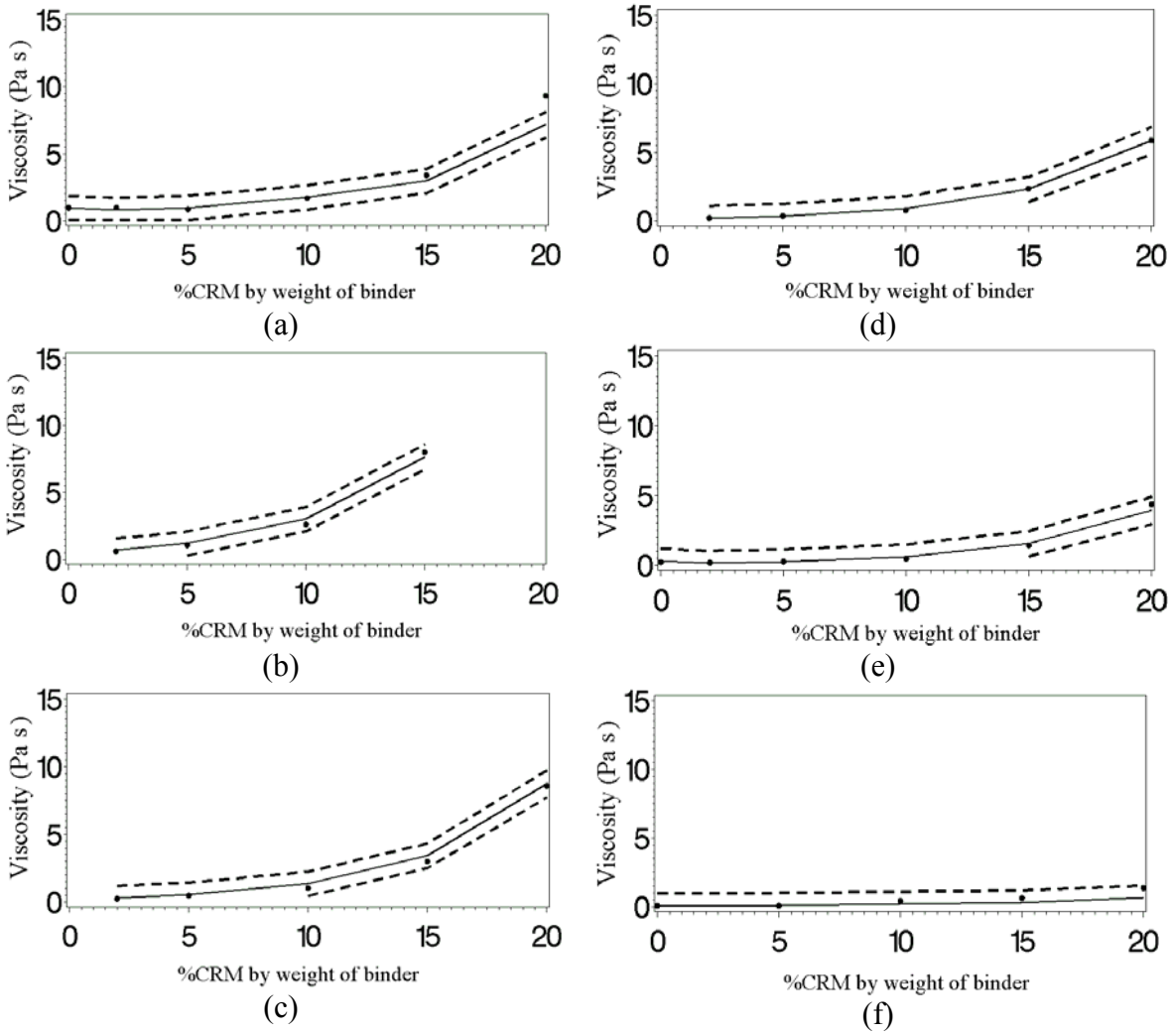

Figure 6.10: Average Experimental and Predicted Values of Binder Viscosity for (a) 135°C,(b) 140°C, (c) 160°C, (d)170°C, (e) 180°C, and (f) 190°C

The upper confidence interval is particularly useful as it provides a conservative estimate of the maximum viscosity achieved with a specific crumb rubber at a given temperature. It is of note that Figure 6.10 is not representative of any one single binder or crumb rubber type, rather it is a summary of the data used in this particular study. Therefore, they should not be compared to one another as the binders are not all of the same source or grade. The value of these figures lies in their representation of the average estimated value of the binder viscosity against the average value of the experimental viscosities. The drawbacks of using such a method are apparent when examining the predicted viscosity at 20% crumb rubber at 135°C. This is the only case where the average experimental value fell outside the prediction interval, this is due to the increasing variability of binder viscosities with increasing crumb rubber concentrations as temperature decreases. The effects of the different virgin binder and crumb rubber types are more pronounced at lower temperatures given the increased viscosity of asphalt at lower temperatures.

Task 4: G*/sinδ and FT Model Results

In this section, the experimental results are compared to the predicted values using the G*/sinδ model and the high end failure temperature model. Of interest in this section was the ability of the 95% confidence interval to capture the experimental values without creating excessively large intervals. Also presented in this section are the various R_{cg} values, these values are compared by base binder, grinding procedure, and crumb rubber source.

G*/sinδ model

Using SAS, the values for K and ϕ were determined to be 837.8 and -0.1047 respectively. The resulting estimated relationship is given by Equation (6.4):

$$\left(\frac{G*}{sin\delta}\right)_{x,t} = \left(\frac{G*}{sin\delta}\right)_{0,64} [e^{R_{cv}x}][837.8e^{-.1047t}] \quad \text{Eq. (6.4)}$$

The standard error of K and ϕ were found to be 90.2 and 0.002, respectively. Equation (6.4) was used to predict values of G*/sinδ for an array of binder and temperature combinations. Upper and lower prediction intervals were also estimated from Equation (6.4). The predicted values and the prediction intervals were plotted along with the actual values. Whenever the actual values fell within the prediction intervals, the predictions based on the model were considered to be accurate. Analysis of the model showed that 92.6% of the time the actual values fell within the prediction intervals.

Figure 6.11 illustrates the increase in G*/sinδ values as crumb rubber content increases. In addition, this figure illustrates the accuracy of the model in predicting the CRM binder properties. Experimental results show that as crumb rubber concentration is increased, the G*/sinδ value increases, a decrease in experimental G*/sinδ values is noted as the temperature increases. At 82 and 88 ^{o}C, binders with less than 10% crumb rubber by weight were seen to not withstand any loading. The average experimental values were consistently encapsulated by the 95% confidence interval; furthermore the 95% confidence interval was seen to be approximately +/- 1.3 kPa.

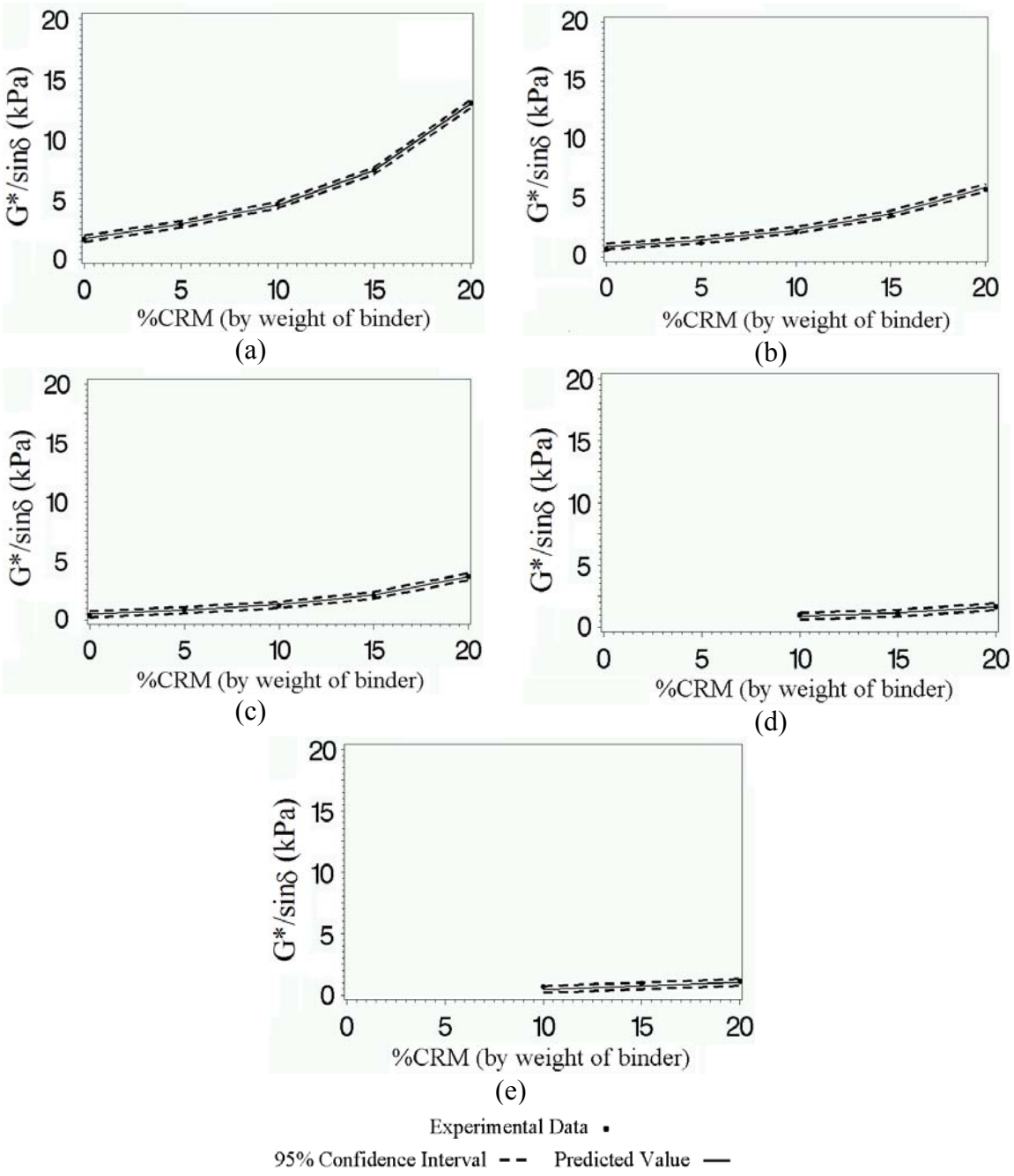

Figure 6.11: Average experimental and predicted G*/sinδ values with 95% confidence intervals for (a) 64°C, (b) 70°C, (c) 76°C, (d) 82°C, and (e) 88°C

Failure Temperature Model

Equation (6.5) is produced by substituting the computed values for K and ϕ into Equation (6.4), this relationship provides an idea of how failure temperature (FT) of CRM binder varies with crumb rubber concentration.

$$ft = \frac{ln\left[\frac{1000}{\left(\frac{G*}{sin\delta}\right)_{0,64}(e^{R_{cg}x})}\right] - ln(837.8)}{-.1047} \quad \text{Eq. (6.5)}$$

A verification of the high end failure temperature model was also performed, as seen in Figure 6.12 where the average values consistently fell within the 95% confidence interval. This suggests that the model derived from the combined model was accurate for the purposes of predicting high end failure temperature given only the virgin G*/sinδ value and other variables (e.g., ambient/cryogenic and particle size) of the crumb rubber to be used. The accuracy of this limited model was seen to be good as the 95% confidence interval was approximately +/- 3^{o}C. Using the 95% confidence interval also provides a factor of safety in the prediction of the CRM binder failure temperature, using the lower value from the confidence interval means that the probability of calculating an inaccurate failure temperature on the high side is less than 2.5%.

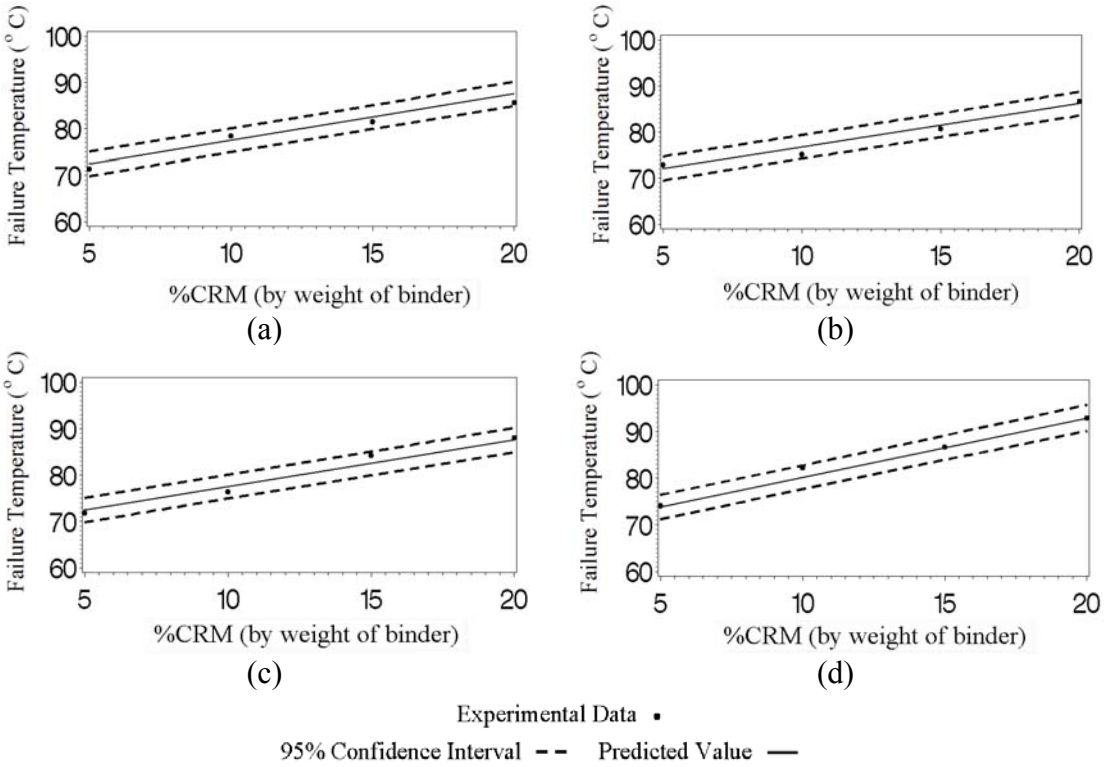

Figure 6.12: Failure temperature fit for crumb rubber Sources (a) 1, (b) 2, (c) 3, and (d) 4

Analysis of R_{cg}

The R_{cg} values were computed for all 462 data points, the R_{cg} values were separated by binder source, crumb rubber grinding procedure, and crumb rubber source (Table 6.3). This analysis indicated that Binder A yielded the highest R_{cg} values regardless of the crumb rubber used to modify the binder. The ambient grinding procedure was seen to produce higher R_{cg} values then cryogenic grinding of the tires, while crumb rubber produced from truck tires tended to yield the highest R_{cg}. Particle size was also an important factor in determining the R_{cg} value, the analysis of the R_{cg} results showed that both ambient and cryogenically ground particles produced higher R_{cg} values as the particle size decreased.

Table 6.3: R_{cg} by (a) Binder source, (b) Grinding Procedure, and (c) crumb rubber Source

(a)

Binder Source	N	Mean R_{cg}	LSD Grouping
Venezuela (a)	202	0.102	A
Blend (b)	180	0.088	B
Middle East (c)	78	0.074	C

(b)

Grinding Procedure	N	Mean R_{cg}	LSD Grouping
Ambient	202	0.103	A
Cryogenic	230	0.093	B

(c)

Crumb Rubber Source	N	Mean R_{cg}	Grinding Procedure	Size	Composition	LSD Grouping
Source 4	32	0.121	Ambient	Gradation [a]	Truck Tire	A
Source 7	36	0.103	Ambient	.18 mm	Passenger Car Tire	B
Source 6	36	0.102	Ambient	.425 mm	Passenger Car Tire	B C
Source 10	36	0.100	Cryogenic	.18 mm	Passenger Car Tire	C
Source 3	62	0.098	Ambient	Gradation [a]	Passenger Car Tire	D
Source 5	36	0.096	Ambient	.85 mm	Passenger Car Tire	D
Source 1	62	0.093	Cryogenic	Gradation [a]	Passenger Car Tire	E
Source 2	60	0.093	Cryogenic	Gradation [a]	Passenger Car Tire	E
Source 9	36	0.092	Cryogenic	.425 mm	Passenger Car Tire	E
Source 8	36	0.088	Cryogenic	.85 mm	Passenger Car Tire	F

[a] Gradation corresponds to specifications provided in Table 3.2(a)

Many of these results are consistent with the literature where ambient ground rubber has been known to exert greater changes on the binder (Blumenthal, 1994; Putman & Amirkhanian, 2006; West et al., 1998), while finer crumb rubber particles have also been seen to produce CRM binders with greater rutting resistance (Putman, 2005).

Task 5: Universal model results

In this section, the results of the nonlinear regression suitability for the test data are presented. First, the model coefficients are presented along with a discussion of their significance. Next, the various models are examined with respect to their ability to predict the experimental values. In this study, R-squared values are presented as a general indication of the model fit; the 95% confidence interval, the interval within which there is a 95% probability of locating the mean, was determined as measure of the variability captured by the model. Therefore, if the mean values of all the experimental data points are calculated, then the 95% confidence interval would provide an estimate of the ability of the model to predict accurate values (Ott & Longnecker, 2001).

Model coefficients

The coefficients produced by conducting the nonlinear regression analysis of the data using SAS are presented in Table 6.4. These coefficients are specific to the binder modification, therefore, coefficients are presented for virgin binder, cryogenic CRM binder, and ambient CRM binder.

Table 6.4: Coefficients for ambient, cryogenic, and virgin binders

Coefficient	Ambient	Cryogenic	Virgin
a	2262.2	3173.0	8212.2
b	0.1036	0.0848	1.000
c	-0.1026	-0.1065	-0.1241

The values from Table 6.4 also confirm findings consistent with the literature. The results indicate that the rate of G*/sinδ increase is greater for ambient ground crumb rubber than cryogenic crumb rubber (*b* value is greater for ambient compared to cryogenic). The fact that the virgin binder *b* value is the highest is irrelevant as the crumb rubber concentration for virgin binder is always zero. Also of note from these findings is the tendency of the *c* values to decrease for the CRM binders with respect to the virgin binder. This indicates the reduced temperature susceptibility of CRM binders compared to virgin binders. When comparing the CRM binders, the *c* coefficient for the ambient crumb rubber is slightly greater than the cryogenic crumb rubber, this indicates that the CRM binders produced with cryogenically ground crumb rubber are slightly more susceptible to temperature variations.

G*/sinδ model

Using the coefficients in Table 6.4, Equation (6.6) was able to encapsulate 94% of all 450 data points used within the 95% confidence interval.

$$\frac{G*}{sin\delta} = \eta_{135,0} a e^{(bx+c(T))} \qquad \text{Eq. (6.6)}$$

The confidence interval was calculated to be approximately +/- 0.5 kPa. Figure 6.13 is an illustration of the average values of all the experimental values recorded as well as the predicted values with the 95% confidence interval. As the viscoelastic behavior of asphalt binder is temperature dependent, the figure is divided into five commonly used performance grades (i.e, 64, 70, 76, 82, and 88^{o}C). In this figure, each experimental value included is actually the average value of all the data points collected at the given crumb rubber concentration and testing temperature. From these figures it can be seen that the experimental data consistently falls within the 95% confidence interval, thus suggesting a good fit for the model. Also, the 95% confidence interval of +/- 0.5 kPa was sufficiently small to produce accurate results. This range of accuracy was seen to be particularly useful for the higher crumb rubber concentrations where the G*/sinδ values are typically quite high.

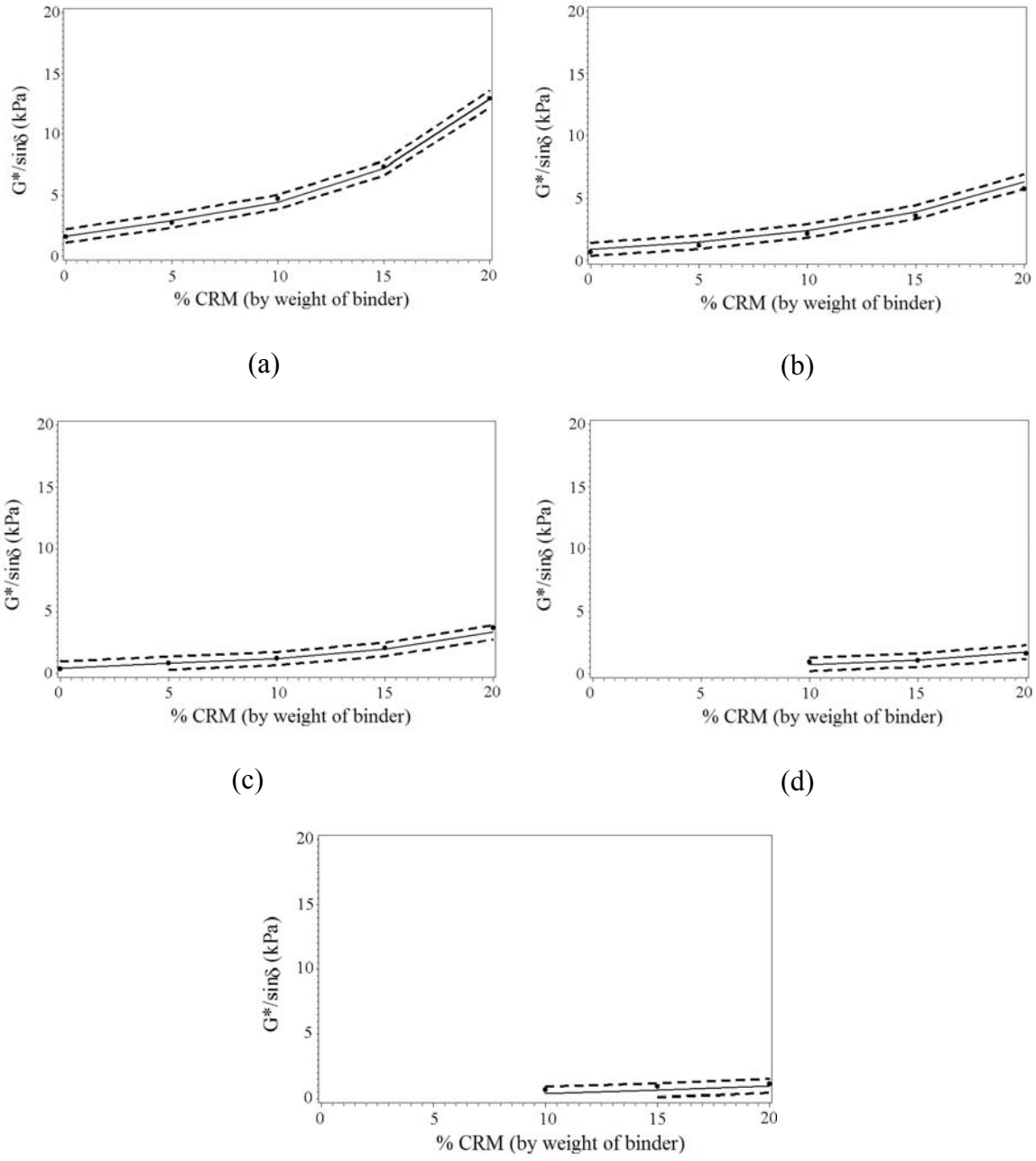

Figure 6.13: Average experimental values with average predicted values for: (a) 64°C, (b)70°C, (c)76°C, (d)82°C, and (e) 88°C.

Figure 6.14 illustrates how the predicted values compare with the experimental values, in this figure the experimental values are plotted together with the predicted values. The line of equality is representative of a perfect fit between model and experimental values and it can be seen that the predicted values are generally quite consistent with the actual values. An R-squared value of 0.86 was determined as an additional measure of goodness of fit. Regardless of the high coefficient of determination, it is still preferable to use the model with the 95% confidence intervals as these provide a measure of the variability inherent in the predictive model.

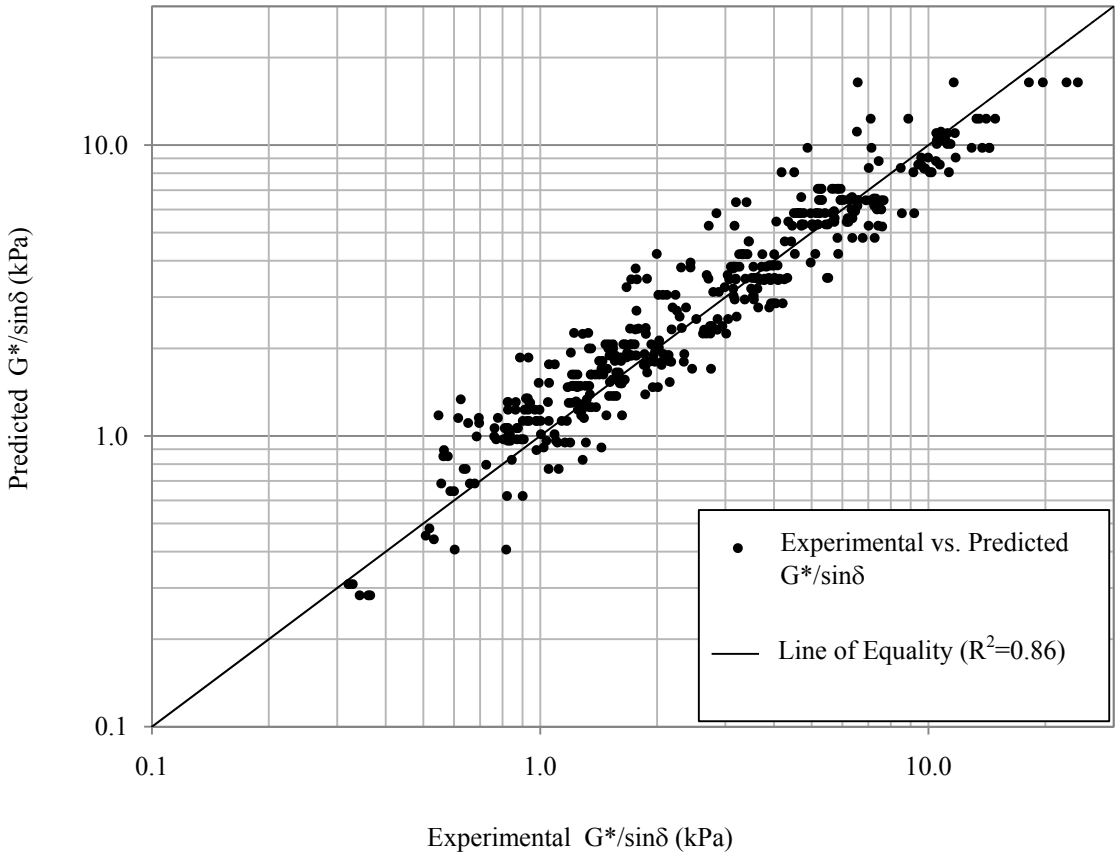

Figure 6.14: Experimental and predicted G*/sinδ values

Temperature model

It was possible to determine the temperature at which a specified CRM binder would fail by using Equation (6.7) with the coefficients in Table 6.4.

$$T = \frac{1}{c}\left\{ ln\left[\frac{\frac{G*}{sin\delta}}{(\eta_{135,0}a)}\right] - bx\right\} \quad \text{Eq. (6.7)}$$

The analysis of the data using SAS suggests that the 95% confidence interval is +/- 2.7°C; this means that there is a 95% probability of estimating the correct failure temperature within the interval between +/- 2.7°C of the predicted value. Figure 6.15 provides an illustration of the average values of all the experimental values at their respective failure temperatures along with the average 95% confidence interval for all the predicted values.

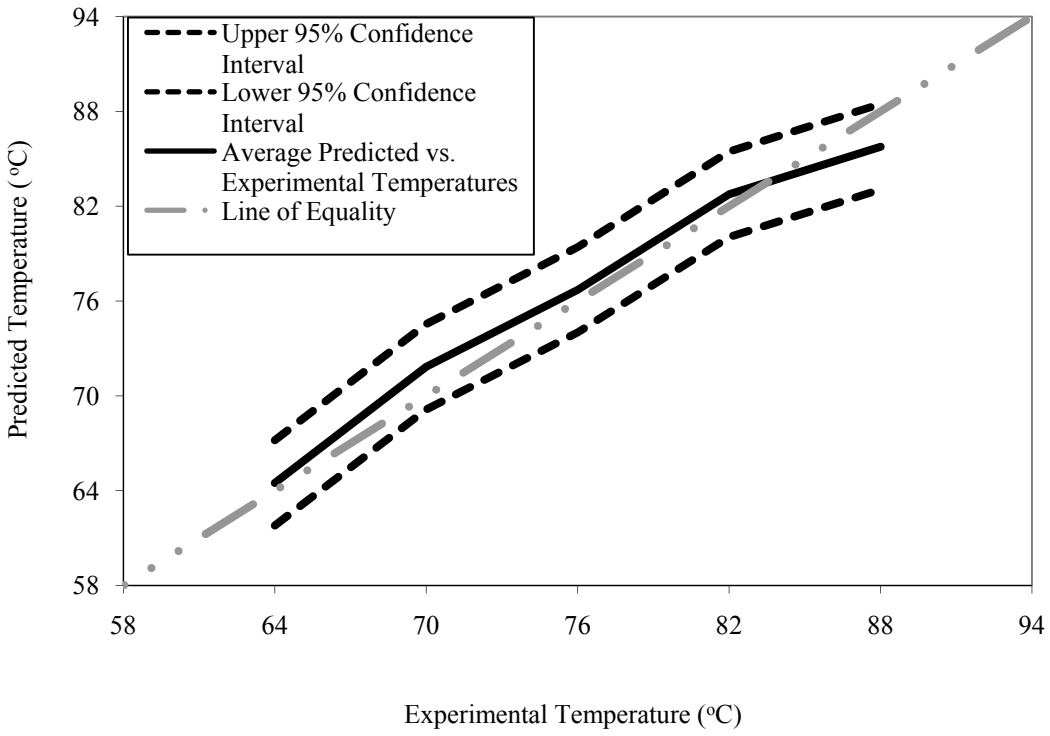

Figure 6.15: Comparison between observed and predicted average values of failure temperature with 95% confidence interval.

From Figure 6.15 it is evident that the model provides an adequate fit for the experimental data. Figure 6.15 illustrates the average values of all the data points studied as well as the average values of the predicted failure temperatures. In the event of a perfect fit between model and experimental values, the line of equality would be followed. In this case, it can be seen that the temperature model typically tends to slightly overestimate the actual value. However, when placed within the context of the 95% confidence interval, the results are seen to be very good. The 95% confidence interval is seen to consistently capture the required experimental values regardless of temperature, meaning that the predictive model is accurate with a level of accuracy of +/- 2.7°C.

Therefore, this shows that given only the unmodified binder viscosity at a temperature of 135°C it is possible to estimate the failure temperature of the binder, for temperatures greater than 64°C, and a level of accuracy of +/- 2.7°C.

The actual experimental and predicted data points were plotted along with the line of equality in Figure 6.16, the R-squared value of 0.88 for the line of equality suggests a good correlation between experimental and predicted values. During testing, G*/sinδ values were determined at temperatures between 64 and 88°C, therefore, all experimental values are at consistent temperatures between 64 and 88°C at intervals of 6°C.

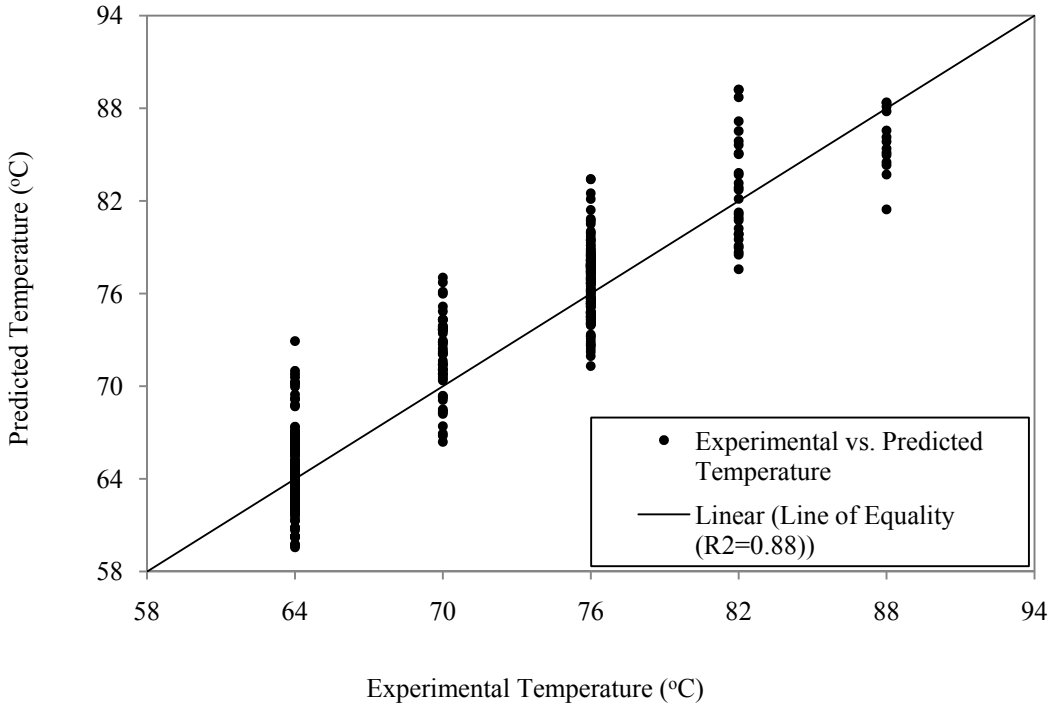

Figure 6.16: Experimental and predicted failure temperatures for the universal model

Crumb Rubber Model

The results relating virgin binder viscosity to CRM binder failure temperature were calculated using Equation (6.8) and the coefficients in Table 6.4.

$$x = \frac{1}{b}\left\{ln\left[\frac{1}{(\eta_{135,0}a)}\right] - cFT\right\} \quad \text{Eq. (6.8)}$$

The average values of all 450 data points were sorted by crumb rubber concentration and presented along with the predicted values and the corresponding 95% confidence interval (Figure 6.17). The goal of this model was to allow the user to estimate the required amount of crumb rubber to be added to the virgin binder to achieve the desired failure temperature. Therefore, to validate the model, the same experimental data was used, but the crumb rubber concentration was assumed to be an unknown variable. Using Equation (6.8) the crumb rubber concentration was solved for using the given G*/sinδ, temperature, virgin viscosity, and appropriate binder coefficients. In the event of a perfect match between predicted values and experimental values the line of equality would be followed. In this case, it can be seen that average predicted values were slightly below the line of equality, which indicates that the predictive model generally tends to produce values which are slightly lower than the actual value. It is therefore necessary to also take into consideration the 95% confidence interval as this interval provides a certain margin of error.

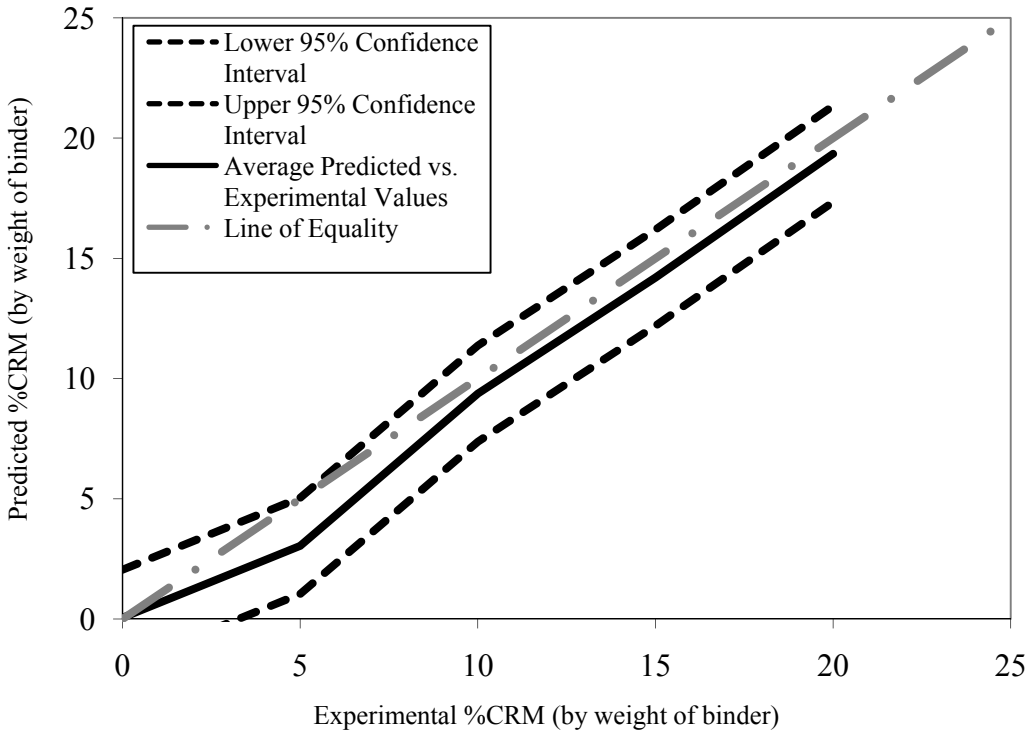

Figure 6.17: Comparison between observed and predicted average values of crumb rubber content with 95% confidence interval

Using the 95% confidence interval, it can be seen that the average experimental values consistently fall within the interval, this means that 95% of the time the predictive model is accurate to within +/- 2%. Generally speaking, the model followed the experimental values quite consistently, the greatest deviation from the experimental values occurred at 5% crumb rubber where the average predicted value was considerably lower than the average experimental value. Another advantage of employing the 95% confidence interval as an indication of the model reliability is that it provides a factor of safety for the predicted values. This is because if the lower value of the confidence interval is assumed, then the probability of calculating an incorrectly high number is less than 2.5%.

Figure 6.18 was derived by calculating the required amounts of crumb rubber needed for achieving the experimental G*/sinδ values, the crumb rubber concentrations were then back calculated using Equation (5.20) and the resulting predicted values were compared with the actual concentrations used.

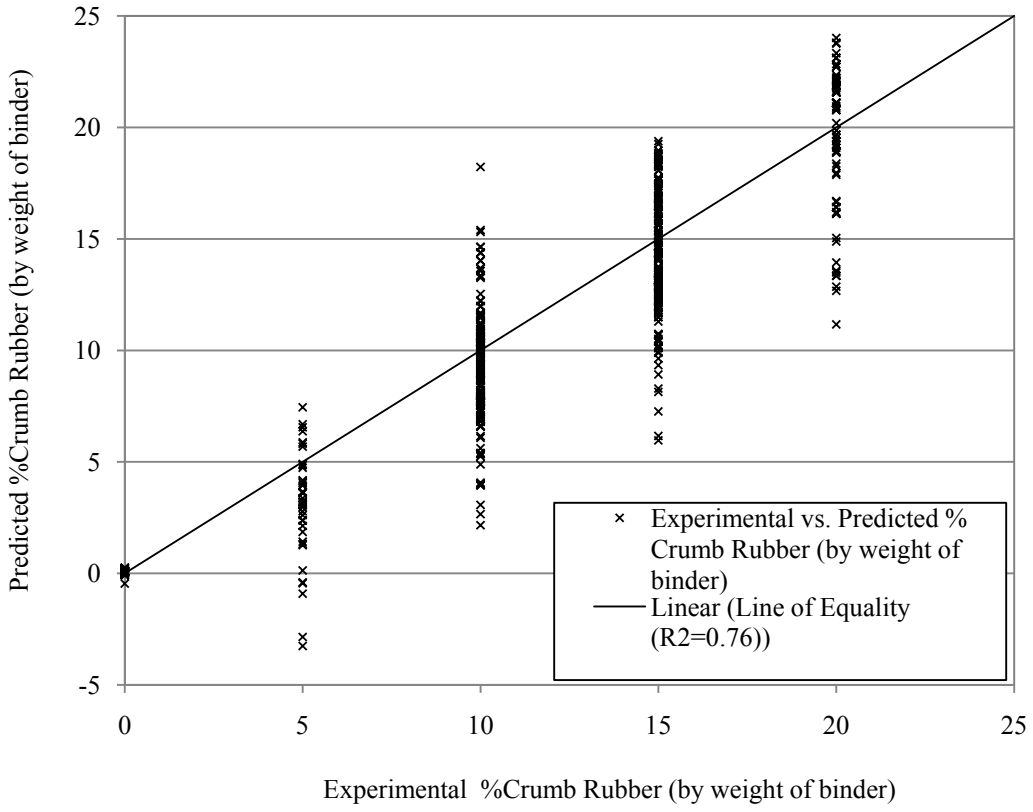

Figure 6.18: Experimental and predicted crumb rubber percentages (by weight of binder)

In this case, the R-squared value was seen to drop to 0.76 thus suggesting slightly more variability than the previous two models. The predicted values can be seen to be slightly skewed under the line of equality indicating that typically the crumb rubber concentration model tends to underestimate the required amount of crumb rubber to achieve a desired G*/sinδ value.

Task 6: Verification Study

Results from the confirmation study indicated that the models developed were sufficiently accurate for predicting the binder properties. The fractional factorial design described in Chapter 3 was used, and resulted in 20 binder testing scenarios. As a result, the predicted values were analyzed with respect to the predicted values and comments made.

Viscosity Equation

Verification of the viscosity equation indicated that the experimental values were closely approximated by the predicted values using Equation 6.3. From Figure 6.19 it can be seen that as the temperature increased the values tended to converge on the predicted values. This is because as the binder heats up, other factors such as binder source, crumb rubber properties, etc. tend to play less of a role in determining the viscosity. As such it appears that the higher the temperature, the more uniform the viscous behavior of the asphalt binder.

Figure 6.20 provides an illustration of the entire verification test data plotted against the line of equality. In the event of a perfect fit between experimental and predicted values all the data points would be located along the line of equality. It can therefore be concluded that the model provided a good fit for the data, as the data points were generally located along the line of equality.

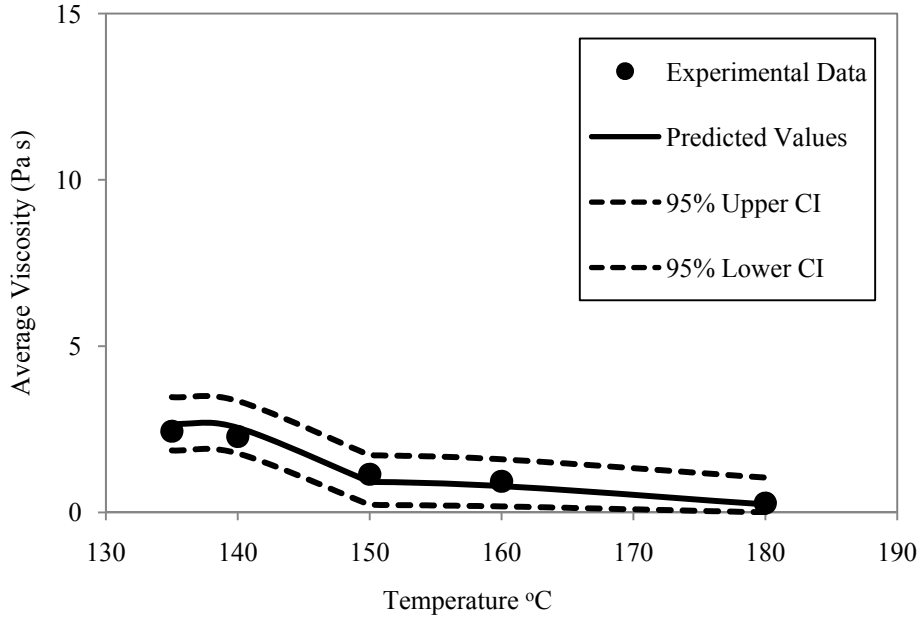

Figure 6.19: Verification of average viscosities vs. temperature for viscosity equation

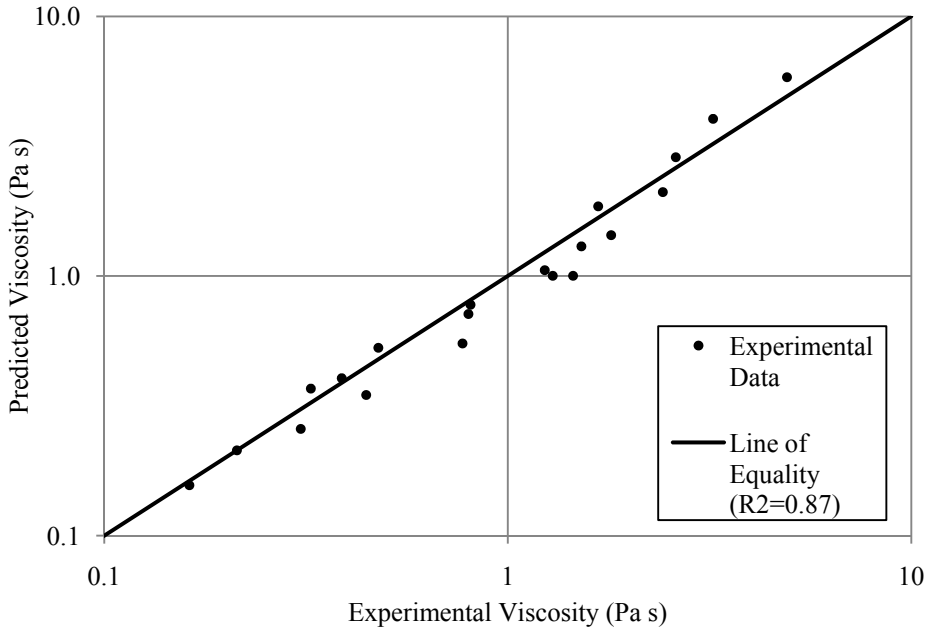

Figure 6.20: Verification of experimental vs. predicted viscosity

G*/sinδ Equation

The verification results also proved the validity of the G*/sinδ model, as seen in Figure 6.21. The model produced accurate results regardless of crumb rubber concentration or temperature. It can also be seen that the predictive model tends to produce the intermediate value between the high and low. For example, it can be seen that at 64°C, the 5% and 10% crumb rubber experimental data is somewhat higher than the predicted value, while for the 15% and 20% it is slightly lower than the predicted value .This suggests that there is a great deal of variability within CRM binder properties, but it also shows that the model will generally select an intermediate value.

These findings are also evident in Figures 6.22 and 6.23, here it can be seen that the experimental data points tend to follow the line of equality. Also, the data does not appear to be skewed to one direction, this can be seen as approximately the same number of data points are located above the line of equality as below the line of equality.

Therefore, it may be concluded that the model was able to determine CRM binder's G*/sinδ and failure temperature given only the virgin binder G*/sinδ value. As it is conservative to underestimate the failure temperature and G*/sinδ for design purposes, it is suggested that the lower confidence interval be used. Doing so, provides an accurate and conservative estimate.

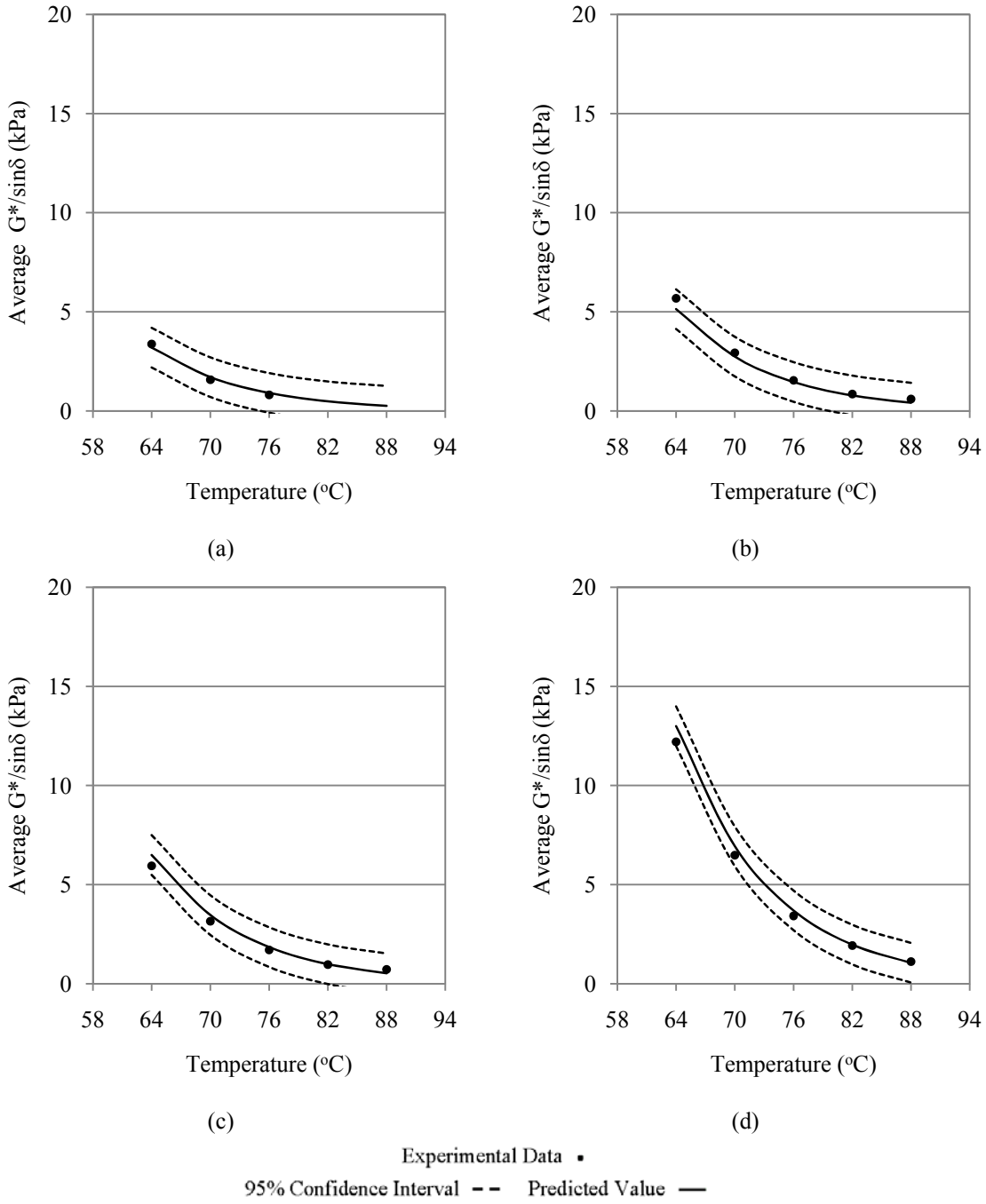

Figure 6.21: Average Experimental and Predicted Values of G*/sinδ using G* equation for (a) 5%, (b) 10%, (c) 15%, and (d) 20% crumb rubber

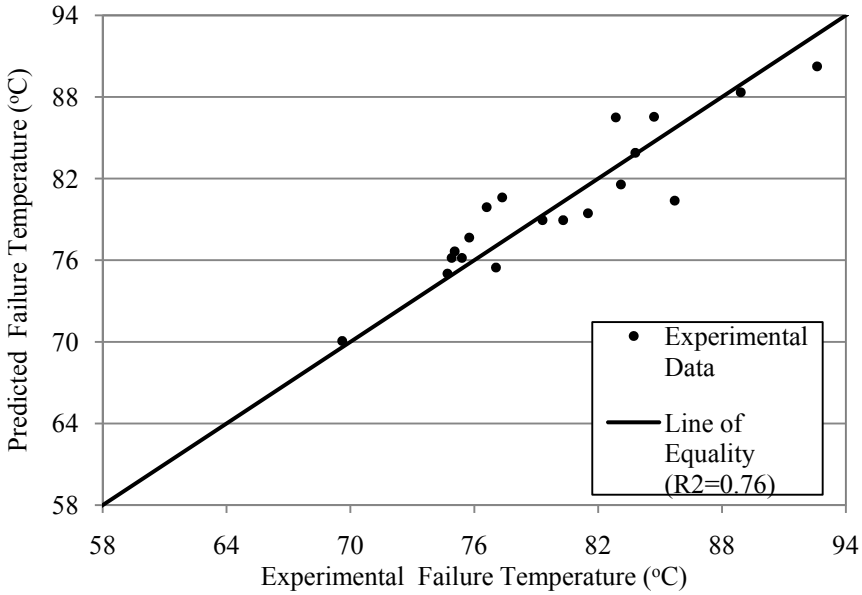

Figure 6.22: Verification of Experimental vs. predicted failure temperature for G* equation

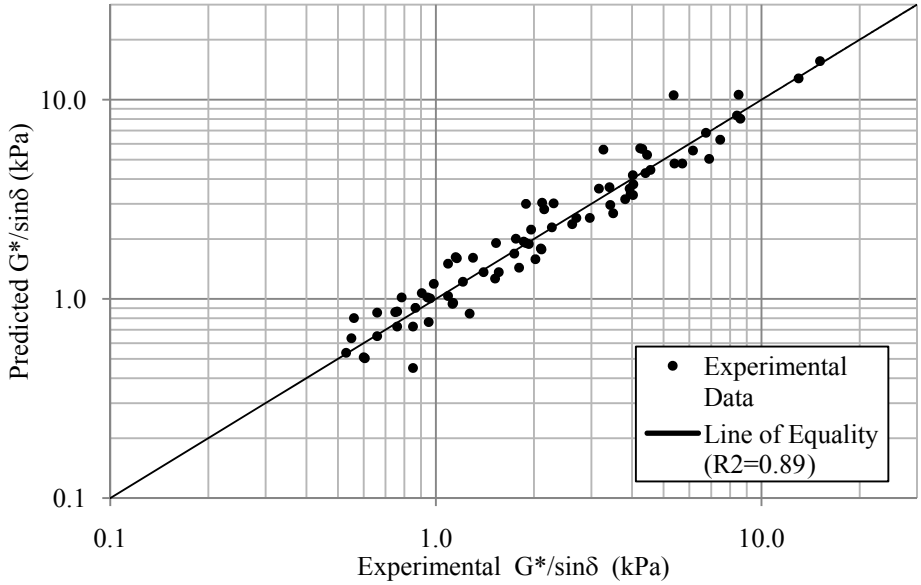

Figure 6.23: Verification of Experimental vs. predicted G*/sinδ for G* equation

Universal model

The verification study suggested that it is possible to predict the rutting susceptibility and failure temperature of a CRM binder given only the virgin binder

viscosity at 135°C. As seen in Figure 6.24 the predicted values tended to be accurately predicted using Equation 6.6. As seen in Figure 6.24, the average experimental values were within the assigned confidence intervals, however, the experimental data tended to be the closest as the testing temperature decreased. This phenomenon, is due to the fact that CRM binders tend to act more uniformly as the temperature increases.

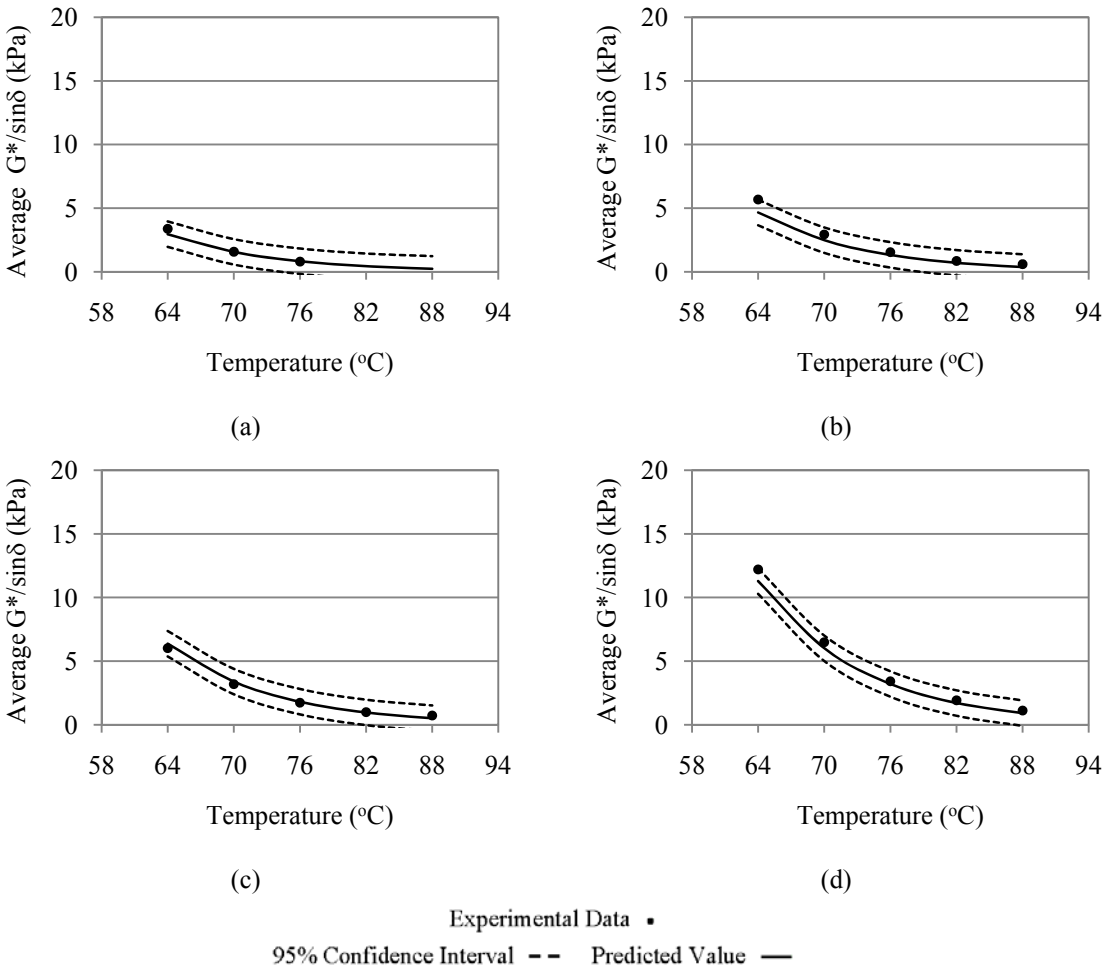

Figure 6.24: Average Experimental and Predicted Values of G*/sinδ using G* equation for (a) 5%, (b) 10%, (c) 15%, and (d) 20% crumb rubber (by weight of binder)

As seen in Figures 6.25-6.27, there was a very strong linear correlation between the predicted data points and the experimental data points. This suggests that the models using the virgin binder viscosity as an input value yielded accurate results regarding the failure temperature, G*/sinδ values, and crumb rubber concentrations. It is also of value to note that the experimental data was scattered evenly on both sides of the line of equality. This indicates that the model was not consistently overestimating or underestimating the actual value, rather it tended to report the average value.

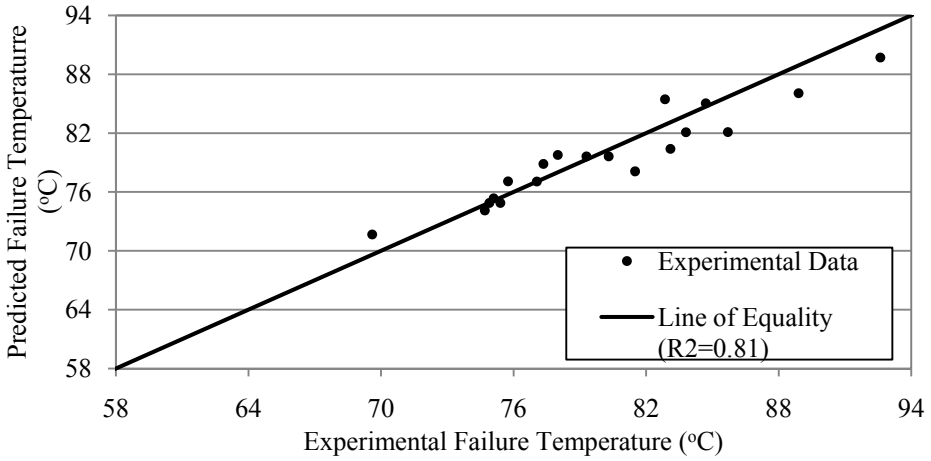

Figure 6.25: Verification of experimental vs. predicted failure temperature for universal equation

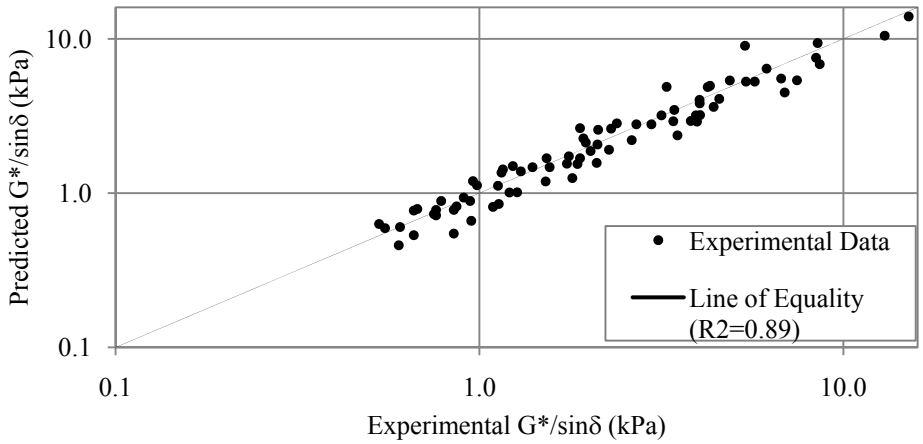

Figure 6.26: Verification of experimental vs. predicted G*/sinδ for universal model

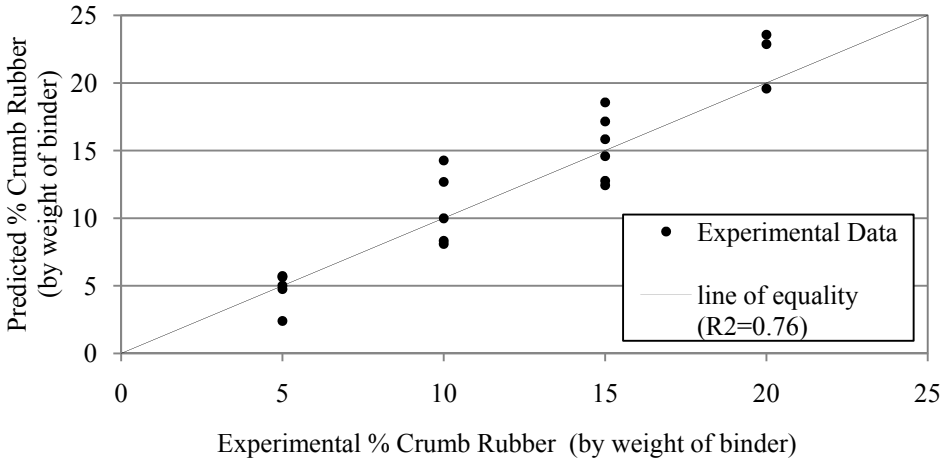

Figure 6.27: Experimental vs. predicted % crumb rubber for universal model

CHAPTER SEVEN

SUMMARY, CONCLUSIONS, AND RECCOMENDATIONS FOR FUTURE RESEARCH

Summary

The purpose of this research was to identify and model critical elements of the asphalt rubber matrix contributing to the CRM binder properties as measured by Superpave testing procedures. Initially, an extensive literature review regarding the use, performance, and estimation of SHRP properties of various CRM binders was conducted. The findings from the literature review indicated that CRM binder was an established paving material with a record of improving pavement performance. Previously, other researchers had attempted to develop models for the prediction of binder properties. These models are today either not applicable (due to new testing procedures) or not practical (due to difficulty of application or lack of accuracy). As such, this research aimed to develop predictive models for estimating binder properties within a certain range of accuracy. Currently, no such models exist, however, for CRM binder to become more established in the field of polymer modified asphalts it is necessary that such models be developed to show the consistency of the product.

The first task in this research involved evaluating the various crumb rubber sources; this was done in order to gain an understanding of the differences between the various crumb rubbers. Doing so would permit identification of the important parameters, thus allowing for an accurate model to be developed. Analysis of the crumb rubbers involved determination of the glass transition temperature, chemical and visual analysis by scanning electron microscope. During the second task, the crumb rubber sources were

reacted at various concentrations (5, 10, 15, and 20% by weight of binder) with two binder sources. Drained binder samples were also obtained to determine the particle and interaction effects of the crumb rubber on the various binders. Subsequently, binder tests were performed on the binders in order to determine which factors had the most effect on the development of binder properties.

Once the critical parameters were established, other test data was obtained from research projects conducted at other labs. Doing so allowed a broader model to be developed, a model which would not be specific to one specific tester and lab facility. Ultimately a total of 17 virgin binder sources from 10 separate regions were evaluated; a further 12 crumb rubber sources were used in conjunction with the various binder sources. These crumb rubber sources used various gradations, grinding mechanisms, and tire types thus allowing numerous variables to be taken into consideration. Three distinct models were developed during this research, these were:

1. Viscosity model: this model permitted the estimation of CRM binder viscosity as a function of crumb rubber content (0-20%) and temperature (135-190^{o}C). The starting parameters for this model were the virgin binder viscosity at 135^{o}C and the crumb rubber type (ambient or cryogenic).
2. G*/sinδ and failure temperature model: this model permitted the estimation of CRM binder's G*/sinδ value and failure temperature as a function of crumb rubber content (0-20%) and temperature (64-94^{o}C). The starting parameters for this model were the virgin binder G*/sinδ value at 64^{o}C or the failure temperature and the crumb rubber type (ambient or cryogenic).

3. Universal model: this model permitted the estimation of the CRM binder G*/sinδ value and failure temperature as a function of crumb rubber content (0-20%). The starting parameters for this model were the virgin binder viscosity at 135°C and the type of crumb rubber (ambient or cryogenic).

The nonlinear empirical models for estimation of CRM binder properties were developed using the nonlinear least squares method. The accuracy of the various models was evaluated by identifying 95% confidence intervals for the binder property estimation. Validation of the models was performed using a fractional factorial design with previously untested CRM binders.

Conclusions

- There is evidence to suggest that increasing crumb rubber concentrations, regardless of crumb rubber or binder type, results in increasing viscosities, failure temperatures, and G*/sinδ values. This confirms that as crumb rubber is added to the binder, the rutting resistance and viscosity are increased; however, the extent of this increase is dependent on the type of binder and crumb rubber properties.
- The effect of the crumb rubber in the binder tends to enhance the effects of the base binder. Therefore, increases in the rutting resistance of CRM binders are still related to the base binder properties. This indicates that, for CRM binder, the properties of the base binder typically have a greater influence on the rutting susceptibility and viscosity of the binder than the properties of the crumb rubber used in the matrix.

- Examination of the interaction and particle effects (IE and PE) indicated that the effects of the crumb rubber on the binder increase as the crumb rubber concentration increases. Particle effects of ambient ground crumb rubbers are generally seen to be higher than particle effects for cryogenically ground crumb rubbers. The particle effect for failure temperature and G*/sinδ of CRM binders is thought to be influenced by the surface morphology of the particle. Findings form the IE and PE indicate that the reaction between rubber and asphalt is largely a physical one, and less due to interaction effects between the crumb rubber and binder..
- From the experimental data it was possible to develop a nonlinear empirical model depicting the viscosity of modified asphalt binders between the temperatures of 135°C and 190°C. Furthermore, this model was seen to be accurate for virgin, polymer modified, and CRM binders in this limited research work. The accuracy of the model was found to be within +/- 0.8 Pa-s. Such a level of precision allows conservative estimates of binder viscosity to be made using the 95% upper confidence interval.
- During the development of the model, the Rubber coefficient for viscosity (R_{cv}) was identified as being critical to the accurate determination of CRM binder properties. This term provides a number which may be used to determine the impact of the specific crumb rubber on the specific binder.
- It was possible to develop an empirical model depicting the changes in G*/sinδ values and failure temperature. The Rubber coefficient for G*/sinδ (R_{cg}), was an

important parameter when estimating the rutting susceptibility of a CRM binder, analysis of the R_{cg} indicated that ambient ground crumb rubber yielded higher R_{cg} values and, therefore, also higher G*/sinδ values.

- The lower confidence interval was found to be the most conservative value. Using the value corresponding to the lower end of the 95% confidence interval, the probability of selecting an inaccurately high failure temperature was reduced to less than 2.5%.
- The universal model showed that it is possible to develop empirical relationships describing the change in G*/sinδ as a function of temperature, virgin binder viscosity, and crumb rubber concentration. The 95% confidence interval for determination of G*/sinδ of binders was found to be approximately +/- 0.5 kPa.
- The 95% confidence intervals used for the estimation of failure temperature and crumb rubber concentration were 2.7^{o}C and 2% crumb rubber (by binder weight), respectively.
- It is suggested that the lower 95% confidence interval be used together with the predicted value as doing so reduces the probability of producing excessively high predicted values to less than 2.5%. Specifically, in the case of failure temperature and G*/sinδ it is preferable to obtain a conservative value rather than obtaining inaccurately high values.
- An exponential growth model was seen to provide a realistic trend of the change in G*/sinδ of binder using both crumb rubber concentration and the temperature as exponents. The rutting susceptibility was shown by the model to increase with

the addition of crumb rubber and decrease with an increase in temperature. Both of these trends are consistent with how the literature describes the change of CRM binder G*/sinδ with respect to temperature and crumb rubber concentration.

Recommendations

- Further testing is required with more binders, specifically the effects of the addition of crumb rubber to other performance grades of binders is of interest. Such testing would reveal the consistency of the trend for temperature less than 64^{o}C.
- It is also suggested that more research is needed in this area to generalize the findings, specifically in the area of generating more R_{cv} and R_{cg} data. In particular, it would be useful to develop more R_{cv} and R_{cg} data for other binders.
- Further research should be undertaken investigating the possibilities of modeling other binder properties such as low failure temperature, and rate of aging of modified binders.
- For viscosity predictions it is recommended to use the upper confidence interval value. Doing so provides a conservative value, and also presents a value which has a probability of 2.5% of being exceeded.
- For failure temperature predications it is recommended to use the lower confidence interval value. This provides a conservative value, and also presents a temperature which has a probability of 97.5% of being exceeded.

- For G*/sinδ predications it is recommended to use the lower confidence interval value. This provides a conservative value, and also presents a G*/sinδ value which has a probability of 97.5% of being exceeded. Using the lower confidence interval provides a minimum expected value.

APPENDICES

Appendix A

Crumb Rubber Elemental Analysis Test Data

Table A.1: Crumb rubber elemental analysis data for Carbon

Crumb Rubber Source	Crumb Rubber Type	% Weight Carbon			
		Raw Data	Average	Standard Deviation	Coefficient of Variation
1	C	78.14 84.51 88.83 88.01 86.62 87.52	85.61	3.94	4.61%
2	C	82.36 84.55 85.23 83.38 86.37 84.05	84.32	1.41	1.67%
3	A	87.62 85.52 85.26 83.64 97.81 91.47	88.55	5.28	5.96%
4	A	83.95 87.58 86.35 91.02 92.76 83.45	87.52	3.75	4.29%

Table A.2: Crumb rubber elemental analysis data for Oxygen

Crumb Rubber Source	Crumb Rubber Type	% Weight Oxygen			
		Raw Data	Average	Standard Deviation	Coefficient of Variation
1	C	17.73 10.98 7.96 9.49 10.35 7.02	10.59	3.80	35.85%
2	C	13.69 9.86 11.1 12.13 9.82 11.87	11.41	1.48	12.97%
3	A	9.34 8.57 10.14 10.45 12.54 9.73	10.13	1.35	13.34%
4	A	10.22 5.72 9.66 3.98 3.38 7.52	6.75	2.87	42.54%

Table A.3: Crumb rubber elemental analysis data for Aluminum

Crumb Rubber Source	Crumb Rubber Type	% Weight, Aluminum			
		Raw Data	Average	Standard Deviation	Coefficient of Variation
1	C	0.29 0.26 0.13 0.15 0.27 0.65	0.29	0.19	64.34%
2	C	0 0.34 0 0 0.32 0.19	0.14	0.16	115.42%
3	A	0 0 0 0 1.2 0.52	0.29	0.49	172.12%
4	A	0 0 0 0 0 0.48	0.08	0.20	244.95%

Table A.4: Crumb rubber elemental analysis data for Silicon

Crumb Rubber Source	Crumb Rubber Type	% Weight, Silicon			
		Raw Data	Average	Standard Deviation	Coefficient of Variation
1	C	0.54 0.32 0.23 0.12 0.2 0	0.24	0.18	78.45%
2	C	0.36 0.63 0.46 0.51 0.28 0.61	0.48	0.14	29.01%
3	A	0 0 0 0.27 3.59 0.27	0.69	1.43	207.41%
4	A	0.25 0 0 0 0 0	0.04	0.10	244.95%

Table A.5: Crumb rubber elemental analysis data for Sulfur

Crumb Rubber Source	Crumb Rubber Type	% Weight, Sulfur			
		Raw Data	Average	Standard Deviation	Coefficient of Variation
1	C	1.5 2.23 1.67 1.51 1.42 2.11	1.74	0.34	19.82%
2	C	1.12 2.04 1.69 1.61 1.99 2.36	1.80	0.43	23.78%
3	A	1.42 2.69 2.34 2.58 1.4 2.13	2.09	0.56	26.93%
4	A	2.56 3.97 2.51 2.06 2.21 2.25	2.59	0.70	27.01%

Table A.6: Crumb rubber elemental analysis data for Calcium

Crumb Rubber Source	Crumb Rubber Type	% Weight, Calcium			
		Raw Data	Average	Standard Deviation	Coefficient of Variation
1	C	1.01 0.41 0 0 0 0.26	0.28	0.40	141.55%
2	C	0 0 0.22 0 0 0	0.04	0.09	244.95%
3	A	0.16 0 0 0.19 0 0.49	0.14	0.19	137.10%
4	A	0 0 0 0 0 0	0.00	0.00	-

Table A.7: Crumb rubber elemental analysis data for Chlorine

Crumb Rubber Source	Crumb Rubber Type	% Weight, Chlorine			
		Raw Data	Average	Standard Deviation	Coefficient of Variation
1	C	0 0 0 0 0 0	0.00	0.00	-
2	C	0 0 0 0 0 0	0.00	0.00	-
3	A	0 0 0 0 0 0	0.00	0.00	-
4	A	0 0 0 1.82 0 0	0.30	0.74	244.95%

Table A.8: Crumb rubber elemental analysis data for Iron

Crumb Rubber Source	Crumb Rubber Type	% Weight, Iron			
		Raw Data	Average	Standard Deviation	Coefficient of Variation
1	C	0 0 0 0 0.19 0	0.03	0.08	244.95%
2	C	0.5 0 1.31 0.53 0 0	0.39	0.52	132.46%
3	A	0 0 0 0 0 0	0.00	0.00	-
4	A	0.25 0 0 0 0 0	0.04	0.10	244.95%

Table A.9: Crumb rubber elemental analysis data for Zinc

Crumb Rubber Source	Crumb Rubber Type	% Weight, Zinc			
		Raw Data	Average	Standard Deviation	Coefficient of Variation
1	C	0.79 1.3 1.18 0.72 0.96 2.45	1.23	0.64	51.57%
2	C	1.98 2.58 0 1.84 1.22 0.92	1.42	0.91	63.95%
3	A	1.45 3.22 2.25 2.87 1.52 3.34	2.44	0.83	34.10%
4	A	2.76 2.72 1.48 1.12 1.65 2.84	2.10	0.76	36.44%

Appendix B

CRM Binder Viscosity Experimental Data

Table B.1:CRM binder viscosity experimental data for crumb rubber Source 1

CRM Source	Binder Source	% CRM*	CRM Type+	Viscosity, Cp Raw Data			Mean	Standard Deviation	Coefficient of Variation
1	A	0	0	647.5	650.0	635.0	645.0	7.6	1.2%
				650.0	650.0	635.0			
				652.5	650.0	635.0			
		5	C	837.5	850.0	912.5	863.9	37.7	4.4%
				825.0	850.0	912.5			
				825.0	850.0	912.5			
		10	C	1888.0	1700.0	1525.0	1679.2	158.9	9.5%
				1875.0	1663.0	1487.0			
				1837.0	1638.0	1500.0			
		15	C	2850.0	2750.0	2912.0	2844.3	77.3	2.7%
				2838.0	2787.0	2912.0			
				2825.0	2750.0	2975.0			
		20	C	4750.0	5113.0	5175.0	5011.1	213.4	4.3%
				4787.0	5050.0	5238.0			
				4675.0	5175.0	5137.0			
	B	0	0	512.5	435.0	455.0	466.1	32.4	7.0%
				512.5	437.5	455.0			
				497.5	435.0	455.0			
		5	C	500.0	487.5	487.5	493.1	6.6	1.3%
				500.0	487.5	487.5			
				500.0	487.5	500.0			
		10	C	787.5	862.5	1112.0	920.7	144.7	15.7%
				787.5	862.5	1112.0			
				787.5	875.0	1100.0			
		15	C	1337.0	1212.0	1650.0	1404.0	180.8	12.9%
				1337.0	1212.0	1625.0			
				1375.0	1263.0	1625.0			
		20	C	2100.0	1875.0	2500.0	2138.9	253.7	11.9%
				2075.0	1862.0	2438.0			
				2075.0	1900.0	2425.0			

*by weight of binder
+0: Virgin; A: Ambient; C: Cryogenic

Table B.2:CRM binder viscosity experimental data for crumb rubber Source 2

CRM Source	Binder Source	% CRM*	CRM Type+	Viscosity, Cp Raw Data			Mean	Standard Deviation	Coefficient of Variation
2	A	0	0	647.5	650.0	635.0	645.0	7.6	1.2%
				650.0	650.0	635.0			
				652.5	650.0	635.0			
		5	C	862.5	850.0	800.0	836.1	30.9	3.7%
				862.5	850.0	800.0			
				862.5	850.0	787.5			
		10	C	1050.0	1013.0	1050.0	1029.3	20.7	2.0%
				1038.0	1000.0	1025.0			
				1038.0	1000.0	1050.0			
		15	C	2563.0	3100.0	3362.0	2996.0	346.0	11.5%
				2575.0	3088.0	3375.0			
				2563.0	3013.0	3325.0			
		20	C	6588.0	7200.0	7025.0	6947.2	352.4	5.1%
				6488.0	7200.0	7050.0			
				6412.0	7275.0	7287.0			
	B	0	0	512.5	435.0	455.0	466.1	32.4	7.0%
				512.5	437.5	455.0			
				497.5	435.0	455.0			
		5	C	675.0	537.5	550.0	581.9	61.3	10.5%
				650.0	537.5	550.0			
				662.5	525.0	550.0			
		10	C	762.5	700.0	712.5	726.4	33.3	4.6%
				762.5	687.5	725.0			
				775.0	687.5	725.0			
		15	C	1288.0	1587.0	1938.0	1605.4	291.5	18.2%
				1300.0	1587.0	1987.0			
				1250.0	1587.0	1925.0			
		20	C	2388.0	3225.0	2487.0	2684.8	392.8	14.6%
				2388.0	3263.0	2450.0			
				2325.0	3112.0	2525.0			

*by weight of binder
+0: Virgin; A: Ambient; C: Cryogenic

Table B.3: CRM binder viscosity experimental data for CRM Source 3

CRM Source	Binder Source	% CRM*	CRM Type+	Viscosity, Cp Raw Data			Mean	Standard Deviation	Coefficient of Variation
3	A	0	0	647.5	650.0	635.0	645.0	7.6	1.2%
				650.0	650.0	635.0			
				652.5	650.0	635.0			
		5	A	962.5	875.0	1000.0	943.1	52.7	5.6%
				962.5	875.0	987.5			
				962.5	875.0	987.5			
		10	A	2750.0	2625.0	3263.0	2861.2	302.5	10.6%
				2737.0	2588.0	3213.0			
				2725.0	2563.0	3287.0			
		15	A	4350.0	4313.0	4488.0	4384.9	112.9	2.6%
				4325.0	4300.0	4600.0			
				4338.0	4262.0	4488.0			
		20	A	10450.0	12213.0	11000.0	11208.3	723.9	6.5%
				10362.0	12062.0	11000.0			
				10700.0	12088.0	11000.0			
	B	0	0	512.5	435.0	455.0	466.1	32.4	7.0%
				512.5	437.5	455.0			
				497.5	435.0	455.0			
		5	A	612.5	550.0	575.0	579.2	27.2	4.7%
				612.5	550.0	575.0			
				612.5	550.0	575.0			
		10	A	1150.0	1087.0	1438.0	1214.0	151.9	12.5%
				1125.0	1100.0	1388.0			
				1150.0	1075.0	1413.0			
		15	A	1788.0	2775.0	2825.0	2450.0	497.5	20.3%
				1775.0	2750.0	2813.0			
				1800.0	2737.0	2787.0			
		20	A	6938.0	6775.0	7412.0	6954.3	221.5	3.2%
				6813.0	6813.0	7113.0			
				6775.0	6813.0	7137.0			

*by weight of binder
+0: Virgin; A: Ambient; C: Cryogenic

Table B.4: CRM binder viscosity experimental data for CRM Source 4

CRM Source	Binder Source	% CRM*	CRM Type+	Viscosity, Cp Raw Data			Mean	Standard Deviation	Coefficient of Variation
4	A	0	0	647.5	650.0	635.0	645.0	7.6	1.2%
				650.0	650.0	635.0			
				652.5	650.0	635.0			
		5	A	1138.0	1100.0	1138.0	1118.0	14.4	1.3%
				1125.0	1100.0	1112.0			
				1112.0	1112.0	1125.0			
		10	A	1825.0	2075.0	2225.0	2041.7	181.1	8.9%
				1825.0	2050.0	2250.0			
				1825.0	2050.0	2250.0			
		15	A	6275.0	6225.0	6600.0	6333.3	192.8	3.0%
				6400.0	6025.0	6550.0			
				6150.0	6275.0	6500.0			
		20	A	20850.0	19425.0	21300.0	20186.1	744.8	3.7%
				19750.0	19350.0	20625.0			
				19700.0	19700.0	20975.0			
	B	0	0	512.5	435.0	455.0	466.1	32.4	7.0%
				512.5	437.5	455.0			
				497.5	435.0	455.0			
		5	A	700.0	812.5	962.5	819.4	106.5	13.0%
				687.5	837.5	925.0			
				687.5	850.0	912.5			
		10	A	950.0	925.0	1163.0	1012.6	113.4	11.2%
				950.0	912.5	1150.0			
				950.0	937.5	1175.0			
		15	A	3600.0	3063.0	3737.0	3434.8	299.1	8.7%
				3588.0	3037.0	3700.0			
				3463.0	3050.0	3675.0			
		20	A	5213.0	4762.0	5150.0	4946.1	279.0	5.6%
				4988.0	4613.0	5025.0			
				5113.0	4438.0	5213.0			

*by weight of binder
+0: Virgin; A: Ambient; C: Cryogenic

Appendix C

G*/sinδ results of CRM binder from binder Sources A and B

Table C.1: G*/sinδ results of CRM binders made with CRM Source 1 tested at 64°C

CRM Source	Binder Source	% CRM*	CRM Type+	G*/sinδ, kPa			
				Raw Data	Mean	Standard Deviation	Coefficient of Variation
1	A	0	0	1.96 2.14	2.05	0.13	6.21%
		5	C	3.19 3.07	3.13	0.08	2.71%
		10	C	7.43 7.01	7.22	0.30	4.11%
		15	C	11.29 10.07	10.68	0.86	8.08%
		20	C	14.85 13.29	14.07	1.10	7.84%
	B	0	0	1.24 1.27	1.26	0.02	1.69%
		5	C	1.78 1.70	1.74	0.06	3.25%
		10	C	3.17 3.04	3.11	0.09	2.96%
		15	C	4.51 4.36	4.44	0.11	2.39%
		20	C	7.10 7.02	7.06	0.06	0.80%

*by weight of binder
+0: Virgin; A: Ambient; C: Cryogenic

Table C.2: G*/sinδ results of CRM binders made with CRM Source 1 tested at 76°C

CRM Source	Binder Source	% CRM*	CRM Type+	G*/sinδ, kPa			
				Raw Data	Mean	Standard Deviation	Coefficient of Variation
1	A	0	0	n/a n/a	n/a	n/a	n/a
		5	C	0.84 0.83	0.84	0.01	0.85%
		10	C	1.95 2.01	1.98	0.04	2.14%
		15	C	3.01 2.74	2.88	0.19	6.64%
		20	C	4.10 3.67	3.89	0.30	7.83%
	B	0	0	- -	-	-	-
		5	C	- -	-	-	-
		10	C	0.78 0.76	0.77	0.01	1.84%
		15	C	1.09 1.05	1.07	0.03	2.64%
		20	C	1.77 1.76	1.77	0.01	0.40%

*by weight of binder
+0: Virgin; A: Ambient; C: Cryogenic

Table C.3: G*/sinδ results of CRM binders made with CRM Source 2 tested at 64°C

CRM Source	Binder Source	% CRM*	CRM Type+	G*/sinδ, kPa			
				Raw Data	Mean	Standard Deviation	Coefficient of Variation
2	A	0	0	1.96 2.14	2.05	0.13	6.21%
		5	C	4.25 3.88	4.07	0.26	6.44%
		10	C	4.71 4.45	4.58	0.18	4.01%
		15	C	9.14 10.18	9.66	0.74	7.61%
		20	C	13.52 14.08	13.80	0.40	2.87%
	B	0	0	1.24 1.27	1.26	0.02	1.69%
		5	C	1.72 1.79	1.76	0.05	2.82%
		10	C	2.72 2.68	2.70	0.03	1.05%
		15	C	4.19 4.06	4.13	0.09	2.23%
		20	C	8.88 8.48	8.68	0.28	3.26%

*by weight of binder
+0: Virgin; A: Ambient; C: Cryogenic

Table C.4: G*/sinδ results of CRM binders made with CRM Source 2 tested at 76°C

CRM Source	Binder Source	% CRM*	CRM Type+	G*/sinδ, kPa			
				Raw Data	Mean	Standard Deviation	Coefficient of Variation
2	A	0	0	- -	-	-	-
		5	C	1.10 1.04	1.07	0.04	3.97%
		10	C	1.25 1.18	1.22	0.05	4.07%
		15	C	2.62 2.68	2.65	0.04	1.60%
		20	C	3.77 3.92	3.85	0.11	2.76%
	B	0	0	- -	-	-	-
		5	C	- -	-	-	-
		10	C	0.70 0.69	0.70	0.01	1.02%
		15	C	1.05 0.99	1.02	0.04	4.16%
		20	C	2.25 2.18	2.22	0.05	2.23%

*by weight of binder
+0: Virgin; A: Ambient; C: Cryogenic

Table C.5: G*/sinδ results of CRM binders made with CRM Source 3 tested at 64°C

CRM Source	Binder Source	% CRM*	CRM Type+	G*/sinδ, kPa			
				Raw Data	Mean	Standard Deviation	Coefficient of Variation
3	A	0	0	1.96 2.14	2.05	0.13	6.21%
		5	A	3.38 3.19	3.29	0.13	4.09%
		10	A	5.64 5.25	5.45	0.28	5.06%
		15	A	14.35 13.75	14.05	0.42	3.02%
		20	A	19.70 18.10	18.90	1.13	5.99%
	B	0	0	1.24 1.27	1.26	0.02	1.69%
		5	A	1.88 1.87	1.88	0.01	0.38%
		10	A	2.84 2.44	2.64	0.28	10.71%
		15	A	4.88 4.70	4.79	0.13	2.66%
		20	A	6.58 6.54	6.56	0.03	0.43%

*by weight of binder
+0: Virgin; A: Ambient; C: Cryogenic

Table C.6: G*/sinδ results of CRM binders made with CRM Source 3 tested at 76°C

CRM Source	Binder Source	% CRM*	CRM Type+	G*/sinδ, kPa			
				Raw Data	Mean	Standard Deviation	Coefficient of Variation
3	A	0	0	- -	-	-	-
		5	A	0.83 0.84	0.84	0.01	0.85%
		10	A	1.49 1.44	1.47	0.04	2.41%
		15	A	4.21 3.93	4.07	0.20	4.86%
		20	A	6.36 5.83	6.10	0.37	6.15%
	B	0	0	- -	-	-	-
		5	A	- -	-	-	-
		10	A	0.62 0.62	0.62	0.00	0.00%
		15	A	1.29 1.20	1.25	0.06	5.11%
		20	A	1.76 1.67	1.72	0.06	3.71%

*by weight of binder
+0: Virgin; A: Ambient; C: Cryogenic

Table C.7: G*/sinδ results of CRM binders made with CRM Source 4 tested at 64°C

CRM Source	Binder Source	% CRM*	CRM Type+	G*/sinδ, kPa			
				Raw Data	Mean	Standard Deviation	Coefficient of Variation
4	A	0	0	1.96 2.14	2.05	0.13	6.21%
		5	A	4.14 3.78	3.96	0.25	6.43%
		10	A	9.19 8.54	8.87	0.46	5.18%
		15	A	14.34 12.92	13.63	1.00	7.37%
		20	A	22.68 24.26	23.47	1.12	4.76%
	B	0	0	1.24 1.27	1.26	0.02	1.69%
		5	A	2.71 2.31	2.51	0.28	11.27%
		10	A	4.97 4.97	4.97	0.00	0.00%
		15	A	7.13 6.36	6.75	0.54	8.07%
		20	A	11.61 10.77	11.19	0.59	5.31%

*by weight of binder
+0: Virgin; A: Ambient; C: Cryogenic

Table C.8: G*/sinδ results of CRM binders made with CRM Source 4 tested at 76°C

CRM Source	Binder Source	% CRM*	CRM Type+	G*/sinδ, kPa			
				Raw Data	Mean	Standard Deviation	Coefficient of Variation
4	A	0	0	- -	-	-	-
		5	A	1.09 1.00	1.05	0.06	6.09%
		10	A	2.75 2.46	2.61	0.21	7.87%
		15	A	3.99 4.05	4.02	0.04	1.06%
		20	A	7.27 6.77	7.02	0.35	5.04%
	B	0	0	- -	-	-	-
		5	A	0.73 0.56	0.65	0.12	18.64%
		10	A	1.32 1.30	1.31	0.01	1.08%
		15	A	1.87 1.67	1.77	0.14	7.99%
		20	A	3.14 2.99	3.07	0.11	3.46%

*by weight of binder
+0: Virgin; A: Ambient; C: Cryogenic

Appendix D

Experimental Drained CRM Binder Viscosity Data

Table D.1: Viscosity results of drained CRM binder made with CRM Source 1 at 135°C

CRM Source	Binder Source	% CRM*	CRM Type+	Viscosity, Cp Raw Data			Mean	Standard Deviation	Coefficient of Variation
1	A	0	0	647.5	650.0	635.0	645.0	7.6	1.2%
				650.0	650.0	635.0			
				652.5	650.0	635.0			
		10	C	922.5	867.5	965.0	918.1	41.4	4.5%
				925.0	870.0	962.5			
				925.0	865.0	960.0			
		20	C	1372.0	1405.0	1428.0	1399.8	23.9	1.7%
				1370.0	1400.0	1425.0			
				1375.0	1395.0	1428.0			
	B	0	0	512.5	435.0	455.0	466.1	32.4	7.0%
				512.5	437.5	455.0			
				497.5	435.0	455.0			
		10	C	530.0	542.5	560.0	545.6	13.5	2.5%
				532.5	545.0	562.5			
				530.0	545.0	562.5			
		20	C	845.0	637.5	670.0	717.5	97.2	13.6%
				847.5	637.5	670.0			
				845.0	637.5	667.5			

*by weight of binder
+0: Virgin; A: Ambient; C: Cryogenic

Table D.2: Viscosity results of drained CRM binder made with CRM Source 2 at 135°C

CRM Source	Binder Source	% CRM*	CRM Type+	Viscosity, Cp Raw Data			Mean	Standard Deviation	Coefficient of Variation
2	A	0	0	647.5	650.0	635.0	645.0	7.6	1.2%
				650.0	650.0	635.0			
				652.5	650.0	635.0			
		10	C	832.5	855.0	857.5	848.6	12.4	1.5%
				832.5	852.5	857.5			
				832.5	855.0	862.5			
		20	C	1298.0	1408.0	1553.0	1418.7	107.3	7.6%
				1303.0	1403.0	1550.0			
				1305.0	1405.0	1543.0			
	B	0	0	512.5	435.0	455.0	466.1	32.4	7.0%
				512.5	437.5	455.0			
				497.5	435.0	455.0			
		10	C	485.0	502.5	500.0	494.7	9.4	1.9%
				482.5	500.0	502.5			
				480.0	497.5	502.5			
		20	C	772.5	610.0	622.5	668.1	77.9	11.7%
				772.5	610.0	622.5			
				770.0	610.0	622.5			

*by weight of binder
+0: Virgin; A: Ambient; C: Cryogenic

Table D.3: Viscosity results of drained CRM binder made with CRM Source 3 at 135°C

CRM Source	Binder Source	% CRM*	CRM Type+	Viscosity, Cp Raw Data			Mean	Standard Deviation	Coefficient of Variation
3	A	0	0	647.5	650.0	635.0	645.0	7.6	1.2%
				650.0	650.0	635.0			
				652.5	650.0	635.0			
		10	A	837.5	857.5	965.0	888.9	60.4	6.8%
				837.5	860.0	970.0			
				840.0	862.5	970.0			
		20	A	1275.0	1265.0	1290.0	1275.6	10.8	0.8%
				1280.0	1265.0	1286.0			
				1278.0	1258.0	1283.0			
	B	0	0	512.5	435.0	455.0	466.1	32.4	7.0%
				512.5	437.5	455.0			
				497.5	435.0	455.0			
		10	A	485.0	490.0	495.0	489.4	3.3	0.7%
				487.5	487.5	492.5			
				487.5	487.5	492.5			
		20	A	617.5	630.0	797.5	681.9	85.5	12.5%
				620.0	630.0	795.0			
				622.5	630.0	795.0			

*by weight of binder
+0: Virgin; A: Ambient; C: Cryogenic

Table D.4: Viscosity results of drained CRM binder made with CRM Source 4 at 135°C

CRM Source	Binder Source	% CRM*	CRM Type+	Viscosity, Cp Raw Data			Mean	Standard Deviation	Coefficient of Variation
2	A	0	0	647.5	650.0	635.0	645.0	7.6	1.2%
				650.0	650.0	635.0			
				652.5	650.0	635.0			
		10	A	1025.0	955.0	920.0	966.1	43.5	4.5%
				1020.0	950.0	925.0			
				1020.0	952.5	927.5			
		20	A	1533.0	1615.0	1740.0	1626.8	92.8	5.7%
				1528.0	1610.0	1737.0			
				1523.0	1610.0	1745.0			
	B	0	0	512.5	435.0	455.0	466.1	32.4	7.0%
				512.5	437.5	455.0			
				497.5	435.0	455.0			
		10	A	472.5	475.0	485.0	477.5	6.7	1.4%
				470.0	475.0	485.0			
				470.0	477.5	487.5			
		20	A	677.5	702.5	705.0	694.2	13.8	2.0%
				675.0	702.5	702.5			
				675.0	705.0	702.5			

*by weight of binder
+0: Virgin; A: Ambient; C: Cryogenic

Appendix E

Experimental Drained G*/sinδ Data

Table E.1: G*/sinδ results of drained CRM binder made with CRM Source 1

CRM Source	Binder Source	% CRM*	CRM Type+	Temperature °C	G*/sinδ, kPa			
					Raw Data	Mean	Standard Deviation	Coefficient of Variation
1	A	0	0	64	1.96 2.14	2.05	0.13	6.27%
		10	C		5.88 5.76	5.82	0.08	1.46%
		20	C		10.12 9.84	9.98	0.20	1.98%
	B	0	0		1.24 1.27	1.26	0.02	1.69%
		10	C		2.65 2.12	2.39	0.37	15.71%
		20	C		2.72 2.75	2.74	0.02	0.78%
	A	0	0	76	- -	-	-	-
		10	C		1.36 1.40	1.38	0.03	2.05%
		20	C		2.39 2.34	2.37	0.04	1.49%
	B	0	0		n/a n/a	n/a	n/a	n/a
		10	C		0.60 0.62	0.61	0.01	2.32%
		20	C		0.58 0.60	0.59	0.01	2.40%

*by weight of binder
+0: Virgin; A: Ambient; C: Cryogenic

Table E.2: G*/sinδ results of drained CRM binder made with CRM Source 2

CRM Source	Binder Source	% CRM*	CRM Type+	Temperature °C	G*/sinδ, kPa			
					Raw Data	Mean	Standard Deviation	Coefficient of Variation
2	A	0	0	64	1.96 2.14	2.05	0.13	6.27%
		10	C		3.74 3.35	3.55	0.28	7.78%
		20	C		7.41 8.29	7.85	0.62	7.93%
	B	0	0		1.24 1.27	1.26	0.02	1.69%
		10	C		2.64 1.96	2.30	0.48	20.91%
		20	C		6.48 5.42	5.95	0.75	12.60%
	A	0	0	76	- -	-	-	-
		10	C		0.92 0.82	0.87	0.07	8.13%
		20	C		1.85 2.03	1.94	0.13	6.56%
	B	0	0		- -	-	-	-
		10	C		- -	-	-	-
		20	C		1.36 1.18	1.27	0.13	10.02%

*by weight of binder
+0: Virgin; A: Ambient; C: Cryogenic

Table E.3: G*/sinδ results of drained CRM binder made with CRM Source 3

CRM Source	Binder Source	% CRM*	CRM Type+	Temperature °C	G*/sinδ, kPa			
					Raw Data	Mean	Standard Deviation	Coefficient of Variation
3	A	0	0	64	1.96 2.14	2.05	0.13	6.27%
		10	C		3.64 3.37	3.51	0.19	5.45%
		20	C		7.33 6.60	6.97	0.52	7.41%
	B	0	0		1.24 1.27	1.26	0.02	1.69%
		10	C		2.58 1.92	2.25	0.47	20.74%
		20	C		3.06 2.52	2.79	0.38	13.69%
	A	0	0	76	- -	-	-	-
		10	C		0.88 0.80	0.84	0.06	6.73%
		20	C		1.80 1.69	1.75	0.08	4.46%
	B	0	0		- -	-	-	-
		10	C		0.54 0.52	0.53	0.01	2.67%
		20	C		0.66 0.57	0.62	0.06	10.35%

*by weight of binder
+0: Virgin; A: Ambient; C: Cryogenic

Table E.4: G*/sinδ results of drained CRM binder made with CRM Source 4

CRM Source	Binder Source	% CRM*	CRM Type+	Temperature °C	G*/sinδ, kPa			
					Raw Data	Mean	Standard Deviation	Coefficient of Variation
4	A	0	0	64	1.96 2.14	2.05	0.13	6.27%
		10	C		4.66 4.66	4.66	0.00	0.00%
		20	C		12.14 11.77	11.96	0.26	2.19%
	B	0	0		1.24 1.27	1.26	0.02	1.69%
		10	C		1.97 1.94	1.96	0.02	1.09%
		20	C		3.95 3.75	3.85	0.14	3.67%
	A	0	0	76	- -	-	-	-
		10	C		1.16 1.14	1.15	0.01	1.23%
		20	C		2.90 2.72	2.81	0.13	4.53%
	B	0	0		- -	-	-	-
		10	C		- -	-	-	-
		20	C		0.87 0.85	0.86	0.01	1.64%

*by weight of binder
+0: Virgin; A: Ambient; C: Cryogenic

Appendix F

Experimental Data for Failure Temperature

Table F.1: Experimental data for failure temperature for CRM Source 1

CRM Source	Binder Source	% CRM*	CRM Type+	Failure Temperature, °C			
				Raw Data	Mean	Standard Deviation	Coefficient of Variation
1	A	0	0	69.8 70.4	70.1	0.4	0.6%
		5	C	74.4 74.1	74.3	0.2	0.3%
		10	C	84.1 82.5	83.3	1.1	1.4%
		15	C	86.9 86.0	86.5	0.6	0.7%
		20	C	90.8 89.1	90.0	1.2	1.3%
	B	0	0	65.7 65.9	65.8	0.1	0.2%
		5	C	68.8 68.4	68.6	0.3	0.4%
		10	C	73.8 73.6	73.7	0.1	0.2%
		15	C	76.8 76.5	76.7	0.2	0.3%
		20	C	81.4 81.4	81.4	0.0	0.0%

*by weight of binder
+0: Virgin; A: Ambient; C: Cryogenic

Table F.2: Experimental data for failure temperature for CRM Source 2

CRM Source	Binder Source	% CRM*	CRM Type+	Failure Temperature, °C			
				Raw Data	Mean	Standard Deviation	Coefficient of Variation
2	A	0	0	69.8 70.4	70.1	0.4	0.6%
		5	C	76.8 76.3	76.6	0.4	0.5%
		10	C	78.0 77.6	77.8	0.3	0.4%
		15	C	84.8 85.9	85.4	0.8	0.9%
		20	C	89.5 89.8	89.7	0.2	0.2%
	B	0	0	65.7 65.9	65.8	0.1	0.2%
		5	C	68.4 70.3	69.4	1.3	1.9%
		10	C	72.7 72.6	72.7	0.1	0.1%
		15	C	76.5 75.9	76.2	0.4	0.6%
		20	C	83.9 83.7	83.8	0.1	0.2%

*by weight of binder
+0: Virgin; A: Ambient; C: Cryogenic

Table F.3: Experimental data for failure temperature for CRM Source 3

CRM Source	Binder Source	% CRM*	CRM Type+	Failure Temperature, °C			
				Raw Data	Mean	Standard Deviation	Coefficient of Variation
3	A	0	0	69.8 70.4	70.1	0.4	0.6%
		5	A	74.4 74.4	74.4	0.0	0.0%
		10	A	82.3 79.4	80.9	2.1	2.5%
		15	A	91.1 89.7	90.4	1.0	1.1%
		20	A	95.8 94.3	95.1	1.1	1.1%
	B	0	0	65.7 65.9	65.8	0.1	0.2%
		5	A	69.4 69.3	69.4	0.1	0.1%
		10	A	72.3 71.8	72.1	0.4	0.5%
		15	A	78.5 77.8	78.2	0.5	0.6%
		20	A	81.3 80.9	81.1	0.3	0.3%

*by weight of binder
+0: Virgin; A: Ambient; C: Cryogenic

Table F.4: Experimental data for failure temperature for CRM Source 4

CRM Source	Binder Source	% CRM*	CRM Type+	Failure Temperature, °C			
				Raw Data	Mean	Standard Deviation	Coefficient of Variation
4	A	0	0	69.8 70.4	70.1	0.4	0.6%
		5	A	76.7 76.0	76.4	0.5	0.6%
		10	A	87.3 84.8	86.1	1.8	2.1%
		15	A	89.9 93.2	91.6	2.3	2.5%
		20	A	93.9 95.2	94.6	0.9	1.0%
	B	0	0	65.7 65.9	65.8	0.1	0.2%
		5	A	73.0 70.8	71.9	1.6	2.2%
		10	A	78.6 78.4	78.5	0.1	0.2%
		15	A	82.4 81.4	81.9	0.7	0.9%
		20	A	88.7 86.7	87.7	1.4	1.6%

*by weight of binder
+0: Virgin; A: Ambient; C: Cryogenic

Appendix G

Experimental Data for Viscosity (Putman)

Table G.1: Viscosity results of CRM binders made with binder Source A tested at 135°C

Binder Source	% CRM*	CRM Type+	CRM Size (mm)	Viscosity, *Pa-s* Raw Data	Mean	Standard Deviation	Coefficient of Variation
A	0	0	0	0.67 0.69 0.73 0.67 0.69 0.73 0.67 0.69 0.73	0.69	0.03	4.02%
	10	A	0.85	2.28 2.34 2.35 2.30 2.35 2.34 2.33 2.36 2.35	2.33	0.03	1.20%
			0.425	2.53 2.56 2.60 2.53 2.56 2.59 2.53 2.56 2.59	2.56	0.03	1.14%
			0.18	2.71 2.73 2.71 2.70 2.71 2.70 2.70 2.71 2.70	2.71	0.01	0.33%
		C	0.85	1.85 1.85 1.93 1.83 1.90 1.85 1.79 1.85 1.86	1.86	0.04	2.13%
			0.425	1.71 1.75 1.75 1.71 1.75 1.74 1.71 1.75 1.74	1.73	0.02	1.02%
			0.18	1.75 1.76 1.78 1.75 1.75 1.76 1.75 1.75 1.76	1.76	0.01	0.52%
	15	A	0.85	4.70 5.00 4.55 4.75 5.74 4.64 4.68 4.63 4.49	4.80	0.38	7.98%
			0.425	5.59 5.40 5.50 5.59 5.38 5.45 5.54 5.38 5.43	5.47	0.09	1.56%
			0.18	6.01 5.96 6.04 5.99 5.94 6.00 5.95 5.90 5.98	5.97	0.04	0.69%
		C	0.85	3.16 3.21 3.31 3.21 3.18 3.26 3.23 3.21 3.30	3.23	0.05	1.60%
			0.425	2.90 3.03 2.99 2.90 3.03 2.96 2.89 3.00 2.96	2.96	0.05	1.82%
			0.18	3.30 3.29 3.34 3.29 3.28 3.33 3.28 3.28 3.33	3.30	0.02	0.75%

*by weight of binder
+0: Virgin; A: Ambient; C: Cryogenic

Table G.2: Viscosity results of CRM binders made with binder Source B tested at 135°C

Binder Source	% CRM*	CRM Type+	CRM Size (mm)	Viscosity, *Pa-s* Raw Data	Mean	Standard Deviation	Coefficient of Variation
B	0	0	0	0.47 0.47 0.47 0.47 0.47 0.47 0.47 0.47 0.47	0.47	0.00	0.23%
	10	A	0.85	1.59 1.63 1.74 1.56 1.31 1.64 1.58 1.33 1.61	1.55	0.14	9.15%
			0.425	1.43 1.40 1.41 1.41 1.39 1.43 1.41 1.39 1.41	1.41	0.01	0.98%
			0.18	1.46 1.45 1.45 1.45 1.44 1.45 1.45 1.44 1.44	1.45	0.01	0.55%
		C	0.85	1.60 1.45 1.38 1.63 1.36 1.38 1.61 1.41 1.39	1.47	0.11	7.66%
			0.425	1.13 1.14 1.11 1.14 1.15 1.11 1.14 1.14 1.11	1.13	0.01	1.27%
			0.18	1.10 1.09 1.08 1.09 1.08 1.08 1.09 1.08 1.08	1.08	0.01	0.83%
	15	A	0.85	2.93 2.84 2.88 2.76 2.86 2.73 2.88 2.81 2.81	2.83	0.06	2.17%
			0.425	3.50 3.58 3.53 3.51 3.56 3.50 3.51 3.53 3.50	3.52	0.03	0.78%
			0.18	3.89 3.94 3.91 3.86 3.91 3.90 3.85 3.89 3.88	3.89	0.03	0.70%
		C	0.85	2.00 2.21 2.26 2.14 2.03 2.20 2.04 2.23 2.16	2.14	0.10	4.53%
			0.425	1.73 1.70 1.79 1.71 1.69 1.79 1.71 1.70 1.78	1.73	0.04	2.32%
			0.18	1.95 1.86 1.85 1.94 1.86 1.85 1.94 1.86 1.85	1.88	0.04	2.31%

*by weight of binder
+0: Virgin; A: Ambient; C: Cryogenic

Table G.3: Viscosity results of CRM binders made with binder Source C tested at 135°C

Binder Source	% CRM*	CRM Type+	CRM Size (mm)	Viscosity, *Pa-s* Raw Data	Mean	Standard Deviation	Coefficient of Variation
C	0	0	0	0.43 0.43 0.43 0.43 0.43 0.43 0.43 0.43 0.43	0.43	0.00	0.54%
	10	A	0.85	1.49 1.39 1.63 1.50 1.40 1.50 1.45 1.35 1.50	1.47	0.08	5.57%
			0.425	1.40 1.30 1.40 1.40 1.29 1.40 1.39 1.30 1.39	1.36	0.05	3.70%
			0.18	1.44 1.46 1.49 1.43 1.46 1.48 1.43 1.45 1.48	1.46	0.02	1.54%
		C	0.85	1.23 1.28 1.19 1.29 1.33 1.19 1.21 1.31 1.24	1.25	0.05	4.16%
			0.425	1.71 1.75 1.75 1.71 1.75 1.74 1.71 1.75 1.74	1.73	0.02	1.02%
			0.18	1.09 1.08 1.06 1.09 1.06 1.06 1.09 1.06 1.06	1.07	0.01	1.09%
	15	A	0.85	3.06 3.14 2.83 3.08 3.03 2.96 3.11 3.29 2.94	3.05	0.13	4.34%
			0.425	3.53 3.55 3.48 3.50 3.55 3.50 3.50 3.53 3.49	3.51	0.03	0.76%
			0.18	3.83 3.85 3.80 3.80 3.84 3.78 3.78 3.81 3.75	3.80	0.03	0.85%
		C	0.85	2.05 2.13 2.18 2.13 2.21 2.29 2.03 2.28 2.21	2.17	0.09	4.25%
			0.425	2.06 1.96 2.00 2.05 1.96 1.99 2.04 1.95 1.98	2.00	0.04	2.09%
			0.18	2.00 1.98 1.95 1.99 1.96 1.94 1.98 1.96 1.94	1.97	0.02	1.08%

*by weight of binder
+0: Virgin; A: Ambient; C: Cryogenic

Appendix H

Experimental Data for G*/sinδ (Putman)

Table H.1: G*/sinδ results of CRM binder made with binder Source A at 64°C

Binder Source	% CRM*	CRM Type+	CRM Size (mm)	G*/sinδ, *kPa*			
				Raw Data	Mean	Standard Deviation	Coefficient of Variation
A	0	0	0	1.98 2.02 2.02	2.01	0.03	1.30%
	10	A	0.85	7.36 7.31 7.23	7.30	0.07	0.96%
			0.425	7.56 7.25 7.32	7.37	0.16	2.19%
			0.18	6.34 6.56 6.28	6.39	0.15	2.30%
		C	0.85	6.16 6.37 6.48	6.33	0.16	2.58%
			0.425	6.22 6.19 6.39	6.27	0.10	1.67%
			0.18	5.72 5.73 5.71	5.72	0.01	0.19%
	15	A	0.85	11.18 10.79 11.69	11.22	0.45	4.04%
			0.425	11.40 11.06 11.20	11.22	0.17	1.49%
			0.18	10.51 10.51 10.47	10.50	0.02	0.20%
		C	0.85	9.75 10.70 11.74	10.73	1.00	9.31%
			0.425	9.77 9.57 9.98	9.77	0.20	2.10%
			0.18	9.80 9.41 9.58	9.60	0.19	2.02%

*by weight of binder
+0: Virgin; A: Ambient; C: Cryogenic

Table H.2: G*/sinδ results of CRM binder made with binder Source A at 76°C

Binder Source	% CRM*	CRM Type+	CRM Size (mm)	G*/sinδ, *kPa*			
				Raw Data	Mean	Standard Deviation	Coefficient of Variation
A	0	0	0	0.53 0.51 0.52	0.52	0.01	2.41%
	10	A	0.85	1.85 1.93 2.35	2.04	0.27	13.25%
			0.425	2.05 2.15 2.08	2.09	0.05	2.43%
			0.18	1.87 1.87 1.86	1.87	0.01	0.54%
		C	0.85	1.62 1.65 1.89	1.72	0.15	8.45%
			0.425	1.62 1.61 1.59	1.61	0.01	0.83%
			0.18	1.60 1.53 1.57	1.57	0.03	2.22%
	15	A	0.85	3.36 3.53 3.49	3.46	0.09	2.57%
			0.425	3.55 3.55 3.63	3.58	0.04	1.25%
			0.18	3.17 3.15 3.14	3.15	0.01	0.45%
		C	0.85	2.86 2.95 3.05	2.95	0.09	3.20%
			0.425	2.68 2.77 2.86	2.77	0.09	3.36%
			0.18	2.64 2.74 2.52	2.64	0.11	4.07%

*by weight of binder
+0: Virgin; A: Ambient; C: Cryogenic

Table H.3: G*/sinδ results of CRM binder made with binder Source B at 64°C

Binder Source	% CRM*	CRM Type+	CRM Size (mm)	G*/sinδ, *kPa*			
				Raw Data	Mean	Standard Deviation	Coefficient of Variation
B	0	0	0	1.54 1.57 1.50	1.54	0.03	2.17%
	10	A	0.85	3.73 3.40 4.01	3.71	0.30	8.10%
			0.425	3.31 3.25 3.34	3.30	0.04	1.35%
			0.18	3.33 3.42 3.31	3.35	0.06	1.77%
		C	0.85	3.72 3.82 3.54	3.69	0.14	3.81%
			0.425	3.18 3.26 3.21	3.21	0.04	1.31%
			0.18	3.15 3.13 3.10	3.13	0.03	0.82%
	15	A	0.85	5.83 5.70 5.29	5.60	0.28	5.01%
			0.425	5.85 5.64 5.94	5.81	0.15	2.64%
			0.18	5.30 5.19 5.24	5.24	0.06	1.08%
		C	0.85	5.41 5.17 5.13	5.24	0.15	2.88%
			0.425	4.77 4.63 4.62	4.67	0.08	1.78%
			0.18	4.68 4.50 4.59	4.59	0.09	1.97%

*by weight of binder
+0: Virgin; A: Ambient; C: Cryogenic

Table H.4: G*/sinδ results of CRM binder made with binder Source B at 76°C

Binder Source	% CRM*	CRM Type+	CRM Size (mm)	G*/sinδ, *kPa*			
				Raw Data	Mean	Standard Deviation	Coefficient of Variation
B	0	0	0	0.32 0.32 0.33	0.32	0.00	1.44%
	10	A	0.85	1.28 1.25	1.27	0.02	1.70%
			0.425	0.93 1.00 0.97	0.96	0.03	3.39%
			0.18	0.83 0.86 0.91	0.87	0.04	4.96%
		C	0.85	0.87 0.87 0.81	0.85	0.04	4.23%
			0.425	0.82 0.82 0.88	0.84	0.03	3.92%
			0.18	0.76 0.83 0.82	0.80	0.04	4.53%
	15	A	0.85	1.71 1.64 1.93	1.76	0.16	8.82%
			0.425	1.72 1.65 1.75	1.71	0.05	2.89%
			0.18	1.54 1.50 1.47	1.50	0.03	2.25%
		C	0.85	1.36 1.39 1.59	1.44	0.12	8.59%
			0.425	1.45 1.42 1.35	1.41	0.05	3.77%
			0.18	1.21 1.25 1.22	1.23	0.02	1.61%

*by weight of binder
+0: Virgin; A: Ambient; C: Cryogenic

Table H.5: G*/sinδ results of CRM binder made with binder Source C at 64°C

Binder Source	% CRM*	CRM Type+	CRM Size (mm)	G*/sinδ, *kPa*			
				Raw Data	Mean	Standard Deviation	Coefficient of Variation
C	0	0	0	1.35 1.34 1.39	1.36	0.03	1.95%
	10	A	0.85	- - -	-	-	-
			0.425	3.99 4.09 3.91	4.00	0.09	2.22%
			0.18	3.96 4.00 3.89	3.95	0.06	1.46%
		C	0.85	5.52 5.48 4.33	5.11	0.68	13.25%
			0.425	4.01 3.88 3.57	3.82	0.22	5.87%
			0.18	3.64 3.56 3.51	3.57	0.07	1.90%
	15	A	0.85	6.59 6.28 6.27	6.38	0.18	2.90%
			0.425	5.95 6.05 5.94	5.98	0.06	1.03%
			0.18	5.28 5.23 5.32	5.28	0.05	0.89%
		C	0.85	5.51 5.19 5.44	5.38	0.17	3.08%
			0.425	5.18 5.01 5.04	5.08	0.09	1.85%
			0.18	4.71 4.77 4.72	4.74	0.03	0.72%

*by weight of binder
+0: Virgin; A: Ambient; C: Cryogenic

Table H.6: G*/sinδ results of CRM binder made with binder Source C at 76°C

Binder Source	% CRM*	CRM Type+	CRM Size (mm)	G*/sinδ, *kPa*			
				Raw Data	Mean	Standard Deviation	Coefficient of Variation
C	0	0	0	0.36 0.34 0.36	0.36	0.01	3.31%
	10	A	0.85	1.00 1.14 1.17	1.10	0.09	8.08%
			0.425	0.98 0.98 1.05	1.00	0.04	4.27%
			0.18	0.90 0.94 0.93	0.92	0.02	1.84%
		C	0.85	0.82 0.89 0.83	0.85	0.04	4.43%
			0.425	0.91 0.90 0.87	0.89	0.02	2.12%
			0.18	0.81 0.77 0.80	0.79	0.02	2.64%
	15	A	0.85	1.72 1.76 1.55	1.68	0.12	6.87%
			0.425	1.72 1.77 1.71	1.73	0.03	1.95%
			0.18	1.52 1.56 1.51	1.53	0.03	1.83%
		C	0.85	1.34 1.21 1.31	1.28	0.07	5.33%
			0.425	1.24 1.26 1.27	1.26	0.02	1.24%
			0.18	1.22 1.23 1.22	1.22	0.01	0.54%

*by weight of binder
+0: Virgin; A: Ambient; C: Cryogenic

Appendix I

Viscosity Verification Data

Table I.1: Viscosity results of CRM binder made with binder Source M

CRM Source	Binder Source	CRM %*	Gradation	CRM Type+	Test Temperature (°C)	Viscosity, Cp					
						Raw Data			Mean	Standard Deviation	Coefficient of Variation
-	M	0	-	0	135	600.00	595.00	602.50	599.72	3.84	0.64%
						600.00	597.50	605.00			
						597.50	595.00	605.00			
3	M	15	ADOT	A	135	3438.00	3138.00	3100.00	3226.67	135.12	4.19%
						3388.00	3237.00	3063.00			
						3350.00	3188.00	3138.00			
13	M	5	SCDOT	C	180	175.00	150.00	162.50	162.50	10.83	6.66%
						175.00	150.00	162.50			
						175.00	150.00	162.50			
2	M	10	ADOT	C	180	400.00	287.50	212.50	306.94	82.47	26.87%
						425.00	300.00	225.00			
						400.00	287.50	225.00			
17	M	5	0.180 mm	C	140	800.00	812.50	800.00	808.33	6.25	0.77%
						812.50	812.50	812.50			
						800.00	812.50	812.50			
12	M	10	SCDOT	A	180	425.00	450.00	462.50	445.83	16.54	3.71%
						425.00	450.00	462.50			
						425.00	450.00	462.50			
20	M	5	0.180 mm	A	160	400.00	375.00	387.50	387.50	10.83	2.79%
						400.00	375.00	387.50			
						400.00	375.00	387.50			
14	M	10	SCDOT	A	135	2463.00	2463.00	2350.00	2422.44	54.59	2.25%
						2450.00	2463.00	2350.00			
						2450.00	2463.00	2350.00			

*by weight of binder

+0: Virgin; A: Ambient; C: Cryogenic

Table I.2: Viscosity results of CRM binder made with binder Source N

CRM Source	Binder Source	CRM %*	Gradation	CRM Type+	Test Temperature (°C)	Viscosity, Cp					
						Raw Data			Mean	Standard Deviation	Coefficient of Variation
-	N	0	-	0	135	550.00	555.00	555.00	552.78	2.32	0.42%
						550.00	552.50	552.50			
						550.00	555.00	555.00			
16	N	5	0.425 mm	C	140	762.50	925.00	712.50	798.61	91.95	11.51%
						762.50	925.00	712.50			
						775.00	900.00	712.50			
2	N	10	ADOT	C	160	475.00	425.00	550.00	477.78	47.51	9.94%
						475.00	425.00	525.00			
						475.00	425.00	525.00			
15	N	15	0.850 mm	C	150	1400.00	1625.00	1575.00	1522.22	107.85	7.09%
						1500.00	1675.00	1525.00			
						1350.00	1600.00	1450.00			
2	N	20	ADOT	C	160	1925.00	1913.00	1612.00	1804.11	135.37	7.50%
						1862.00	1938.00	1625.00			
						1837.00	1875.00	1650.00			
14	N	20	SCDOT	A	140	4675.00	5225.00	5025.00	4919.44	248.99	5.06%
						4550.00	5000.00	5100.00			
						4600.00	4950.00	5150.00			

*by weight of binder
+0: Virgin; A: Ambient; C: Cryogenic

Table I.3: Viscosity results of CRM binder made with binder Source O

CRM Source	Binder Source	CRM %*	Gradation	CRM Type+	Test Temperature (°C)	Viscosity, Cp					
						Raw Data			Mean	Standard Deviation	Coefficient of Variation
-	O	0	-	0	135	500.00	495.00	492.50	495.83	3.31	0.67%
						500.00	495.00	492.50			
						500.00	495.00	492.50			
16	O	20	0.425 mm	C	140	2900.00	2750.00	2225.00	2608.33	305.93	11.73%
						2875.00	2750.00	2200.00			
						2850.00	2725.00	2200.00			
17	O	10	0.180 mm	C	180	200.00	275.00	275.00	252.78	34.11	13.49%
						200.00	275.00	275.00			
						225.00	275.00	275.00			

*by weight of binder
+0: Virgin; A: Ambient; C: Cryogenic

Table I.4: Viscosity results of CRM binder made with binder Source P

CRM Source	Binder Source	CRM %*	Gradation	CRM Type+	Test Temperature (°C)	Viscosity, Cp					
						Raw Data			Mean	Standard Deviation	Coefficient of Variation
-	P	0	-	0	135	435.00	430.00	432.50	432.50	2.17	0.50%
						435.00	430.00	432.50			
						435.00	430.00	432.50			
2	P	15	ADOT	C	135	1900.00	1500.00	1700.00	1675.00	183.71	10.97%
						1850.00	1425.00	1675.00			
						1825.00	1425.00	1775.00			

*by weight of binder
+0: Virgin; A: Ambient; C: Cryogenic

Table I.5: Viscosity results of CRM binder made with binder Source Q

CRM Source	Binder Source	CRM %*	Gradation	CRM Type+	Test Temperature (°C)	Viscosity, Cp					
						Raw Data			Mean	Standard Deviation	Coefficient of Variation
-	Q	0	-	0	135	435.00	430.00	432.50	432.50	2.17	0.50%
						435.00	430.00	432.50			
						435.00	430.00	432.50			
19	Q	10	0.425 mm	A	160	675.00	762.50	875.00	772.22	85.42	11.06%
						687.50	775.00	875.00			
						675.00	750.00	875.00			
17	Q	15	0.180 mm	C	160	1400.00	1313.00	1275.00	1329.33	58.35	4.39%
						1413.00	1313.00	1275.00			
						1400.00	1300.00	1275.00			
16	Q	15	0.425 mm	C	150	1313.00	1438.00	1587.00	1451.44	133.59	9.20%
						1288.00	1487.00	1625.00			
						1275.00	1475.00	1575.00			
18	Q	15	0.850 mm	A	160	1150.00	1438.00	1138.00	1234.89	141.16	11.43%
						1175.00	1362.00	1050.00			
						1163.00	1438.00	1200.00			
17	Q	5	0.180 mm	C	150	325.00	325.00	325.00	325.00	0.00	0.00%
						325.00	325.00	325.00			
						325.00	325.00	325.00			

*by weight of binder
+0: Virgin; A: Ambient; C: Cryogenic

Appendix J

G*/sinδ Verification Data

Table J.1: G*/sinδ results of CRM binder made with binder Source M at 64°C

CRM Source	Binder Source	CRM %*	Gradation	CRM Type+	Test Temperature (°C)	G*/sinδ kPa			
						Raw Data	Mean	Standard Deviation	Coefficient of Variation
-	M	0	-	0	64	2.48 1.88	2.18	0.42	19.46%
3	M	15	ADOT	A	64	4.94 5.80	5.37	0.61	11.32%
13	M	5	SCDOT	C	64	3.22 3.11	3.17	0.08	2.46%
2	M	10	ADOT	C	64	4.02 4.46	4.24	0.31	7.34%
17	M	5	0.180 mm	C	64	3.90 4.18	4.04	0.20	4.90%
12	M	10	SCDOT	A	64	7.61 7.31	7.46	0.21	2.84%
20	M	5	0.180 mm	A	64	4.33 3.54	3.94	0.56	14.20%

*by weight of binder
+0: Virgin; A: Ambient; C: Cryogenic

Table J.2: G*/sinδ results of CRM binder made with binder Source M at 70°C

CRM Source	Binder Source	CRM %*	Gradation	CRM Type+	Test Temperature (°C)	G*/sinδ kPa			
						Raw Data	Mean	Standard Deviation	Coefficient of Variation
-	M	0	-	0	70	1.31 0.89	1.10	0.30	27.00%
3	M	15	ADOT	A	70	3.22 3.31	3.27	0.06	1.95%
13	M	5	SCDOT	C	70	1.57 1.49	1.53	0.06	3.70%
2	M	10	ADOT	C	70	1.89 2.35	2.12	0.33	15.34%
17	M	5	0.180 mm	C	70	1.89 1.63	1.76	0.18	10.45%
12	M	10	SCDOT	A	70	4.03 3.89	3.96	0.10	2.50%
20	M	5	0.180 mm	A	70	1.99 1.79	1.89	0.14	7.48%

*by weight of binder
+0: Virgin; A: Ambient; C: Cryogenic

Table J.3: G*/sinδ results of CRM binder made with binder Source M at 76°C

CRM Source	Binder Source	CRM %*	Gradation	CRM Type+	Test Temperature (°C)	G*/sinδ kPa			
						Raw Data	Mean	Standard Deviation	Coefficient of Variation
-	M	0	-	0	76	0.81 -	0.81	-	-
3	M	15	ADOT	A	76	1.85 1.92	1.89	0.05	2.63%
13	M	5	SCDOT	C	76	0.80 0.77	0.79	0.02	2.70%
2	M	10	ADOT	C	76	0.97 1.33	1.15	0.25	22.14%
17	M	5	0.180 mm	C	76	0.96 0.85	0.91	0.08	8.59%
12	M	10	SCDOT	A	76	2.15 2.05	2.10	0.07	3.37%
20	M	5	0.180 mm	A	76	1.00 0.89	0.94	0.08	8.03%

*by weight of binder
+0: Virgin; A: Ambient; C: Cryogenic

Table J.4: G*/sinδ results of CRM binder made with binder Source M at 82°C

CRM Source	Binder Source	CRM %*	Gradation	CRM Type+	Test Temperature (°C)	G*/sinδ kPa			
						Raw Data	Mean	Standard Deviation	Coefficient of Variation
-	M	0	-	0	82	- -	-	-	-
3	M	15	ADOT	A	82	1.10 1.21	1.16	0.08	6.73%
13	M	5	SCDOT	C	82	- -	-	-	-
2	M	10	ADOT	C	82	0.76 -	0.76	-	-
17	M	5	0.180 mm	C	82	- -	-	-	-
12	M	10	SCDOT	A	82	1.17 1.08	1.13	0.06	5.66%
20	M	5	0.180 mm	A	82	- -	-	-	-

*by weight of binder
+0: Virgin; A: Ambient; C: Cryogenic

Table J.5: G*/sinδ results of CRM binder made with binder Source M at 88°C

CRM Source	Binder Source	CRM %*	Gradation	CRM Type+	Test Temperature (°C)	G*/sinδ kPa			
						Raw Data	Mean	Standard Deviation	Coefficient of Variation
-	M	0	-	0	88	- -	-	-	-
3	M	15	ADOT	A	88	0.64 0.67	0.66	0.02	3.24%
13	M	5	SCDOT	C	88	- -	-	-	-
2	M	10	ADOT	C	88	- -	-	-	-
17	M	5	0.180 mm	C	88	- -	-	-	-
12	M	10	SCDOT	A	88	0.64 0.58	0.61	0.04	6.96%
20	M	5	0.180 mm	A	88	- -	-	-	-

*by weight of binder
+0: Virgin; A: Ambient; C: Cryogenic

Table J.6: G*/sinδ results of CRM binder made with binder Source N at 64°C

CRM Source	Binder Source	CRM %*	Gradation	CRM Type+	Test Temperature (°C)	G*/sinδ kPa			
						Raw Data	Mean	Standard Deviation	Coefficient of Variation
-	N	0	-	0	64	1.96 1.90	1.93	0.04	2.20%
16	N	5	0.425 mm	C	64	3.67 3.94	3.81	0.19	5.02%
2	N	10	ADOT	C	64	6.90 6.96	6.93	0.04	0.61%
15	N	15	0.850 mm	C	64	8.98 8.24	8.61	0.52	6.08%
2	N	20	ADOT	C	64	13.70 12.28	12.99	1.00	7.73%
14	N	20	SCDOT	A	64	15.13 15.10	15.12	0.02	0.14%

*by weight of binder
+0: Virgin; A: Ambient; C: Cryogenic

Table J.7: G*/sinδ results of CRM binder made with binder Source N at 70°C

CRM Source	Binder Source	CRM %*	Gradation	CRM Type+	Test Temperature (°C)	G*/sinδ kPa			
						Raw Data	Mean	Standard Deviation	Coefficient of Variation
-	N	0	-	0	70	0.92 0.85	0.89	0.05	5.59%
16	N	5	0.425 mm	C	70	1.72 1.76	1.74	0.03	1.63%
2	N	10	ADOT	C	70	3.48 3.47	3.48	0.01	0.20%
15	N	15	0.850 mm	C	70	4.55 4.24	4.40	0.22	4.99%
2	N	20	ADOT	C	70	7.06 6.44	6.75	0.44	6.49%
14	N	20	SCDOT	A	70	8.30 8.51	8.41	0.15	1.77%

*by weight of binder
+0: Virgin; A: Ambient; C: Cryogenic

Table J.8: G*/sinδ results of CRM binder made with binder Source N at 76°C

CRM Source	Binder Source	CRM %*	Gradation	CRM Type+	Test Temperature (°C)	G*/sinδ kPa			
						Raw Data	Mean	Standard Deviation	Coefficient of Variation
-	N	0	-	0	76	- -	-	-	-
16	N	5	0.425 mm	C	76	0.83 0.90	0.87	0.05	5.72%
2	N	10	ADOT	C	76	1.78 1.78	1.78	0.00	0.00%
15	N	15	0.850 mm	C	76	2.36 2.18	2.27	0.13	5.61%
2	N	20	ADOT	C	76	3.44 3.38	3.41	0.04	1.24%
14	N	20	SCDOT	A	76	4.41 4.71	4.56	0.21	4.65%

*by weight of binder
+0: Virgin; A: Ambient; C: Cryogenic

Table J.9: G*/sinδ results of CRM binder made with binder Source N at 82°C

CRM Source	Binder Source	CRM %*	Gradation	CRM Type+	Test Temperature (°C)	G*/sinδ kPa			
						Raw Data	Mean	Standard Deviation	Coefficient of Variation
-	N	0	-	0	82	- -	-	-	-
16	N	5	0.425 mm	C	82	- -	-	-	-
2	N	10	ADOT	C	82	0.96 0.94	0.95	0.01	1.49%
15	N	15	0.850 mm	C	82	1.25 1.16	1.21	0.06	5.28%
2	N	20	ADOT	C	82	1.90 1.82	1.86	0.06	3.04%
14	N	20	SCDOT	A	82	2.52 2.72	2.62	0.14	5.40%

*by weight of binder
+0: Virgin; A: Ambient; C: Cryogenic

Table J.10: G*/sinδ results of CRM binder made with binder Source N at 88°C

CRM Source	Binder Source	CRM %*	Gradation	CRM Type+	Test Temperature (°C)	G*/sinδ kPa			
						Raw Data	Mean	Standard Deviation	Coefficient of Variation
-	N	0	-	0	70	- -	-	-	-
16	N	5	0.425 mm	C	70	- -	-	-	-
2	N	10	ADOT	C	70	- -	-	-	-
15	N	15	0.850 mm	C	70	0.69 0.62	0.66	0.05	7.56%
2	N	20	ADOT	C	70	1.10 1.07	1.09	0.02	1.96%
14	N	20	SCDOT	A	70	1.41 1.63	1.52	0.16	10.23%

*by weight of binder
+0: Virgin; A: Ambient; C: Cryogenic

Table J.11: G*/sinδ results of CRM binder made with binder Source O at 64°C

CRM Source	Binder Source	CRM %*	Gradation	CRM Type+	Test Temperature (°C)	G*/sinδ kPa			
						Raw Data	Mean	Standard Deviation	Coefficient of Variation
-	O	0	-	0	64	1.65 1.56	1.61	0.06	3.97%
16	O	20	0.425 mm	C	64	8.05 8.19	8.12	0.10	1.22%
17	O	10	0.180 mm	C	64	3.91 4.14	4.03	0.16	3.97%

*by weight of binder
+0: Virgin; A: Ambient; C: Cryogenic

Table J.12: G*/sinδ results of CRM binder made with binder Source O at 70°C

CRM Source	Binder Source	CRM %*	Gradation	CRM Type+	Test Temperature (°C)	G*/sinδ kPa			
						Raw Data	Mean	Standard Deviation	Coefficient of Variation
-	O	0	-	0	70	0.85 0.86	0.86	0.01	0.83%
16	O	20	0.425 mm	C	70	4.09 4.16	4.13	0.05	1.20%
17	O	10	0.180 mm	C	70	1.91 2.01	1.96	0.07	3.61%

*by weight of binder
+0: Virgin; A: Ambient; C: Cryogenic

Table J.13: G*/sinδ results of CRM binder made with binder Source O at 76°C

CRM Source	Binder Source	CRM %*	Gradation	CRM Type+	Test Temperature (°C)	G*/sinδ kPa			
						Raw Data	Mean	Standard Deviation	Coefficient of Variation
-	O	0	-	0	76	- -	-	-	-
16	O	20	0.425 mm	C	76	0.94 1.03	0.99	0.06	6.46%
17	O	10	0.180 mm	C	76	2.27 2.23	2.25	0.03	1.26%

*by weight of binder
+0: Virgin; A: Ambient; C: Cryogenic

Table J.14: G*/sinδ results of CRM binder made with binder Source O at 82°C

CRM Source	Binder Source	CRM %*	Gradation	CRM Type+	Test Temperature (°C)	G*/sinδ kPa			
						Raw Data	Mean	Standard Deviation	Coefficient of Variation
-	O	0	-	0	82	- -	-	-	-
16	O	20	0.425 mm	C	82	0.55 -	0.55	-	-
17	O	10	0.180 mm	C	82	1.22 1.26	1.24	0.03	2.57%

*by weight of binder
+0: Virgin; A: Ambient; C: Cryogenic

Table J.15: G*/sinδ results of CRM binder made with binder Source O at 88°C

CRM Source	Binder Source	CRM %*	Gradation	CRM Type+	Test Temperature (°C)	G*/sinδ kPa			
						Raw Data	Mean	Standard Deviation	Coefficient of Variation
-	O	0	-	0	88	- -	-	-	-
16	O	20	0.425 mm	C	88	- -	-	-	-
17	O	10	0.180 mm	C	88	0.71 0.71	0.71	0.00	0.00%

*by weight of binder
+0: Virgin; A: Ambient; C: Cryogenic

Table J.16: G*/sinδ results of CRM binder made with binder Source P at 64°C

CRM Source	Binder Source	CRM %*	Gradation	CRM Type+	Test Temperature (°C)	G*/sinδ kPa			
						Raw Data	Mean	Standard Deviation	Coefficient of Variation
-	P	0	-	0	64	1.36 1.18	1.27	0.13	10.02%
2	P	15	ADOT	C	64	4.89 4.86	4.88	0.02	0.44%

*by weight of binder
+0: Virgin; A: Ambient; C: Cryogenic

Table J.17: G*/sinδ results of CRM binder made with binder Source P at 70°C

CRM Source	Binder Source	CRM %*	Gradation	CRM Type+	Test Temperature (°C)	G*/sinδ kPa			
						Raw Data	Mean	Standard Deviation	Coefficient of Variation
-	P	0	-	0	70	0.60 0.55	0.58	0.04	6.15%
2	P	15	ADOT	C	70	2.39 2.38	2.39	0.01	0.30%

*by weight of binder
+0: Virgin; A: Ambient; C: Cryogenic

Table J.18: G*/sinδ results of CRM binder made with binder Source P at 76°C

CRM Source	Binder Source	CRM %*	Gradation	CRM Type+	Test Temperature (°C)	G*/sinδ kPa			
						Raw Data	Mean	Standard Deviation	Coefficient of Variation
-	P	0	-	0	76	- -	-	-	-
2	P	15	ADOT	C	76	1.24 1.23	1.24	0.01	0.57%

*by weight of binder
+0: Virgin; A: Ambient; C: Cryogenic

Table J.19: G*/sinδ results of CRM binder made with binder Source P at 82°C

CRM Source	Binder Source	CRM %*	Gradation	CRM Type+	Test Temperature (°C)	G*/sinδ kPa			
						Raw Data	Mean	Standard Deviation	Coefficient of Variation
-	P	0	-	0	82	- -	-	-	-
2	P	15	ADOT	C	82	0.69 0.66	0.68	0.02	3.14%

*by weight of binder
+0: Virgin; A: Ambient; C: Cryogenic

Table J.20: G*/sinδ results of CRM binder made with binder Source P at 88°C

CRM Source	Binder Source	CRM %*	Gradation	CRM Type+	Test Temperature (°C)	G*/sinδ kPa			
						Raw Data	Mean	Standard Deviation	Coefficient of Variation
-	P	0	-	0	88	- -	-	-	-
2	P	15	ADOT	C	88	- -	-	-	-

*by weight of binder
+0: Virgin; A: Ambient; C: Cryogenic

Table J.21: G*/sinδ results of CRM binder made with binder Source Q at 64°C

CRM Source	Binder Source	CRM %*	Gradation	CRM Type+	Test Temperature (°C)	G*/sinδ kPa			
						Raw Data	Mean	Standard Deviation	Coefficient of Variation
-	Q	0	-	0	64	1.14 1.15	1.15	0.01	0.62%
19	Q	10	0.425 mm	A	64	4.06 4.01	4.04	0.04	0.88%
17	Q	15	0.180 mm	C	64	5.50 5.91	5.71	0.29	5.08%
16	Q	15	0.425 mm	C	64	5.62 5.17	5.40	0.32	5.90%
18	Q	15	0.850 mm	A	64	6.17 6.14	6.16	0.02	0.34%
17	Q	5	0.180 mm	C	64	2.03 1.82	1.93	0.15	7.71%

*by weight of binder
+0: Virgin; A: Ambient; C: Cryogenic

Table J.22: G*/sinδ results of CRM binder made with binder Source Q at 70°C

CRM Source	Binder Source	CRM %*	Gradation	CRM Type+	Test Temperature (°C)	G*/sinδ kPa			
						Raw Data	Mean	Standard Deviation	Coefficient of Variation
-	Q	0	-	0	70	0.57 0.56	0.57	0.01	1.25%
19	Q	10	0.425 mm	A	70	2.13 2.08	2.11	0.04	1.68%
17	Q	15	0.180 mm	C	70	2.90 3.03	2.97	0.09	3.10%
16	Q	15	0.425 mm	C	70	2.86 2.58	2.72	0.20	7.28%
18	Q	15	0.850 mm	A	70	3.23 3.62	3.43	0.28	8.05%
17	Q	5	0.180 mm	C	70	1.02 0.89	0.96	0.09	9.63%

*by weight of binder
+0: Virgin; A: Ambient; C: Cryogenic

Table J.23: G*/sinδ results of CRM binder made with binder Source Q at 76°C

CRM Source	Binder Source	CRM %*	Gradation	CRM Type+	Test Temperature (°C)	G*/sinδ kPa			
						Raw Data	Mean	Standard Deviation	Coefficient of Variation
-	Q	0	-	0	76	- -	-	-	-
19	Q	10	0.425 mm	A	76	1.16 1.09	1.13	0.05	4.40%
17	Q	15	0.180 mm	C	76	1.55 1.56	1.56	0.01	0.45%
16	Q	15	0.425 mm	C	76	1.48 1.33	1.41	0.11	7.55%
18	Q	15	0.850 mm	A	76	1.83 2.20	2.02	0.26	12.98%
17	Q	5	0.180 mm	C	76	0.53 -	0.53	-	-

*by weight of binder
+0: Virgin; A: Ambient; C: Cryogenic

Table J.24: G*/sinδ results of CRM binder made with binder Source Q at 82°C

CRM Source	Binder Source	CRM %*	Gradation	CRM Type+	Test Temperature (°C)	G*/sinδ kPa			
						Raw Data	Mean	Standard Deviation	Coefficient of Variation
-	Q	0	-	0	82	- -	-	-	-
19	Q	10	0.425 mm	A	82	0.62 0.59	0.61	0.02	3.51%
17	Q	15	0.180 mm	C	82	0.87 0.83	0.85	0.03	3.33%
16	Q	15	0.425 mm	C	82	0.81 0.71	0.76	0.07	9.30%
18	Q	15	0.850 mm	A	82	1.10 1.43	1.27	0.23	18.45%
17	Q	5	0.180 mm	C	82	- -	-	-	-

*by weight of binder
+0: Virgin; A: Ambient; C: Cryogenic

Table J.25: G*/sinδ results of CRM binder made with binder Source Q at 88°C

CRM Source	Binder Source	CRM %*	Gradation	CRM Type+	Test Temperature (°C)	G*/sinδ kPa			
						Raw Data	Mean	Standard Deviation	Coefficient of Variation
-	Q	0	-	0	88	- -	-	-	-
19	Q	10	0.425 mm	A	88	- -	-	-	-
17	Q	15	0.180 mm	C	88	- -	-	-	-
16	Q	15	0.425 mm	C	88	- -	-	-	-
18	Q	15	0.850 mm	A	88	0.66 1.03	0.85	0.26	30.96%
17	Q	5	0.180 mm	C	88	- -	-	-	-

*by weight of binder
+0: Virgin; A: Ambient; C: Cryogenic

Appendix K

Failure Temperature Verification Data

Table K.1: Failure temperature results of CRM binder made with binder Source M

CRM Source	Binder Source	CRM %*	Gradation	CRM Type+	Failure Temperature (°C)			
					Raw Data	Mean	Standard Deviation	Coefficient of Variation
-	M	0	-	0	73.30 69.00	71.15	3.04	4.27%
3	M	15	ADOT	A	83.00 83.90	83.45	0.64	0.76%
13	M	5	SCDOT	C	73.90 73.60	73.75	0.21	0.29%
2	M	10	ADOT	C	75.70 79.00	77.35	2.33	3.02%
17	M	5	0.180 mm	C	75.70 74.40	75.05	0.92	1.22%
12	M	10	SCDOT	A	83.50 82.70	83.10	0.57	0.68%
20	M	5	0.180 mm	A	75.90 74.90	75.40	0.71	0.94%

*by weight of binder
+0: Virgin; A: Ambient; C: Cryogenic

Table K.2: Failure temperature results of CRM binder made with binder Source N

CRM Source	Binder Source	CRM %*	Gradation	CRM Type+	Failure Temperature (°C)			
					Raw Data	Mean	Standard Deviation	Coefficient of Variation
-	N	0	-	0	69.20 68.80	69.00	0.28	0.41%
16	N	5	0.425 mm	C	74.40 75.00	74.70	0.42	0.57%
2	N	10	ADOT	C	81.60 81.40	81.50	0.14	0.17%
15	N	15	0.850 mm	C	84.20 83.40	83.80	0.57	0.68%
2	N	20	ADOT	C	89.00 88.80	88.90	0.14	0.16%
14	N	20	SCDOT	A	91.40 93.80	92.60	1.70	1.83%

*by weight of binder
+0: Virgin; A: Ambient; C: Cryogenic

Table K.3: Failure temperature results of CRM binder made with binder Source O

CRM Source	Binder Source	CRM %*	Gradation	CRM Type+	Failure Temperature (°C)			
					Raw Data	Mean	Standard Deviation	Coefficient of Variation
-	O	0	-	0	68.40 68.50	68.45	0.07	0.10%
16	O	20	0.425 mm	C	84.30 84.30	84.30	0.00	0.00%
17	O	10	0.180 mm	C	75.30 76.20	75.75	0.64	0.84%

*by weight of binder
+0: Virgin; A: Ambient; C: Cryogenic

Table K.4: Failure temperature results of CRM binder made with binder Source P

CRM Source	Binder Source	CRM %*	Gradation	CRM Type+	Failure Temperature (°C)			
					Raw Data	Mean	Standard Deviation	Coefficient of Variation
-	P	0	-	0	66.10 65.10	65.60	0.71	1.08%
2	P	15	ADOT	C	78.10 77.90	78.00	0.14	0.18%

*by weight of binder
+0: Virgin; A: Ambient; C: Cryogenic

Table K.5: Failure temperature results of CRM binder made with binder Source Q

CRM Source	Binder Source	CRM %*	Gradation	CRM Type+	Failure Temperature (°C)			
					Raw Data	Mean	Standard Deviation	Coefficient of Variation
-	Q	0	-	0	65.10 65.10	65.10	0.00	0.00%
19	Q	10	0.425 mm	A	77.30 76.80	77.05	0.35	0.46%
17	Q	15	0.180 mm	C	80.40 80.20	80.30	0.14	0.18%
16	Q	15	0.425 mm	C	79.90 78.70	79.30	0.85	1.07%
18	Q	15	0.850 mm	A	83.00 88.40	85.70	3.82	4.46%
17	Q	5	0.180 mm	C	70.20 69.00	69.60	0.85	1.22%

*by weight of binder
+0: Virgin; A: Ambient; C: Cryogenic

REFERENCES

Abdelrahman, M. A., & Carpenter, S. H. (1999). Mechanism of Interaction of Asphalt Cements with Crumb Rubber Modifier. *Transportation Research Record* , 106-113.

Abdelrahman, M. (2006). Controlling the Performance of Crumb Rubber Modifier (CRM) Binders through the Addition of Polymer Modifiers. *Transportation Research Record* .

American Association of State Highway and Transportation Officials. (2005). *AASHTO M 320 Standard Specification for Performance-Graded Asphalt Binder.* Washington DC: AASHTO.

American Association of State Highway and Transportation Officials. (2005). *AASHTO T 313: Standard Test Method for Determining the Flexural Creep Stiffness of Asphalt Binder Using the Bending Beam.* Washington DC: AASHTO.

American Association of State Highway and Transportation Officials. (2006). *AASHTO T 315 Standard Method of Test for Determining the Rheological Properties of Asphalt Binder Using a Dynamic Shear Rheometer (DSR).* Washington DC: AASHTO.

American Association of State Highway Officials. (2006). *AASHTO T 316 Viscosity Determination of Asphalt Binder using Rotational Viscometer.* Washington DC: AASHTO.

American Society of Testing and Materials. (2001). D 6114 Standard Specification for Asphalt Rubber Binder. In A. B. Standards, *Road and Paving Materials: Vehicle Pavement Systems.* West Conshohoken, PA: ASTM.

Amirkhanian, S. N. (2003). Establishment of an Asphalt-Rubber Technology Service (ARTS). *Proceedings of the Asphalt Rubber 2003 Conference*, *2*, pp. 577-588. Brasilia, Brazil.

Asphalt Institute. (2003). *Performance Graded Asphalt Binder Specification and Testing, Superpave Series No.1 (SP-1).* Lexington, KY: Asphalt Institute.

Bahia, H. U., & Davies, R. (1996). Factors Controlling the Effect of Crumb Rubber on Critical Properties of Asphalt Binders. *Journal of the Association of Asphalt Paving Technologists , 64*, 130-162.

Bahia, H. U., & Davis, R. (1994). Effect of Crumb Rubber Modifiers (CRM) on Performance Related properties of Asphalt Binders. *Journal of the Association of Asphalt Paving Technologists , 63*, 414-449.

Blumenthal, M. H. (1994). *Producing Ground Scrap Tire: A Comparison Between Ambient and Cryogenic Technologies.* Washington, D.C.: Rubber Manufacturer's Association.

California Department of Transportation. (2003). *Asphalt Rubber Usage Guide.* Sacramento, CA.

Chehoveits, J. G., Dunning, R. L., & Morris, G. R. (1982). Characteristics of Asphalt-Rubber by the Sliding Plate Microviscometer. *Association of Asphalt Paving Technologies* , 240.

Cramer, S., & Swanson, M. (1973). An Evaluation of Ten Pairwise Multiple Comparison Procedures by Monte Carlo Methods. *Journal of the American Statistical Association* , 66-74.

Dantas Neto, S. A., Farias, M. M., Pais, J. C., Pereira, .. A., & Picado Santos, L. (2003). Behavior of Asphalt-Rubber Hot Mixes Obtained with High Crumb Rubber Contents. *Proceedings of the Asphalt Rubber 2003 Conference*, *2*, pp. 147-158. Brasilia, Brazil.

Environmental Protection Agency. (2007, January 2007). Retrieved August 29, 2007, from Management of Scrap Tires: http://www.epa.gov/garbage/tires/

Environmental Protection Agency. (2007, August 17). *Green Buildings*. Retrieved August 29, 2007, from Why Build Green: http://www.epa.gov/greenbuilding/

Environmental Protection Agency. (2007, September 6). *Management of Scrap Tires*. Retrieved January 7, 2008, from Tire Fires: http://www.epa.gov/garbage/tires/fires.htm

Environmental Protection Agency. (2006). *Municipal Solid Waste Generation, Recycling, and Disposal in the United States: Facts and Figures for 2006.* Washington, DC: Environmental Protection Agency.

Eyring, H. (1936). Viscosity, Plasticity, and Diffusion as Examples of Absolute Reaction Rates. *Journal of Chemical Physics* , 283-291.

Fisher, R. A. (1949). *The Design of Experiments.* Edinburgh: Oliver and Boyd.

Griffith, J. M., & Puzinauskas, V. P. (1963). *Relation of Empirical Tests to Fundamental Viscosity of Asphalt Cement.* Philadelphia, PA: ASTM Special Technical Publication No. 328.

Jennrich, R. I. (1995). *An Introduction to Computational Statistics: Regression Analysis.* Englewood Cliffs, NJ: Prentics-Hall, Inc.

Khalid, H. A., & Artamendi, I. (2004, March). Mechanical Properties of used-tyre Rubber. *Engineering Sustainability* , pp. 37-43.

Kyari, M., Cunliffe, & Williams, P. (2005). Characterization of Oils, Gases, and Char in Relation to the Pyrolysis of Different Brands of Scrap Automotive Tires. *Energy and Fuels Vol. 19* .

Lee, K. W., & Mahboub, K. C. (2006). *Asphalt Mix Design: Past, Present, and Future.* Washington, D.C.: American Society of Civil Engineers.

Lee, S., Amirkhanian, S., Thodesen, C., & Shatanawi, K. (2006). Effect of Compaction Temperatures on Rubber Asphalt Mixes. *Asphalt Rubber Conference.* Palm Springs, CA.

Lougheed, T. J., & Pappagiannakis, A. T. (1996). Viscosity Characteristics of Rubber Modified Asphals. *Journal of Materials in Civil Engineering* , 153-156.

Maze, M. (1996). Viscosity of EVA Modified Polymerzed Bitumens. *Eurasphalt and Eurobitume Congress* (p. No. 5117). Strasbourg, France: Eurobitume.

Oliver, J. W. (1982). Optimizing the Improvements Obtained by the Digestion of Comminuted Scrap Rubbers in Paving Asphalts. *Association of Asphalt Paving technologies* , 169.

Ott, R. L., & Longnecker, M. (2001). An Introduction to Statistical Methods and Data Analysis. In R. L. Ott, & M. Longnecker. Pacific Grove, CA, USA: Duxbury.

Painter, P. C., & Coleman, M. M. (1997). *Fundamentals of Polymer Science - An Introductory Text.* Lancaster, PA: Technomic Publishing Co. Inc.

Pellinen, T. K., Witczak, M. W., & Bonaquist, R. F. (2002). Asphalt Mix Master Curve Construction using Sigmoidal Fitting Function with Non-linear Least Squares

Optimization. *15th ASCE Engineering Mechanics Conferences.* New York, NY: ASCE.

Putman, B. J. (2005). *Quantification of the Effects of Crumb Rubber in CRM Binders.* PhD Dissertation, Clemson University, Department of Civil Engineering, Clemson, SC.

Putman, B. J., & Amirkhanian, S. N. (2006). Crumb Rubber Modification of Binders: Interaction and Particle Effects. *Proceedings of the Asphalt Rubber 2006 Conference*, *3*, pp. 655-677. Palm Springs,Ca.

Puzinauskas, V. P. (1967). Evaluation of Properties of Asphalt Cements with Emphasis on Consistencies at Low Temperatures. *Association of Asphalt Paving Technologists* (pp. 489-540). Denver, CP: AAPT.

Rasmussen, R. O., Lytton, R. L., & Chang, G. K. (2002). Method to Predict Temperature Susceptibilty of an Asphalt Binder. *Journal of Materials in Civil Engineering* , 246-252.

Rieck, J. (2005). *Experimental Statistics 801: Statistical Methods Class Notes.* Clemson, SC: Clemson University.

Roberts, F. L., Kandhal, P. S., Brown, E. R., Lee, D., & Kennedy, T. (1996). *Hot Mix Asphalt Materials Design and Construction.* Lanham, MD, Md: NAPA Educational Fund.

Rubber Manufacturers Association. (2006). *Scrap Tire Markets in the United States.* Washington DC: Rubber Manufacturers Association.

Rubber Manufacturers Association. (2004). *State Legislation of Scrap Tires.* Washington DC: Rubber Manufacturers Association.

Salomon, D., & Zhai, H. (2003). *Asphalt Binder Flow Activation Energy and its Significance for Compaction Effort.* Nampa, ID: Idaho Asphalt Supply, Inc.

Specht, L. P., Khatchatourian, O., Teixeira Brito, L. A., & Pereira Ceratti, J. A. (2007). Modeling of Asphalt-Rubber Rotational Viscosities by Statistical Analysis and Neural Networks. *Materials Research* , 69-74.

Stroup-Gardiner, M., Newcomb, D. E., & Tanquist, B. (1993). Asphalt-rubber interactions. *Transportation Research Record* , 99-108.

Stuart, K. D. (2001). *Methodology for Determining Compaction Temperatures for Modified Asphalt Binders (FHWA-RD-02-016).* McLean, VA: FHWA.

Takallou, B. (1991). Recycling Tires in Rubber Asphalt Pavign Yields Cost Disposal Benefits. *Elastomerics* , pp. 19-24.

Tayebali, A. A., Vyas, B. B., & Malpass, G. A. (1990). Effect of Crumb Rubber Particle Size and Concentration on Performance Grading of Rubber Modified Asphalt Binders. *ASTM Special Technical Publication* , 30-47.

Toler, J. (2006). *Experimental Statistics 805: Design and Analysis of Experiments Class Notes.* Clemson, SC: Clemson University.

Toyo Tires. (2001). *Toyo Global Web Page.* Retrieved August 29, 2007, from Toyo Tire Talk: http://www.toyojapan.com/tires/pdf/TTT_06.pdf

Transportation Research Board. (1984). *TRB Special Report 202: America's Highways: Accelerating the Search for Innovation.* Washington DC: TRB.

Ucar, S., Karagoz, S., Yanik, J., Saglam, M., & Yuksel, M. (2005). Copyrolysis of Scrap Tires with Waste Lubricant Oil. *Fuel Processing Technology , 87*, 53-58.

US Army Corps of Engineers. (2000). *Hot-Mix Asphalt Paving Handbook, AC 150/5370-14A.* Washington DC: Library of Congress.

Ward, I. M., & Hadley, D. W. (1993). *An Introduction to the Mechanical Properties of Solid Polymers.* New York, NY: Wiley.

West, R. C., Page, G. C., Veilleux, J. G., & Choubane, B. (1998). Effect of Tire Grinding Method on Asphalt Rubber Binder Characteristics. *Transportation Research Record* (1638), 134-140.

Xiao, F., Amirkhanian, S. N., & Juang, C. H. (2007). Rutting Resistance of Rubberized Asphalt Concrete Pavements Containing Reclaimed Asphalt Pavement Mixtures. *Journal of Materials in Civil Engineering , 19* (6), 475-483.